UiT The Arctic University of Norway
University of South-Eastern Norway
Western Norway University of Applied Sciences
NTNU Norwegian University of Science and Technology

Faculty of Science and Technology
Department of Technology and Safety

An Integrated Data Analytics Framework for Enhancing the Environmental and Life-cycle Economic Performance in Shipping

Khanh Quang Bui

A dissertation for the degree of Philosophiae Doctor

October 2022

UiT The Arctic University of Norway
Faculty of Science and Technology
Department of Technology and Safety

Norwegian University of Science and Technology
Faculty of Engineering
Department of Ocean Operations and Civil Engineering

University of South-Eastern Norway
Faculty of Technology, Natural Sciences and Maritime Studies
Department of Maritime Operations

Western Norway University of Applied Sciences
Faculty of Business Administration and Social Sciences
Department of Maritime Studies

An Integrated Data Analytics Framework for Enhancing the Environmental and Life-cycle Economic Performance in Shipping

Khanh Quang Bui

Doctoral thesis in partial fulfilment of the requirements for the degree of Philosophiae Doctor

UiT The Arctic University of Norway

Faculty of Science and Technology
Department of Technology and Safety

October 2022

Abstract

Shipping has been recognized as the most efficient mode of transport, carrying over 80% of international trade volume. The shipping industry is at the beginning of one of its greatest energy and technology transition driven by decarbonization drivers in terms of stringent emission regulations and commercial pressure. Digitalization can enable the transition by leveraging Machine Learning (ML) and Data Analytics (DA) techniques with a focus on enhancing energy efficiency during ship operations. Furthermore, such a transition is expected to exert tremendous impacts on the life-cycle costs of ships' assets and systems. Under the scope of maritime decarbonization, the main aim of this thesis is to develop an integrated data analytics framework for enhancing the environmental and life-cycle economic performance in the shipping industry. In order to achieve the stated aim, a set of objectives are specified under two distinct frameworks which are developed in individual methodologies and applied in unique case studies illustrating their effectiveness in the respective objectives.

Firstly, an advanced data analytics framework (ADAF) is proposed to quantify the operational performance of a bulk carrier on a local scale with respect to its operational conditions. The ADAF includes appropriate data analytics along with domain knowledge for the detection of data anomalies, the investigation of the ship's localized operational conditions via data clustering, the identification of the relative correlations among the investigated parameters and the quantification of the ship's performance in each of the respective conditions (i.e., engine modes and trim-draft modes). Given the data set used for the implementation of the ADAF, a ship performance index (SPI) is derived to find the best performance trim-draft mode under the engine modes of the ship. The findings generated from the ADAF add to the growing field of fault diagnostics, ship performance and condition monitoring in the maritime research domain and are particularly relevant for ship-owners and ship operators.

Secondly, a life-cycle cost framework (LCCF) is developed to evaluate the total cost performance of an innovative marine dual-fuel engine compared to that of a conventional diesel engine. The LCCF is built upon the fundamental assumption that the selected ship from the ADAF will be retrofitted with the dual-fuel engine. The LCCF includes the development of a cost model with an engineering build-up approach considering the uncertainties involved over the lifetime of such engines, resulting in interpretable and effective results using data from numerous sources. Furthermore,

several measures of economic performance such as the Net Present Cost (NPC), the Net Saving (NS) and the Saving-to-Investment Ratio (SIR) are derived from the LCCF to compare the life-cycle cost performances of these engines. The findings indicate that the dual-fuel engine is more cost-effective than the diesel engine under a given fuel price scenario. The uncertainties are meticulously treated by performing scenario sensitivity analyses and a Monte Carlo simulation. Results from the scenario sensitivity analyses indicate that the cost-effectiveness of the dual-fuel engine is sensitive to higher gas price scenarios. Results from the Monte Carlo simulation within the initial fuel price setting reveal an adequate degree of confidence when opting for the dual-fuel engine. Furthermore, it is found that fuel prices are the most influential cost driver. Different foreseeable carbon pricing scenarios are also simulated to show that the dual-fuel engine is still more competitive than the diesel engine. One of the more significant findings is that regardless of fuel price and carbon pricing scenarios, the dual-fuel engine offers an environmental impact (EI) with a CO_2 emission reduction potential of 33% compared to the diesel engine. The findings contribute to the current literature on shipping investment appraisals. Furthermore, the findings could be of interest to ship-owners and investors wishing to make retrofitting decisions. The findings also have policy implications for the development of market-based measures (MBMs) for emissions reduction in shipping achieved through future energy technologies.

Taken together, this thesis marks the first attempt to develop an integrated data analytics framework encompassing ML/DA approaches and the life-cycle cost approach with the creation of various KPIs (i.e. Key Performance Indicators) including the SPI, NPC, NS, SIR and EI to enable better decision-making towards enhanced environmental and life-cycle economic performance in the shipping industry.

Acknowledgements

Pursuing this PhD degree is an important milestone in my life. Throughout the course of my PhD studies, I had an opportunity to elevate my research skills and invest in my own personal development. It has been a journey with its ups and downs, but there have been a great number of people who have always been by my side with their support, friendship and love.

Most of all, I wish to express my gratitude to my main supervisor Professor Lokukaluge Prasad Perera for his constant support during my PhD studies. Without his guidance and wise advice, this PhD thesis would not have been possible.

My gratitude is also extended to my co-supervisors Professor Halvor Schøyen and Professor Peter Wide for their input in supervisor meetings during this PhD process. I would like to thank Halvor for his constructive and helpful comments on the first draft of this PhD thesis.

Besides, I would like to acknowledge the valuable feedback provided by Professor Jan Emblemsvåg in the second half of this research study. In addition, I am deeply grateful to Professor Aykut I. Ölcer who offered interesting comments and precious suggestions to enhance the quality of this thesis. Extraordinary thanks are due to Professor Egil Pedersen who always made time to provide me with interesting discussions.

A very special thank you goes out to colleagues at the Department of Technology and Safety, UiT. In particular, I must express my sincere appreciation to Associate Professor Bjørn-Morten Batalden and Gunn-Helene Turi for their tremendous support. Thanks to the members of the nautical science team at the department for their continuous encouragement. I would also like to express gratitude to my PhD and Postdoc friends in the department: Lise, Minh Tuan, Brian, Per, Nikolai, Yufei, Hadi, Afshin, Behrooz, Bright, Leikny, Jibola, Sushmit, Helene, Hao and many more.

There was a multitude of individuals who helped me to arrive at this point. My special thanks go to Yaser and Phuong Chau for their invaluable support. To Martin and Silje, thank you for being with me in difficult times during the pandemic. I would like to thank the Vietnamese community in Tromsø for all the social gatherings throughout these years.

I am fortunate enough to come from a shipping family with many of my family members working on ocean-going vessels. Maritime expertise from my uncle Thanh Phong Nguyen, my cousins Anh Phan and Cuong Tran, who are experienced Chief Engineers, was essential in helping me complete this PhD thesis.

Lastly, I would not have been able to afford to undertake this endeavor without the unconditional love and support from my parents, my sister and family members. Words cannot express how much I love them. It is essential that I thank my long-term friends, Vuong Nguyen, Truong Vu, Viet Dung, Thao Pham and Khue Tran, for their friendship, wisdom and empathy.

Khanh Quang Bui

Tromsø, Norway

October 2022

Contents

List of Figures

List of Tables

Nomenclature

Acronyms

ADAF	Advanced Data Analytics Framework
AER	Annual Efficiency Ratio
AI	Artificial Intelligence
ANNs	Artificial Neural Networks
APS	Announced Pledges Scenario
CBS	Cost Breakdown Structure
CII	Carbon Intensity Indicator
CO_2	Carbon Dioxide
DA	Data Analytics
DCS	Data Collection System
DWT	Deadweight Ton
EBS	Engine Breakdown Structure
ECAs	Emission Control Areas
EEDI	Energy Efficiency Design Index
EEOI	Energy Efficiency Operational Indicator
EEXI	Energy Efficiency Existing Ship Index
EI	Environmental Impact
EM	Expectation-Maximization
ETS	Emissions Trading System
EU	European Union
GHG	Greenhouse Gas
GMMs	Gaussian Mixture Models
HFO	Heavy Fuel Oil
IMO	International Maritime Organization
IoT	Internet of Things
ISO	International Organization for Standardization
KDE	Kernel Density Estimation
KPIs	Key Performance Indicators
LCC	Life-cycle Costing

LCCA	Life-cycle Cost Analysis
LCCF	Life-cycle Cost Framework
LNG	Liquefied Natural Gas
LOA	Length Overall
MARPOL	International Convention for the Prevention of Pollution from Ships
MBMs	Market-based Measures
MCR	Maximum Continuous Rating
ME	Main Engine
MEPC	Marine Environment Protection Committee
MGO	Marine Gas Oil
ML	Machine Learning
MRV	Monitoring, Reporting and Verification
NO_x	Nitrogen Oxide
NZE	Net Zero Emissions by 2050 Scenario
O&MMs	Operation & Maintenance Manuals
PM	Particulate Matter
RO	Research Objective
SCR	Selective Catalytic Reduction
SDGs	Sustainable Development Goals
SDS	Sustainable Development Scenario
SEEMP	Ship Energy Efficiency Management Plan
SO_x	Sulphur Oxide
SOG	Speed Over Ground
SPI	Ship Performance Index
STEPS	Stated Policies Scenario
STW	Speed Through Water
SVD	Singular Value Decomposition
SVs	Singular Vectors
ULSD	Ultra Low Sulphur Diesel
VLSFO	Very Low Sulphur Fuel Oil
WEO2021	World Energy Outlook 2021

Symbols

$\boldsymbol{\mu}$	Mean vector
$\boldsymbol{\Sigma}$	Covariance
$\mathcal{N}$	The number of years in study period
$\mathcal{P}$	Price of a product [€]
$\gamma(z_{nk})$	The responsibility that component k takes for explaining the observation of data point $\mathbf{x}_n$
$\hat{f}$	Kernel density estimator
$\hat{L}$	The maximized value of the likelihood function of the model
I_t	The additional investment-related costs in year t associated with the alternative
$\mathcal{N}$	A component of the Gaussian mixture
M_{CO_2}	The annual amount of CO_2 emissions generated from fuel combustion [t-CO_2/y]
ϕ	Kernel function
π_k	The prior probability or the mixing coefficients of the k^{th} Gaussian component
σ	Singular values
$\mathbf{S}$	Diagonal matrix of the SVD, $\mathbf{S} \in \mathbb{R}^{n \times m}$
$\mathbf{U}$	Square matrix of the SVD, $\mathbf{U} \in \mathbb{R}^{n \times n}$
$\mathbf{V}$	Square matrix of the SVD, $\mathbf{V} \in \mathbb{R}^{m \times m}$
$\mathbf{X}$	Data matrix $\mathbf{X} \in \mathbb{R}^{n \times m}$
$\mathbf{x}$	Data
AIC	Akaike Information Criterion
BIC	Bayesian Information Criterion
C_F	Carbon emission conversion factor [t-CO_2/t-Fuel]
C_j	CO_2 emissions in voyage j
D_j	Distance traveled in voyage j
H	The annual operating hours for each engine mode [h/y]
h	Bandwidth of kernel density estimator
I	Inflation rate [%]
i	The i^{th} engine mode associated with the corresponding engine load
K	Number of Gaussian component
k^{th}	The k^{th} Gaussian component
M	The total number of engine modes
n	Observations
N_k	The effective number of points assigned to cluster k
P	The engine power required for each engine mode [kW]
p	A mixture of Gaussians
r	Discount rate [%]
S_t	The savings in year t in operational costs associated with the alternative
t	Year of occurrence, $t = 0$ is the base year
CST	Construction cost [€]

EOL	End-of-life value [€]
FC	The annual fuel consumption [t-Fuel/y]
FGC	The annual fuel gas consumption [t-Fuel/y]
FOC	The annual fuel oil consumption [t-Fuel/y]
FV	Future value of the cost or benefit [€]
LOC	The annual lubricating oil consumption [t-Fuel/y]
MTN	Maintenance cost [€]
NPC	Net present cost [€]
NS	Net saving [€]
OPR	Operation cost [€]
PFC	The annual pilot fuel consumption [t-Fuel/y]
PV	Present value of the cost or benefit [€]
SFGC	The specific fuel gas consumption [g/kWh] under specific engine power output, as the function of the engine load [g/kWh]
SFOC	The specific fuel oil consumption [g/kWh] under specific engine power output, as the function of the engine load [g/kWh]
SIR	The saving-to-investment ratio of the alternative relative to the base case
SLOC	The specific lubricating oil consumption under specific engine power output [g/kWh]
SPFC	The specific pilot fuel consumption under specific engine power output [g/kWh]

Chapter 1

Introduction

This chapter draws together an overview of the research in this thesis. First of all, the essential background information and motivation are presented. Afterwards, the direction of this thesis regarding the research question, the aim and objectives are presented. Subsequently, a brief description of the appended papers is given. Finally, the structure of this thesis is outlined.

1.1 Background and motivation

Each year nearly 100,000 commercial ships move around 11 billion tons of goods around the world from port to port. With more than 80% of international goods by volume transported by sea, shipping has been playing an indispensable role in the global economy (UNCTAD, 2021). Without shipping, the vast scale of global development over the last decades would not have been possible. Albeit being considered the most efficient mode of transport per ton transported, shipping was still responsible for 2.89% of global anthropogenic greenhouse gas (GHG) emissions in 2018 (IMO, 2020). If the shipping industry had been a country, it would have been the world's sixth GHG-emitting country (Balcombe et al., 2019). Following the "Business-as-usual" scenario, by 2050, the GHG emissions from shipping are predicted to result in an increase between 90% and 130% of 2008 levels, and of up to 50% of 2018 levels (IMO, 2020).

The shipping industry is taking its first step to dramatically decarbonize itself and undergo the transition towards green shipping. In order to contribute to the ambitions of the Paris Agreement, the International Maritime Organization (IMO) laid out the Initial IMO Strategy on the reduction of GHG emissions from ships. Two main targets derived from this strategy are summarized as follows. First, to halve the international shipping annual GHG emissions by 2050, compared to the 2008 benchmark. Second, to reduce CO_2 emissions intensity by at least 40% by 2030, and pursue efforts towards 70% by 2050, compared to the 2008 benchmark (IMO, 2018). The Initial IMO GHG Strategy will be revised in the 80^{th} session of the IMO's Marine Environment Protection Committee (MEPC 80) on July 2023. Discussions are currently in progress with a target of 100%

decarbonization (i.e. net zero) by 2050 (IMO, 2022). Given such ambitious targets, the shipping industry should be well-prepared because changes are inevitable to improve the sustainability of its operations.

Similar to other sectors, there is no silver bullet for achieving the IMO emission targets. Instead, the IMO has provided a wide range of short-, mid-, and long-term measures, as shown in Table 1.1. To be simplified, these measures can be divided into the following interconnected groups: a) technical measures, b) operational measures, c) low carbon or zero carbon fuels, and d) market-based measures (MBMs) (Halim, Kirstein, Merk, & Martinez, 2018). It is perceived that a combination of these measures is needed to meet the IMO emission targets (Andersson, 2022; Balcombe et al., 2019; Bouman, Lindstad, Rialland, & Strømman, 2017; IMO, 2021b). Technical measures include the following indexes:

- The Efficiency Design Index (EEDI): Applies to new ships to promote the use of more energy-efficient equipment and engines.
- The Energy Efficiency Existing Ship Index (EEXI): Comes into force in 2023, applying to existing ships. The EEXI calculation is essentially similar to the EEDI calculation, with some changes.

Solutions for technical measures are related to emission reduction technologies adopted under the design, construction, and retrofit phases of ships, including weight reduction, hull form optimization, air lubrication, optimal propulsion systems, and waste heat recovery (Brynolf, Baldi, & Johnson, 2016) or green technologies such as wind-assisted ship propulsion (Metzger, 2022).

Operational measures include:

- The Carbon Intensity Indicator (CII): A rating scheme (A-E) to determine how efficiently a ship transports goods or passengers on an annual basis, in terms of the mass of carbon dioxide (CO_2) emitted per the annual transport work (i.e., cargo-carrying capacity and nautical mile). The CII applies to all ships above 5,000 GT.
- The Ship Energy Efficiency Management Plan (SEEMP): A management tool for assisting ship owners in improving their fleet efficiency performance.

Solutions for operational measures are associated with the operation phase of ships such as optimal handling of ships (e.g., trim and ballast optimization), voyage optimization (e.g., weather routing and slow steaming), good hull, engine, propeller maintenance and ship-port integrative solutions (e.g. just-in-time arrival) (Ölçer, 2018).

MBMs are related to carbon or emission pricing. It can be seen as a levy (also called a tax or fee) on emitted GHG emissions. Apart from the IMO MBMs, another carbon pricing mechanism is the European Union Emission Trading System (ETS), which would sponsor emission savers and punish polluters (Lagouvardou & Psaraftis, 2022; Lagouvardou, Psaraftis, & Zis, 2022).

Table 1.1: Measures for GHG reduction

Short-term Measures (2018-2023)	Mid-term Measures (2023-2030)	Long-term Measures (beyond 2030)
EEDI (Technical Measure)	Market-based Measures (MBMs)	Zero-carbon Fuel Development
EEXI (Technical Measure)		Develop other Emission Reduction Mechanisms
CII (Operational Measure)		
SEEMP (Operational Measure)		

It is believed that the shipping industry is steering its course towards Shipping 4.0 with digitalization playing a pivotal role. In this respect, Artificial Intelligence (AI), Machine Learning (ML), Data Analytics (DA), and Internet of Things (IoT) are expected to accelerate the digital transformation of the shipping industry. It is envisaged that the shipping industry will spend USD 931 million on AI-related solutions in 2022. More than a twofold increase in this number is expected in the next five years, which is equal to USD 2.7 billion by 2027, a compound annual growth rate of 23% (Palmejar & Chubb, 2022). Recently, the adoption of such technologies has been growing at a rapid pace with numerous applications. One of these applications is digitally-enabled optimization solutions that are estimated to produce up to a 38% reduction in GHG emissions by 2050 (Ricardo Energy & Environment, 2022). The use of such solutions can provide accurate vessel performance insights into speed, trim and fuel consumption. Such solutions can also be integrated into onboard decision support systems that can be served in the context of operational measures.

Taking the above into consideration, an effective operational efficiency framework is desirable to monitor a vessel's performance using a number of parameters associated with engine, weather and voyage data, detect data anomalies pertaining to sensor faults and abnormal events, provide a quantification of the vessel's operational conditions under engine and trim-draft modes and support decision making as regards vessel operational efficiency.

Simultaneously, the shipping industry is at the beginning of one of its greatest technical transformation to achieve the IMO emission targets. Apart from being a capital-intensive industry with long-life assets, shipping is relying on a global supply of energy-dense fuels. These attributes make the technical transformation complex and expensive, with one study estimating that at least $1 trillion USD in investments is needed for decarbonizing shipping (Carlo, Marc, Fuente, Smith, & Søgaard, 2020). In addition, if MBMs are implemented, the operating costs of conventional ships will rise considerably. Consequently, ship owners will have three following options for their ships: paying to offset their emissions, retrofitting or retiring their ships earlier than expected (Bourboulis, Krantz, & Mouftier, 2022). Given that most ships have more than 20 years of lifetime and almost 100,000 ships on the waters are needed to decarbonize, retrofitting the existing vessels with the latest engine technologies is drawing attention to ship owners for regulatory compliance. Besides, it is an opportunity for them to improve their fleet's environmental footprint and operational

standards.

From this perspective, an innovative dual-fuel engine is under consideration within this thesis. The dual-fuel engine can be retrofitted on existing ships as the main propulsion system. The dual-fuel engine can be run either in gas or liquid-fueled diesel operating mode. In addition, the dual-fuel engine can operate flexibly between the operating modes within certain limits, without interruption of power generation. Due to the high efficiency and the use of clean fuel (i.e. LNG), the overall emissions performance of the dual-fuel engine is improved with extremely low exhaust gas emissions in the gas mode (Wärtsilä, 2020). From the ship owner's perspective, aiming to make technology investments, there is a grey area where decision-making is made under uncertainties over the long lifetime of such an engine technology. Furthermore, the outcomes of their decisions are determined by a number of criteria, such as technical, economic, environmental, and social criteria. It is important to stress that the economic factor is of paramount importance among these criteria (Bui, Ölçer, Kitada, & Ballini, 2021).

Bearing the above in mind, it is required to develop a life-cycle cost framework to quantify the total life-cycle cost performance of the dual-fuel engine compared to that of a conventional diesel engine and reflect the uncertainties over the engines' lifespan.

1.2 Research question

The research question of this thesis is formulated as follows.

How to develop and implement a holistic strategy to enhance the operational efficiency and life-cycle economic performance in the shipping industry by utilizing ML/DA approaches for ship performance monitoring and the life-cycle cost approach for innovative emissions reduction technologies to be retrofitted on existing ships?

1.3 Research aim and objectives

The main aim of this thesis is to answer the research question above through the development of an integrated data analytics framework encompassing ML/DA methods and the life-cycle cost analysis. The integrated data analytics framework is applied for a bulk carrier with the assumption that it will be retrofitted with the dual-fuel engine technology. In order to fulfill the stated aim, the following research objectives (RO) are specified.

RO1 The development of an advanced data analytics framework (ADAF) for ship performance monitoring under localized operational conditions.

(i) Provide the ADAF with a number of data analytics approaches together with domain knowledge for ship performance quantification.

(ii) Investigate the ship's localized operational conditions, including its main engine modes and associated trim-draft modes.

(iii) Detect data anomalies existing in the data set for improving data quality.

(iv) Identify the relative correlations among ship performance and navigation parameters.

(v) Derive an operational efficiency key performance indicator (KPI), i.e. the ship performance index (SPI), for ship performance quantification in order to identify the best performance trim-draft mode under the engine modes.

RO2 The development of a life-cycle cost framework (LCCF) for the dual-fuel engine under uncertainties.

(i) Provide a methodological procedure with an engineering build-up approach for conducting the life-cycle cost analysis.

(ii) Compare the life-cycle cost performance of the dual-fuel engine with that of a conventional diesel engine by considering several economic KPIs, including the Net Present Cost (NPC), the Net Saving (NS), and the Saving-to-Investment Ratio (SIR).

(iii) Deal with uncertainties by conducting sensitivity analyses and a Monte Carlo simulation.

(iv) Assess the implications of MBMs on the life-cycle cost performances of the studied engines.

(v) Derive an environmental KPI from the environmental impact (EI) of switching over to the dual-fuel engine.

Figure 1.1 depicts the integrated data analytics framework including the two main legs (i.e. the ADAF and the LCCF), the associated objectives and the contributed papers towards the respective objectives. The two-way arrow in the figure shows that the ADAF and the operation phase of the LCCF are interconnected. Since the implementation of ADAF is showcased through the performance of a selected ship in operation, results obtained from the ship's operational conditions (i.e. engine modes) in the ADAF can be utilized by the LCCF for calculating the operation costs of the studied engines. The expected outcomes of the proposed framework are various KPIs comprising the SPI, NPC, NS, SIR, and EI that can be used as effective metrics for improving the environmental and life-cycle cost performance in shipping.

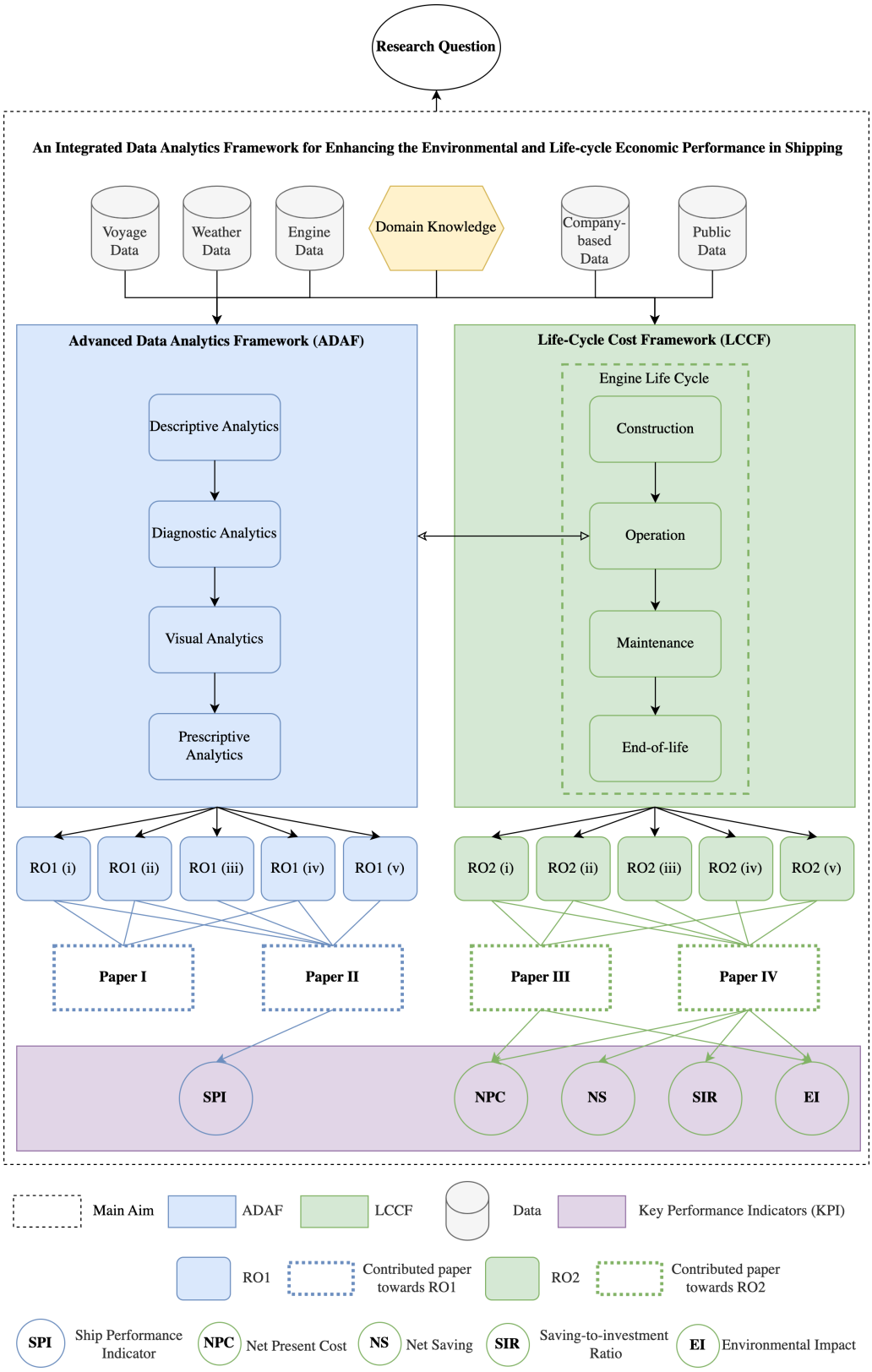

Figure 1.1: The development of the integrated data analytics framework proposed in this thesis.

1.4 Publications

Appended papers

(I) Bui, K. Q., & Perera, L. P. (2020). A Decision Support Framework for Cost-Effective and Energy-Efficient Shipping. *Proceedings of the ASME 2020 39th International Conference on Ocean, Offshore and Arctic Engineering. Volume 6A: Ocean Engineering.* Virtual, Online. August 3–7, 2020. V06AT06A026. ASME. https://doi.org/10.1115/OMAE2020-18368.

(II) Bui, K. Q., & Perera, L. P. (2021). Advanced data analytics for ship performance monitoring under localized operational conditions. *Ocean Engineering, 235*, 109392. https://doi.org/10.1016/j.oceaneng.2021.109392.

(III) Bui, K. Q., Perera, L. P., Emblemsvåg, J., & Schøyen, H. (2022). Life-Cycle Cost Analysis on a Marine Engine Innovation for Retrofit: A Comparative Study. *Proceedings of the ASME 2022 41st International Conference on Ocean, Offshore and Arctic Engineering. Volume 5A: Ocean Engineering.* Hamburg, Germany. June 5–10, 2022. V05AT06A029. ASME. https://doi.org/10.1115/OMAE2022-79488.

(IV) Bui, K. Q., Perera, L. P., & Emblemsvåg, J. (2022). Life cycle cost analysis of an innovative marine dual-fuel engine under uncertainties. *Journal of Cleaner Production, 380*, 134847. https://doi.org/10.1016/j.jclepro.2022.134847.

Published papers but not included in the thesis

1. Bui, K. Q., & Perera, L. P. (2019). The Compliance Challenges in Emissions Control Regulations to Reduce Air Pollution from Shipping. *OCEANS 2019 - Marseille*, 2019, 1-8. https://doi.org/10.1109/OCEANSE.2019.8867420.

2. Bui, K. Q., Perera, L. P., & Emblemsvåg, J. (2021). Development of a Life-cycle Cost Framework for Retrofitting Marine Engines towards Emission Reduction in Shipping. *13th IFAC Conference on Control Applications in Marine Systems, Robotics, and Vehicles CAMS 2021, 54*, 181–187. https://doi.org/10.1016/j.ifacol.2021.10.091.

3. Bui, K. Q., Ölçer, A. I., Kitada, M., & Ballini, F. (2021). Selecting technological alternatives for regulatory compliance towards emissions reduction from shipping: An integrated fuzzy multi-criteria decision-making approach under vague environment. *Proceedings of the Institution of Mechanical Engineers, Part M: Journal of Engineering for the Maritime Environment, 235*(1), 272–287. https://doi.org/10.1177/1475090220917815.

1.5 Thesis outline

Chapter 1 sets the scene of this thesis by presenting the background and motivation, research questions, research aim and objectives, and the overview of the appended papers.

The remaining parts of this thesis proceed as follows:

Part I - Context and Methodology: This part covers two chapters.

Chapter 2 presents the context of maritime decarbonization and the focus of this thesis in relation to this context. The methodology with a focus on ML and DA techniques and the life-cycle cost analysis are discussed in chapter 3.

Part II - Research Outcomes: This part is divided into three chapters.

The summary of research in light of the ADAF and the LCCF is presented in chapter 4. Discussions on the fulfillment of the research aim and objectives, research novelty, limitations, and the connection between the ADAF and the LCCF are reported in chapter 5. The conclusions outlining the concluding remarks and suggestions for future work are given in chapter 6.

Part III - Appended Papers: This part consists of the included papers within this thesis.

Part I

Context and methodology

Chapter 2

Maritime decarbonization

This chapter contextualizes the research by providing an account of maritime decarbonization. The first section gives a glimpse at air emissions from shipping. The second section attempts to classify the drivers for maritime decarbonization. The third section narrows the focus of the thesis with regard to maritime decarbonization.

2.1 Air emissions from shipping

The period from 2012 to 2018 saw an increase, i.e. from 2.76% to 2.89%, in the share of shipping emissions in global anthropogenic emissions (IMO, 2020). A consistent increase in shipping emissions has been observed since 1990, which is aligned with the increase in world seaborne trade. The biggest polluters of GHG emissions within shipping are container ships, bulk carriers, and oil tankers. This is attributed to the international and intercontinental routes, rather than the domestic ones (Balcombe et al., 2019).

Apart from that, international shipping is responsible for emitting sulphur oxides (SO_x) and nitrogen oxides (NO_x) emissions. Respectively, 13% and 15% of global anthropogenic SO_x and NO_x are ascribed to international shipping (IMO, 2014).

2.2 Drivers for maritime decarbonization

The fundamental regulation for controlling air emissions resulting from international shipping is the International Convention for the Prevention of Pollution from Ships (MARPOL) 73/78 Annex VI.

SO_x emissions are addressed in Chapter 3, Regulation 14 of MARPOL 73/78 Annex VI. Originally, the global sulphur content limit in bunker fuel was at 4.5%. In 2020, a new regulation was enforced by the IMO, capping this limit to 0.5% (Zis & Cullinane, 2020). Stricter SO_x emission limits were

set with the introduction of Emission Controlled Areas (ECA), covering the oceans and seas in Europe and North America. NO_x emissions are regulated in Chapter 3, Regulation 13 of MARPOL 73/78 Annex VI. Different NO_x emission levels, i.e., Tier I, Tier II, and Tier III, are applied to ships with different construction dates. The strictest tier, i.e. tier III offers a NO_x reduction of about 80% compared with tier I, applying only to ships in ECAs. It should be borne in mind that the introduction of ECAs contributes not only to SO_x and NO_x emissions reduction but also to GHG emissions reduction.

On top of that, GHG emissions are addressed via two measures within Chapter 4 of MARPOL 73/78 Annex VI, which entered into force on 1 January 2013 (IMO, 2011). The first one is the technical measure called the Energy Efficiency Design Index (EEDI), the second one is the operational measure namely Ship Energy Efficiency Management Plan (SEEMP Part I). The purpose of the EEDI is to facilitate technical improvements for new-built ships with a target of a 10% reduction of CO_2 levels (grams of CO_2 per tonne mile) by 2015, 20% by 2020, and 30% by 2025 respectively. The SEEMP Part I, a continuous energy efficiency improvement plan, is required to be kept on board. From 2019, through the Data Collection System (DCS), which came into force on 1 January 2019, ships above 5,000 gross tonnage are required to report their actual fuel consumption and CO_2 emissions under the SEEMP Part II. Similar to the DCS, the EU came up with the Monitoring, Reporting and Verification (MRV) scheme for fuel consumption and CO_2 emissions from ships operating within the EU, entering into force on 1 January 2018.

In 2018, the IMO announced the Initial IMO Strategy on reducing GHG emissions from international shipping with main targets of i) reducing CO_2 emissions intensity (i.e. emission per transport work) by at least 40% by 2030, with a vision of 70% by 2050, compared to the 2008 level as the benchmark; ii) reducing annual GHG emissions from ships by at least 50% by 2050 (IMO, 2018).

In the MEPC76 held in June 2021, the IMO adopted three new energy efficiency measures applicable to existing ships, entering into force from 2023. First, the SEEMP Part III, i.e. the enhanced SEEMP, will focus on continuous carbon intensity improvement and addressing the management system. Second, the Energy Efficiency Existing Ship Index (EEXI), considered the sister of the EEDI, is introduced for existing ships, requiring ships to calculate the EEXI values (i.e. attained EEXI). Such values should fall below the baseline (i.e. required EEXI) which is at the same level as required EEDI phase 2 or phase 3. In order to meet the required EEXI, ship owners can adopt several methods such as shaft/engine power limitation, utilizing alternative fuels, retrofitting with energy-saving technologies and so on (Schinas & Bergmann, 2021). Third, the Carbon Intensity Indicator (CII), a yearly score of a ship's energy efficiency, is introduced to address the operational efficiency. In this respect, all ships above 5000 GT will be required to calculate the yearly CII based on the reported IMO DCS data. The ship is then allocated a rating from A to E. For ships rated as D for three consecutive years or E in a single year, a plan of improvement actions will be required as part of the SEEMP (IMO, 2021a).

In terms of measuring shipping emissions, the GHG Fuel Standard from the IMO and the Fuel

EU Maritime from the EU are underdevelopment to provide a more comprehensive view on the environmental impacts of marine fuels. Such mechanisms are based on the well-to-wake approach, which assesses the GHG emissions from the fuel production to the end-use by a ship.

Regarding market-based measures, the IMO MBMs have been discussed, setting a price on CO_2 emissions emitted. Another market-based measure developed by the EU, called the EU ETS, has also been discussed. The EU ETS is based on the principle of 'cap-and-trade' (Lagouvardou & Psaraftis, 2022; Lagouvardou et al., 2022). It is noted that the IMO MBMs and the EU ETS have not yet entered into force.

In addition, the IMO has shown a commitment to the United Nations Sustainable Development Goals (SDGs). In particular, SDG 7 (affordable and clean energy), 12 (responsible consumption and production), and 13 (climate action) are relevant to maritime decarbonization.

Furthermore, maritime decarbonization can be attributed to the business driver. Commercial pressure is impacting ship owners in a way that they can be less attractive on the charter market due to high expectations from cargo owners and consumers. Additionally, they may experience difficulty in accessing to investors and capital (DNV, 2021). For this reason, ship owners are interested in upgrading their fleet to higher operational standards and improving their emission profiles.

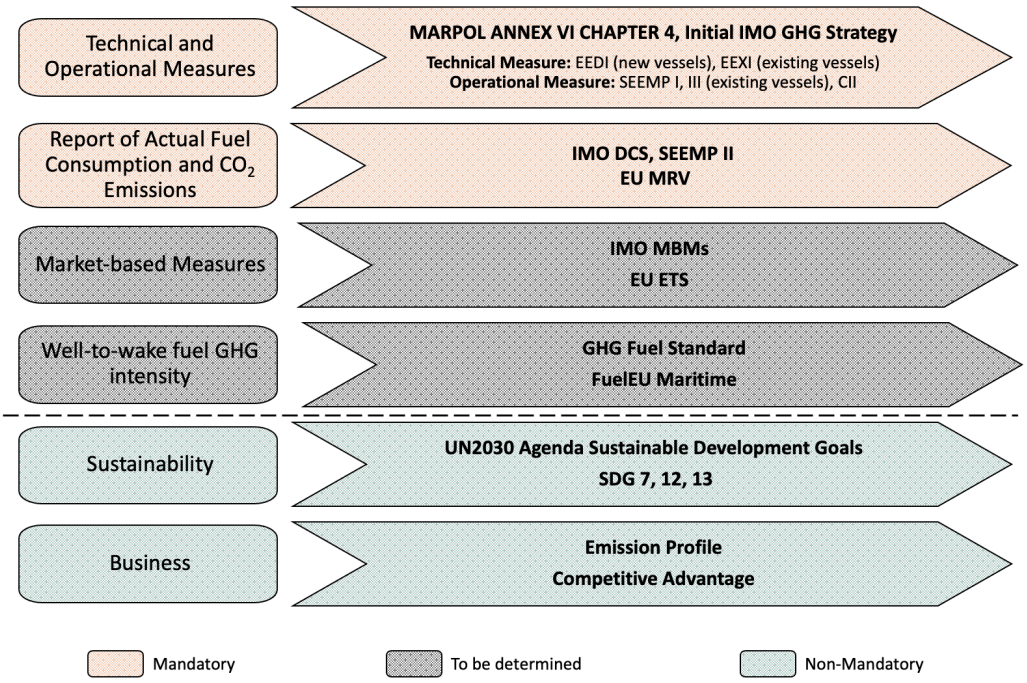

Figure 2.1: Drivers of maritime decarbonization

As schematically demonstrated in Figure 2.1, the mandatory, non-mandatory, and to-be-determined drivers are the fundamentals of maritime decarbonization, advancing the shipping industry towards

a more energy-efficient or sustainable industry. A target of achieving a carbon-neutral or zero-carbon shipping industry by 2050 is currently under discussion (IMO, 2022). In order to achieve this target, dramatic emissions reduction will be required with a paradigm change from fossil fuels to non-fossil fuels (i.e. zero-carbon fuels) such as ammonia, hydrogen, bio-fuels, green methanol (i.e. including bio-methanol and e-methanol). However, they are not yet broadly available at the moment from the technological readiness level. It will take time to the point where such zero-carbon fuels are commercially viable at the scale needed (Shell, 2020). Therefore, the zero-carbon target is arguably regarded as ambitious. This indicates a need for low-carbon fuels to be entered into the near future fuel mix used by shipping.

In this respect, LNG is leading the race with 534 new-building orders, accounting for 30.2% of the total gross tonnage on order. Currently, there are 923 LNG-fuelled ships, constituting 5.39% of the total gross tonnage of ships in operation (DNV, 2022).

2.3 How does this thesis fit into the maritime decarbonization picture?

Achieving the IMO's emission targets towards maritime decarbonization requires a broad array of solutions. This thesis is carried out with an eye to the IMO's technical and operational measures.

From the technical perspective, more recently, there have been growing interests and investments in dual-fuel engine technologies. It has been argued that dual-fuel engines are sensible options that are expected to dominate the current order book. It is attributed to the flexibility the dual-fuel engine can bring to ship owners. Retrofitting existing ships with such engine technologies should be part of solutions for maritime decarbonization, given the fact that roughly 100,000 ships on the oceans need to be decarbonized. In this regard, the assessed subject of this thesis is an innovative dual-fuel engine. When the dual-fuel engine operates in the gas mode, the exhaust gas emissions are very low. This is attributed to its high efficiency and the utilization of LNG as fuel. In the dual-fuel engine, due to the high air-fuel ratio through the lean burn combustion process, peak temperatures are reduced and lower NO_x emissions are produced (Wärtsilä, 2020).

Nonetheless, there is a trade-off between adhering to existing and soon-to-be-enforced emission regulations and investing in such an engine technology at a high cost. This is due to the fact that economic factor is the most significant contributory factor to the investment decision-making process (Bui et al., 2021). Another factor that should be considered is that a ship and its associated assets (i.e. engine and equipment) have over 20-year lifespans, adding complexity to the decision-making process. These support the notion that there is a need to evaluate the cost performance of such an engine technology over its complete life. In this respect, this thesis develops a life-cycle cost framework (LCCF) which enables decision-makers (i.e., ship-owners and investors) to investigate an investment opportunity by comparing the total costs, over time, of the dual-fuel engine versus

that of a traditional diesel engine. Indirectly, the proposed LCCF could possibly support decision-makers in investing in technologies that constitute technical measures contributing to maritime decarbonization.

From the operational perspective, emission reduction potential can also be achieved through operational measures, thus contributing to maritime decarbonization. In this respect, the operational phase is considered a fruitful area for maritime decarbonization through digitalization. The utilization of digital tools can result in up to 15% of GHG emission savings required by 2050 (DNV, 2022). In this respect, leveraging AI, ML, and DA techniques will bring immense value to decision-makers (i.e. ship-owners) with regard to energy efficiency improvement for ships in operation. Taking this into account, this thesis attempts to develop an advanced data analytics framework (ADAF) for ship performance monitoring that could be a useful aid for ship-owners.

Chapter 3

Methodology

This chapter describes the specific methods by which the ADAF and the LCCF were conducted. With respect to the ADAF, ML and DA techniques for ship performance monitoring are presented in the first section. In terms of the LCCF, the life-cycle cost method to estimate the life-cycle cost of the dual-fuel engine is demonstrated in the second section.

3.1 Machine Learning (ML) and Data Analytics (DA)

ML is a sub-field of AI that enables models to operate autonomously without explicit programming. With the use of data and algorithms to mimic human's manners, the accuracy of models is gradually improved. In this respect, models are trained to make clustering, classifications or predictions, and to reveal important insights that can drive decision-making.

Generally, ML can be grouped into supervised and unsupervised learning. In supervised learning, the labels of data sets are given. Such labels are used to train the models to produce the desired output. Supervised learning is applied for either classification or regression purposes. While classification deals with predicting the value of discrete variables, regression attempts to predict the value of a continuous variable (Ayodele, 2010). However, the implementation of supervised learning techniques lies beyond the scope of this thesis.

Unlike supervised learning, unsupervised learning does not have labels for data sets. The models aim to uncover hidden patterns or data grouping without mapping between inputs and known outputs. Unsupervised learning is capable of discovering similarities and differences in properties within the data set. One of the common unsupervised learning approaches is data clustering which processes raw, unclassified data into groups described by patterns in the information (Bishop, 2006).

The following will attempt to introduce relevant unsupervised learning techniques used in this thesis for ship performance monitoring.

3.1.1 Kernel Density Estimation (KDE)

KDE is a useful technique to show a sense of what the underlying distribution looks like for a given data set. KDE, a non-parametric technique, is able to estimate the probability density function from the data set by weighting the distances of observations from a particular point. Given a sample of n observations $\mathbf{x} = \{\mathbf{x}_1, ..., \mathbf{x}_n\}$. The kernel density estimator can be expressed mathematically as follows (Silverman, 2017).

$$\hat{f}(\mathbf{x}) = \frac{1}{nh} \sum_{i=1}^{n} \phi \left(\frac{\mathbf{x} - \mathbf{x}_i}{h} \right) \tag{3.1}$$

where ϕ represents the kernel function and h is the bandwidth. In this thesis, ϕ is the Gaussian kernel.

3.1.2 Gaussian Mixture Models (GMMs)

GMMs relate to the probabilistic clustering method, which involves density estimation or 'soft' clustering. Data points are grouped according to the likelihood that they belong to a specific distribution. GMMs formulate an unspecified number of probability distribution functions and find out which Gaussian or probability distribution a given data point belongs to. Since the parameters of such distribution (i.e., the mean and variance) are unknown, it is assumed that a latent variable exists to cluster data points adequately. The Expectation-Maximization (EM) algorithm is used to estimate the assignment probabilities for a given data point to a specific data cluster.

The Gaussian distribution of a d-dimensional vector $\mathbf{x}$ takes the form (Bishop, 2006)

$$\mathcal{N}(\mathbf{x}|\boldsymbol{\mu}, \boldsymbol{\Sigma}) = \frac{1}{(2\pi)^{d/2}\sqrt{|\boldsymbol{\Sigma}|}} exp \left(-\frac{1}{2}(\mathbf{x} - \boldsymbol{\mu})^T \boldsymbol{\Sigma}^{-1} (\mathbf{x} - \boldsymbol{\mu}) \right) \tag{3.2}$$

where $\boldsymbol{\mu}$ is the mean vector and $\boldsymbol{\Sigma}$ is the covariance matrix.

The Gaussian mixture distribution can be expressed by a linear superposition of K Gaussian densities

$$p(\mathbf{x}) = \sum_{k=1}^{K} \pi_k \mathcal{N}(\mathbf{x}|\boldsymbol{\mu}_k, \boldsymbol{\Sigma}_k) \tag{3.3}$$

which is called a mixture of Gaussians where each Gaussian density $\mathcal{N}(\mathbf{x}|\boldsymbol{\mu}_k, \boldsymbol{\Sigma}_k)$ is a component of the mixture with its mean vector $\boldsymbol{\mu}_k$ and covariance $\boldsymbol{\Sigma}_k$ for the k^{th} Gaussian component, π_k is the prior probability of the k^{th} Gaussian. π_k is also called the mixing coefficients with the constraint that $\sum_{k=1}^{K} \pi_k = 1$.

EM algorithm for Gaussian Mixtures

Given Eq. (3.3), the log of the likelihood function can be defined as

$$ln\ p(\mathbf{X}|\pi,\boldsymbol{\mu},\boldsymbol{\Sigma}) = \sum_{n=1}^{N} ln\left(\sum_{k=1}^{K}\pi_k\mathcal{N}(\mathbf{x}_n|\boldsymbol{\mu}_k,\boldsymbol{\Sigma}_k)\right) \tag{3.4}$$

The expectation-maximization (EM) algorithm is used to find maximum likelihood solutions for the Gaussian mixture model as regards the parameters, including the means $\boldsymbol{\mu}_k$, the covariances of the components $\boldsymbol{\Sigma}_k$, and the mixing coefficients π_k.

- Step 1: Initialize $\boldsymbol{\mu}_k$, $\boldsymbol{\Sigma}_k$, π_k, and evaluate the log likelihood function.
- Step 2 (E-step): Evaluate the responsibilities $\gamma(z_{nk})$ by using the current parameter values. $\gamma(z_{nk})$ is given by

$$\gamma(z_{nk}) = \frac{\pi_k\mathcal{N}(\mathbf{x}_n|\boldsymbol{\mu}_k,\boldsymbol{\Sigma}_k)}{\sum_{j=1}^{K}\pi_j\mathcal{N}(\mathbf{x}_n|\boldsymbol{\mu}_j,\boldsymbol{\Sigma}_j)} \tag{3.5}$$

  $\gamma(z_{nk})$ is the responsibility that component k has for explaining the observation of data point $\mathbf{x}_n$.

- Step 3 (M-step): Re-estimate the parameters by using the current responsibilities

$$\mu_k^{new} = \frac{1}{N_k}\sum_{n=1}^{N}\gamma(z_{nk})\mathbf{x}_n \tag{3.6}$$

$$\gamma_k^{new} = \frac{1}{N_k}\sum_{n=1}^{N}\gamma(z_{nk})(\mathbf{x}_n-\mu_k^{new})(\mathbf{x}_n-\mu_k^{new})^T \tag{3.7}$$

$$\pi_k^{new} = \frac{N_k}{N} \tag{3.8}$$

  where

$$N_k = \sum_{n=1}^{N}\gamma(z_{nk}) \tag{3.9}$$

  N_k can be viewed as the effective number of points assigned to cluster k

- Step 4: Evaluate the log likelihood function

$$ln\ p(\mathbf{X}|\pi,\boldsymbol{\mu},\boldsymbol{\Sigma}) = \sum_{n=1}^{N} ln\left(\sum_{k=1}^{K}\pi_k\mathcal{N}(\mathbf{x}_n|\boldsymbol{\mu}_k,\boldsymbol{\Sigma}_k)\right) \tag{3.10}$$

and check for convergence of either the parameters or the log likelihood function. If not, return to Step 2.

3.1.3 Finding the optimal number of clusters

The GMMs are required to specify the number of components K. Several techniques can be used to find the most likely number of components K. The silhouette metric is unreliable if the clusters are not spherical or have different sizes, shapes, and orientations. Another approach is to find the model that minimizes a theoretical criterion information such as the Bayesian Information Criterion (BIC) or the Akaike Information Criterion (AIC) (Akaike, 1974; Schwarz, 1978).

$$BIC = ln\ (n)m - 2\ ln\ (\hat{L}) \tag{3.11}$$

$$AIC = 2m - 2\ ln\ (\hat{L}) \tag{3.12}$$

where n is the number of observations, m is the number of parameters learned by the model, $\hat{L}$ is the maximized value of the likelihood function of the model. The most likely number of components (i.e. the number of clusters) is the one with the lowest BIC and AIC values.

3.1.4 Data anomaly detection

"Garbage in - garbage out" is a classic saying about the importance of the quality of input data in ML models (Pyle, 1999). It is therefore important to prepare high-quality data to employ a ML implementation free of errors. This can be achieved through data anomaly detection which relates to detecting anomalies or outliers that deviate strongly from the norm. Removing such data anomalies before training the model can greatly enhance the performance of the resulting model.

This thesis deals with data anomaly detection by two approaches. The first one is a limit check approach based on the minimum-maximum values (Isermann, 2006; Perera, 2016). In this regard, the minimum and maximum values of the parameters in the data set are defined by domain knowledge. Such values normally express the general range of the parameters. Data points will be flagged as outliers and be removed if they are out of the defined minimum and maximum thresholds.

The second approach is based on Singular Value Decomposition (SVD), which is a numerically robust matrix decomposition technique (Brunton & Kutz, 2019). Given a time-series data set $\mathbf{X} \in \mathbb{R}^{n \times m}$ (n is the number of observations, m is the number of parameters and $n > m$), the SVD is a unique matrix decomposition, given by

$$\mathbf{X} = \mathbf{U}\mathbf{S}\mathbf{V}^{\top} \tag{3.13}$$

where $\mathbf{U} \in \mathbb{R}^{n \times n}$ is a square matrix, the column of $\mathbf{U}$ are called the left-singular vectors. $\mathbf{V} \in \mathbb{R}^{m \times m}$ is a square matrix, the column of $\mathbf{V}$ are called the right-singular vectors. $\mathbf{S} \in \mathbb{R}^{n \times m}$ is diagonal, hierarchically ordered with singular values $\sigma_i, i = 1, ..., m$. The singular values are sorted from

largest to smallest $\sigma_1 \geqslant \sigma_2 \geqslant ...\sigma_m \geqslant 0$.

The SVD is closely associated with an eigenvalue problem in terms of the correlation matrix $\mathbf{X}^\top\mathbf{X}$ (i.e. the normalized covariance matrix). The SVD formula can be rewritten as follows.

$$\mathbf{X}^\top\mathbf{X} = \mathbf{V}\hat{\mathbf{S}}^2\mathbf{V}^\top \implies \mathbf{X}^\top\mathbf{X}\mathbf{V} = \mathbf{V}\hat{\mathbf{S}}^2 \tag{3.14}$$

The intuition behind the SVD is that it takes a high-dimensional data set and reduces it into a lower dimensional space that extracts the substructure of the original data intuitively. It can be seen from Equation (3.14), the columns of $\mathbf{V}$ (i.e. the right-singular vectors) are eigenvectors of the correlation matrix $\mathbf{X}^\top\mathbf{X}$. For this reason, the columns of $\mathbf{V}$ are the principal directions for projections of the original data onto a linear subspace. Furthermore, the hierarchical representation of the data in the new subspace is arranged by the dominant features within the data from the most variation to the least variation. Therefore, the top singular vectors capture the most important combination of the data. In contrast, the bottom singular vectors represent the least important combination of the data. In this respect, data anomalies can be observed in such bottom singular vectors.

3.1.5 Identifying the relative correlations among parameters

The following is a brief description of a technique for visualizing high dimensional data. The structure of a data cluster in a high-dimensional space can be properly visualized by a set of singular vectors (SVs) through SVD. By doing this, the relative relationships or correlations among parameters within a data cluster can be explored. As depicted in Figure 3.1, there are three SVs Z_1, Z_2 and Z_3 expressed by dotted circles in descending order from the outermost circle to the innermost one. The singular values associated with the SVs, which express the descending variance directions, can be used to form colored circles on each SV circle. In this regard, the relative correlations among parameters (X_1, X_2 and X_3) can be perceived through the size and color of each colored circle. The color of each colored circle shows the positive correlation (in red) and negative correlations (in blue). The size of each colored circle represents how significant the correlation is. An example of such correlations among parameters can be observed in the top singular vector Z_1, where parameter X_2 increases considerably while parameter X_2 decreases considerably. It can also be seen from the top singular vector that there is a decrease in parameter X_1.

It is important to stress that the most useful information extracted from the parameter correlations is accommodated in the top singular vector Z_1 (i.e. expresses the greatest variance direction). In contrast, the bottom singular vector Z_3, i.e. expresses the smallest variance direction, may provide insignificant parameter correlations.

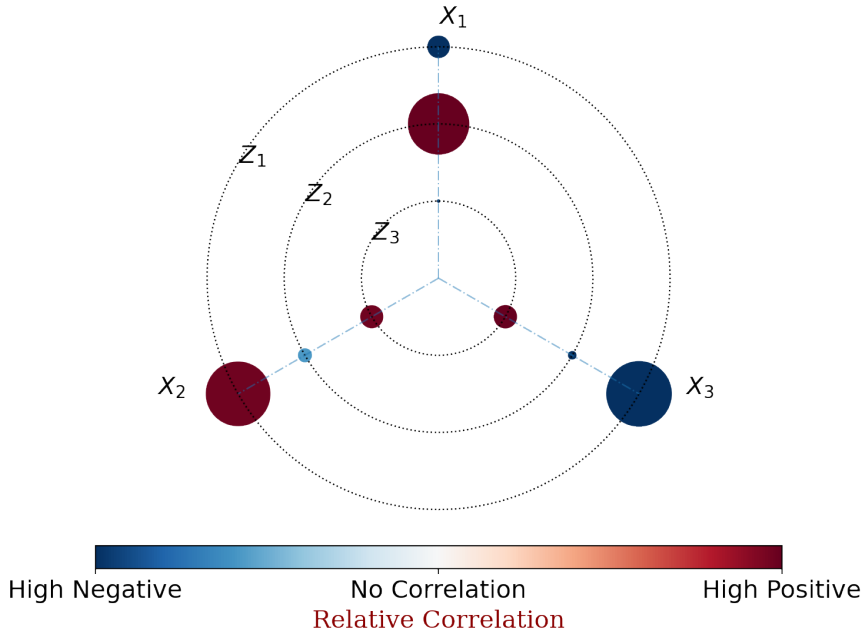

Figure 3.1: Visual analytics on a high dimensional singular vector space

3.2 Life-cycle cost analysis (LCCA)

As decarbonization technologies are under development at a rapid pace, there are tremendous opportunities for existing ships to be retrofitted with such technologies. Sound economic decisions on technological investments are important for decision-makers (i.e. ship-owners) to improve their environmental profiles and efficiency performance. When the capital cost of an innovative technology is increased, LCCA can identify whether such technologies are economically justified by looking into reduced operational costs and other cost implications throughout the technology's lifespan.

LCCA, originally introduced in the 1960s by the US Department of Defence Sherif and Kolarik (1981), is an economic technique for evaluating the life-cycle costs of an asset, product, or system over its lifetime, from raw material acquisition to salvage by determining environmental impacts and assigning monetary values Cheremisinoff (2016); Rödger, Kjær, and Pagoropoulos (2018).

LCCA represents an effective tool for any capital investment decision where higher initial costs are exchanged for reduced future costs. LCCA offers a considerably better assessment of the cost effectiveness of a product in the long term compared with other economic methods that deal with first costs or operating-related costs in the short term.

The payback method is one of the popular methods for economic analysis. However, there are certain drawbacks associated with the use of the payback method. It is concerned with when the initial investment will be recovered. In addition, costs and savings occurring after the time when

payback is reached are not taken into consideration. Alternatives can have different useful lives, which is not addressed by the payback method. It also uses an arbitrary threshold. Furthermore, the time value of money is not included when the future stream of savings is compared with the initial investment cost. In contrast to the payback method, LCCA is a powerful method which tabulates the costs, revenues and savings that a project is expected to generate, taking into account the effects of the time value of money. Furthermore, it provides measures of long-term economic performance or profitability Kneifel and Webb (2022). Due to the nature of LCCA with long-term considerations, in-depth data information is needed. Moreover, understanding of discounted cash flow and inflation is required.

3.2.1 Inflation and discounting

In LCCA, the monetary flows occur at different points in time because all the costs are accumulated throughout a lifespan. As such, one should consider the two following aspects.

The first accounts for the change in the purchasing power of currency over time, a concept known as inflation. For example, one dollar in 2000 has a different value than one dollar in 2022. Another example is that all the costs in the ship building sector such as steel, labor, fuel, and taxes are probably increased over time. This is attributable to the market dynamics. Therefore, all the costs need to be adjusted to a chosen base year using an inflation rate. With an inflation rate I, the price $\mathcal{P}$ of a product at time t (in years) can be calculated as expressed in Equation (3.15)

$$\mathcal{P}(t) = (1 + I)^t \times \mathcal{P}(0) \tag{3.15}$$

where $\mathcal{P}(0)$ is the price at the base year ($t = 0$).

The second relates to discounting, which translates future costs into today's equivalent. In other words, future costs will need to be adjusted for what is called the time value of money. It means that a given amount of money today is more valuable than the same amount of money in the future. The adjustment is necessary to identify present values because future costs occur at different times. This can be done by using a chosen discount rate. All future costs are adjusted to present value with the help of the following equation.

$$PV = FV \frac{1}{(1 + r)^t} \tag{3.16}$$

where PV is the present value of the cost or benefit [€], FV is the future value of the cost or benefit [€], r is the discount rate [%], and t is the year of occurrence (where $t = 0$ is the base year).

3.2.2 Cost components included in the LCCA

In this thesis, key cost components in the LCCA include initial construction costs and all relevant future costs related to operation, required maintenance, possible part replacement, and disposal, as

shown in Figure 3.2. Since the engines will be recycled, the disposal costs are the residual values of the engines at the end of their life cycles.

As shown by the color scheme in Figure 3.2, the cost components can be classified into internal and external costs. The internal costs are borne by actors directly connected with the life cycle phases of the engines, i.e., construction, operation, maintenance, and end-of-life. The scope of the LCCA conducted in this thesis is expanded with the inclusion of the external costs, i.e. carbon emissions costs, resulting from air pollution emitted from the engines. The cost components are briefly described in Table 3.1 and further elaborated as follows.

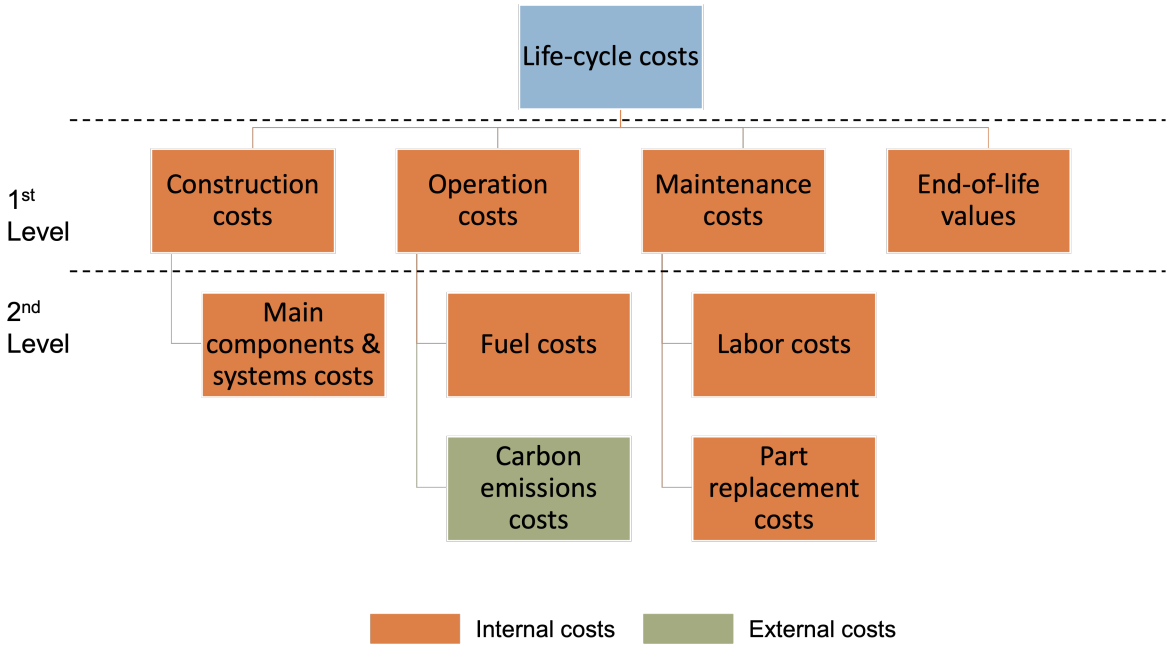

Figure 3.2: Scope of costs.

Construction costs

In order to have an overview of the construction costs of the studied engines, it is recommended to use an Engine Breakdown Structure (EBS) of a traditional diesel engine as a basis, as presented in Table 3.2. In connection with the construction costs shown in Figure 3.2, the EBS provides every cost component of these engines with a high level of detail. The fuel injection systems of these engines are different because the dual-fuel engine has a fuel gas system on top of a fuel oil system. In addition, the dual-fuel engine does not need the Selective Catalytic Reduction (SCR) technology to achieve the NO_x limits set by the IMO Tier III because of low emissions when running in the gas mode.

Table 3.1: Description of the cost components.

Cost component	Description
Construction costs	The construction expenses, i.e. the costs of the main components and systems of the engines.
Operation costs	The expenses borne by the engines' routine operations, i.e., fuel costs.
External costs	Carbon emission costs, i.e., the costs of emitting CO_2 equivalent emissions
Maintenance costs	The costs for preventive maintenance tasks in a regular basis recommended by O&MM
Labor costs	Labor costs for doing the maintenance tasks
Part replacement costs	The costs of replacing engine component's parts
End-of-life values	The residual values of the engines at the end of their lives

O&MMs: Operation & Maintenance Manuals obtained from the engine manufacturer.

Table 3.2: A general Engine Breakdown Structure (EBS). Table from Paper IV.

2nd Level	3rd Level	Cost	
		Diesel Engine	Dual-fuel Engine
Main components & systems	Engine Basement		
	Camshaft & Valve Mechanism		
	Fuel Injection System		
	Turbocharging & Scavenging System		
	Ancillary System		
	Automation System		
	Low-value Parts		
	Exhaust Gas Cleaning System*		N/A
	Total	989K	1,200K

* Selective Catalytic Reduction (SCR) technology for NO_x reduction. The SCR cost for the diesel engine was adopted from the International Association for Catalytic Control of Ship Emissions to Air (IACCSEA) (IACCSEA, n.d.). SCR is not required for the dual-fuel engine. Other costs were obtained from the engine manufacturer (Wärtsilä, 2021b).
Unit K = 1000 €.

Operation costs

Fuel costs are considered the most significant contributory factor to a ship's voyage costs, constituting about two-thirds of the total (Stopford, 2009). In the case of a large container ship, it accounts for roughly three-quarters of the operating cost when bunker fuel price is about 500 USD per ton (Ronen, 2011). For this reason, throughout the LCCA conducted in this thesis considering the

internal costs, the operation costs refer to fuel costs. Such costs are influenced by fuel consumption and lubricating oil consumption. The following are formulae for calculating the total annual fuel oil consumption (FOC) and the total annual lubricating oil consumption (LOC) H. Wang, Oguz, Jeong, and Zhou (2019).

$$FOC = \sum_{i=1}^{M} P_i \times SFOC_i \times H_i \tag{3.17}$$

$$LOC = \sum_{i=1}^{M} P_i \times SLOC_i \times H_i \tag{3.18}$$

where FOC is the annual fuel oil consumption [t-Fuel/y], P is the engine power required for each engine mode [kW], SFOC is the specific fuel oil consumption [g/kWh] under specific engine power output, as the function of the engine load [g/kWh], H is the annual operating hours for each engine mode [h/y], i is the i^{th} engine mode associated with the corresponding engine load, LOC is the annual lubricating oil consumption [t-Fuel/y], SLOC is the specific lubricating oil consumption under specific engine power output [g/kWh], and M is the total number of engine modes.

As far as the diesel engine is concerned, the annual FOC and LOC can be determined with the help of Equation (3.17) and Equation (3.18).

With respect to the dual-fuel engine, it can run in either liquid-fueled diesel mode or gas mode. The engine operates based on the lean-burn Otto principle in the gas mode. In this respect, there is a lean premixed air-gas mixture in the combustion chamber. The mixture of air and gas in the cylinder has more air than it is required to complete combustion, thereby reducing peak temperatures. The mixture is ignited with a small amount of diesel fuel, i.e. pilot injection. The main fuel in the gas mode is LNG (Wärtsilä, 2020). The total annual fuel gas consumption (FGC) is defined by the following formula.

$$FGC = \sum_{i=1}^{M} P_i \times SFGC_i \times H_i \tag{3.19}$$

where FCG is the annual fuel gas consumption [t-Fuel/y], and SFGC is the specific fuel gas consumption [g/kWh] under specific engine power output, as the function of the engine load [g/kWh].

For the total annual pilot fuel consumption (PFC), the calculation can be done by using Equation (3.17). In the diesel mode, the operating principle is identical to the normal diesel concept. Therefore, the total FOC and LOC of the dual-fuel engine can be calculated by using Equation (3.17) and Equation (3.18).

Carbon emissions costs

The carbon emissions costs are the external costs that are anticipated to be internalized in the near future. This stems from recent MBMs which apply the 'polluter pay' principle on emitted CO_2 equivalent emissions. These costs are monetized for quantification in the LCCA in the case of carbon pricing. To do so, this thesis captures the latest carbon pricing data from World Energy Outlook 2021 (WEO2021). Apart from that, it is required to calculate the CO_2 emissions released during the combustion of fuels, as defined in Equation (3.20).

$$\mathsf{M}_{CO_2} = FC \times C_F \tag{3.20}$$

where M_{CO_2} is the annual amount of CO_2 emissions emitted during fuel combustion [t-CO_2/y], FC is the annual fuel consumption [t-Fuel/y], and C_F is carbon emission conversion factor [t-CO_2/t-Fuel].

Maintenance costs

The main components and systems of these engines, which correspond to the third level of the EBS as shown in Table 3.2, consist of various parts that need to be regularly maintained according to the O&MMs given by the engine manufacturer. The O&MMs document is a scheduled maintenance plan that contains information about the maintenance intervals and the maintenance tasks for numerous parts of the engines' main components and systems. The maintenance tasks include a wide range of activities: Check/ Inspect, Check oil sample, Clean, Maintain, Replace, and Overhaul. Such maintenance tasks are normally performed by either crew members on board or technical personnel from the engine manufacturer.

There are two types of costs falling under the maintenance costs, which are: (1) the labor costs for doing the maintenance tasks and (2) the part replacement costs.

- The labor costs: The labor costs are attributed to several factors, as depicted in Figure 3.3. The maintenance intervals vary depending on the fuel type and the annual operating hours. The maintenance hour consumption for doing the maintenance tasks was acquired by using questionnaires and conducting in-depth interviews with crew members (Chief Engineers, Engine Officers) who have at least 5-year ocean-going experience.

- The part replacement costs: The costs of part replacement (i.e. spare part) recommended by the O&MMs. Estimating these costs can be done by doing several interviews with a Technical Manager and Chief Engineers from various shipping companies. By using their domain knowledge together with an analogous cost estimation technique to find similarities between engines in a historical database, the part replacement costs can be obtained with a reasonable estimation.

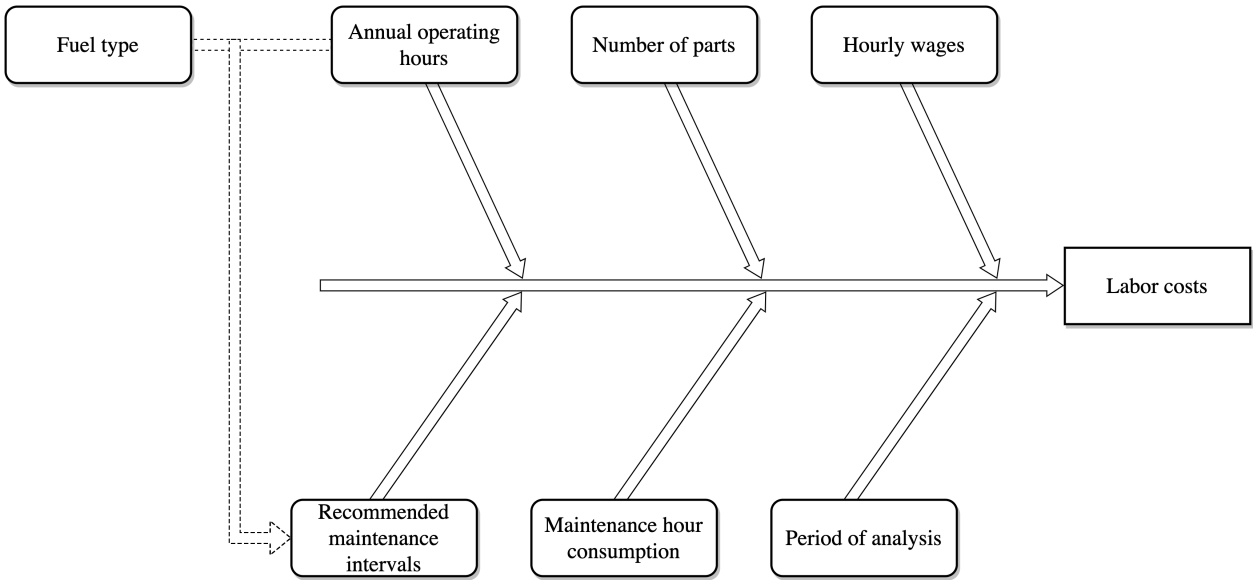

Figure 3.3: Factors contributing to the labor costs

End-of-life values

The engines will undergo the disposal and recycling process when they reach the final point of their lives. The end-of-life values are the benefits gained at this point when the materials used in the engines and the associated components can be recycled.

3.2.3 Net present cost (NPC)

Net present cost or the total present value cost is the total cost of constructing, operating, maintaining, replacing, and disposing of an engine over a given study period (i.e. the entire lifetime of the engine), adjusted for the time value of money. The NPC formula can be expressed as follows.

$$NPC = PV(CST) + PV(OPR) + PV(MTN) - PV(EOL) \tag{3.21}$$

where CST is the construction cost [€], OPR is the operation cost [€], MTN is the maintenance cost [€], and EOL is the end-of-life value [€].

The NPC for the alternative (i.e. the dual-fuel engine) and the base case (i.e. the diesel engine) are computed and compared to determine which engine is more cost-effective, i.e. the one with the lowest NPC.

3.2.4 Measures of economic performance

In line with the NPC, Net saving (NS) and Saving-to-investment Ratio (SIR) are the measures of economic performance. Both of them are calculated under the same stream of costs and savings

over the same study period. The NS method is used when benefits are mainly derived from future operational cost reductions. The NS is expressed by the net amount, in present value terms, that an alternative is expected to save over the study period. The NS for an alternative, relative to a base case, can be calculated from the difference between the NPC of the base case and the NPC of the alternative, as expressed as follows.

$$NS = NPC_{BaseCase} - NPC_{Alternative} \tag{3.22}$$

An alternative investment is considered cost-effective if its NS is greater than zero. This also means that the NPC of the alternative is lower than the NPC of the base case. Therefore, the NPC and NS methods are interconnected and can be used interchangeably.

The SIR represents the relation between the savings of the alternative and its increased investment cost, expressed in present value terms, as a ratio. It is an alteration of the benefit-cost ratio under a condition that benefits occur mainly in the form of operational cost reductions Kneifel and Webb (2022). The following is the general formula for the SIR

$$SIR = \sum_{t=0}^{\mathcal{N}} \frac{S_t}{(1+r)^t} \Bigg/ \sum_{t=0}^{\mathcal{N}} \frac{\Delta I_t}{(1+r)^t} \tag{3.23}$$

where SIR is the saving-to-investment ratio of the alternative relative to the base case, S_t is the savings in year t in operational costs associated with the alternative, ΔI_t is the additional investment-related costs in year t associated with the alternative, t is the year of occurrence (where $t = 0$ is the base year), r is the discount rate, and $\mathcal{N}$ is the number of years in the study period.

An alternative investment is considered economically justified compared to the base case if its SIR is greater than 1.0. This is equivalent to acquiring its NS greater than zero.

3.2.5 Data collection

Gathering reliable data is essential during the course of the LCCA in this thesis. The research data needed for the LCCA can be divided into three main categories: a) Company-based data source, b) Public database, and c) Indirectly derived data, as presented in Table 3.3.

- Company-based data source: Accessing the data in this category requires collaboration with an engine manufacturer (i.e. Wärtsilä). It should be noted that some of the data can be confidential.
- Public database: Several public databases can be used for obtaining market prices for fuels, material recycling, discount rate, inflation rate, and currency exchange rates. It is necessary to check the database with regard to comprehensiveness and validity for the studied region, currency, and time period.

Table 3.3: Data categories and sources.

Category	Source
Company-based data source	
Construction costs	(Wärtsilä, 2021a)
Operational profile	Wärtsilä
Engine technical data	Wärtsilä (n.d.)
Maintenance schedule (O&MMs)	Wärtsilä
Engine materials	Wärtsilä
Engine weights	Engine Product Guide Wärtsilä (2020); Wärtsilä (2021b)
Public database	
Material recycling rates	(Greengate Metals, n.d.)
Marine fuel (gas, oil) prices	Global Maritime Hub (2021); Ship & Bunker (2021)
Wages	Eurostat (2022a)
Currency exchange rates	xe.com/currencyconverter
Discount rate	Hunkeler, Lichtenvort, and Rebitzer (2008); Rödger et al. (2018)
Inflation rate	Eurostat (2022b); The World Bank (n.d.)
Expert knowledge-based data	
Maintenance hour consumption	Questionnaires & Interviews
Part replacement costs	Interviews

O&MMs: Operation & Maintenance Manuals.

- Expert knowledge-based data: In this category, questionnaires and interviews were conducted to gain domain knowledge from experts for calculating the maintenance costs.

3.2.6 Dealing with uncertainty

Assumptions regarding future cost behaviors are always made in LCCA. For this reason, it is required to include considerations of uncertainty in LCCA. The level of uncertainty relies on the quality of available data, pricing assumptions, the robustness of the defined scope, cost estimation methods, and many other factors that can impact the final outcomes (ISO, 2017).

In the literature, two types of approaches for dealing with uncertainty exist: deterministic and probabilistic approaches. The deterministic approaches are based on single-value input variables. As such, they examine the impacts on the outcomes by varying one or a combination of key uncertain variables one at a time. The results reveal how changes in an uncertain variable can affect the outcomes, while keeping all the others unchanged. The probabilistic approaches offer a more complete consideration of the uncertainty in input variables than the deterministic approaches by considering the probabilities associated with different outcomes.

In the LCCA conducted in this thesis, scenario sensitivity analysis, which falls under the deterministic approach, is undertaken. This can be achieved by varying uncertain variables, one at a time and recalculating the NPC, NS and SIR. The degree of uncertainty can be found by assessing the

resulting changes.

Regarding the probabilistic approaches, Monte Carlo simulation is performed to model the probabilities of different possible outcomes of the NPC that cannot easily be predicted due to the intervention of uncertain variables. This can be done by 'random sampling', which generates multiple possible outcomes and calculates the average result. Performing the Monte Carlo simulation in this thesis is done through the use of the @RISK software involving the three following steps. Firstly, a life-cycle cost model is developed to predict the NPC. Secondly, it is required to model uncertain variables by using triangular distributions. In this regard, a range of likely values is assigned to uncertain variables. Thirdly, the simulation is run repeatedly to calculate the NPC outcomes using a different set of random values from the triangular distributions. As a result, the probability distributions of the NPC outcomes can be produced in the cost prediction model. A key strength of the Monte Carlo simulation is that it allows the assessment of simultaneous changes in uncertain variables with respect to a probability distribution of the NPC.

Part II

Research outcomes

Chapter 4

Summary of research

In this chapter, the appended papers are summarized. The first section presents the ADAF for ship performance monitoring under localized operational conditions. In this respect, the findings from Paper I and II are summarized. Afterwards, the LCCF for an innovative engine technology under uncertainties is demonstrated, followed by the findings from Paper III and IV.

4.1 ADAF for ship performance monitoring under localized operational conditions

In this section, the proposed ADAF for ship performance monitoring under localized operational conditions is presented. The ADAF was applied to a data set collected from a bulk carrier. This is a time-series data set of 3 years with a sampling rate of 15 min. The ship's principal particulars are shown in Table 4.1. The data set contains twelve ship performance and navigation parameters with respect to voyage, weather, and engine data, as shown in Table 4.2.

Table 4.1: Ship particulars.

Feature	Value [Unit]
Ship length	225 [m]
Beam	33 [m]
Gross tonnage	38.889 [N/A]
Deadweight at max draft	72.562 [Ton]
2-stroke Main Engine with maximum continuous rating (MCR)	7564 [kW]
Main Engine - shaft rotational speed	105 [rpm]
2 Auxiliary engines with MCR	850 [kW]
Auxiliary engines - shaft rotational speed	800 [rpm]
Fixed pitch propeller with 6.20 [m] in diameter and four blades	

Table 4.2: Ship performance and navigation parameters.

Parameter	Unit
Auxiliary (Aux) fuel consumption (cons)	[Ton/day]
Main Engine (ME) fuel consumption (cons)	[Ton/day]
Auxiliary (Aux) power	[kW]
Main Engine (ME) power	[kW]
Shaft speed	[rpm]
Relative (Rel) wind speed	[m/s]
Relative (Rel) wind direction (dir)	[deg]
Course	[deg]
Speed over ground (SOG)	[Knots]
Speed through water (STW)	[Knots]
Trim	[m]
Average (Avg) draft	[m]

Paper I: A Decision Support Framework for Cost-effective and Energy-efficient Shipping

Paper I is a background study that presents an overview of the proposed framework integrating the ADAF and the LCCF. The discussion on the LCCF in this paper was still in its infancy. From the ADAF perspective, the paper developed a digital model for data clustering. The GMMs were deployed to cluster the engine representations that reflect the engine operating modes. The performance of the GMMs is dependent on determining the number of components (i.e. number of clusters). In order to have an initial understanding on the number of clusters, the KDE was employed to provide a smooth representation of the underlying probability density function of the data. In addition, the number of clusters can be determined with the help of domain knowledge. It can be seen from Figure 4.1 that three data clusters (A_1, A_2 and A_3) are generated through the implementation of the KDE and the GMMs. Such data clusters are equivalent to three engine modes the ship operated. Data cluster A_2, among other clusters, is considered the transient mode of the engine.

Further investigation on the ship's operational conditions on a local scale can be done through data clustering of data cluster A_1 under trim-draft conditions. Figure 4.2 illustrates two data clusters A_{11} and A_{12}, expressing trim-draft modes with respect to data cluster A_1.

Furthermore, visual analytics was embedded in the ADAF presented in this paper. The visual analytics aimed to discover the relative relationships or correlations among parameters within each cluster. The results of the visual analytics for data cluster A_{12} under trim-draft mode are demonstrated in Figure 4.3. The results can be illustrated briefly as follows. The top singular vector demonstrates an increase in the shaft speed and the main engine (ME) power. The second singular

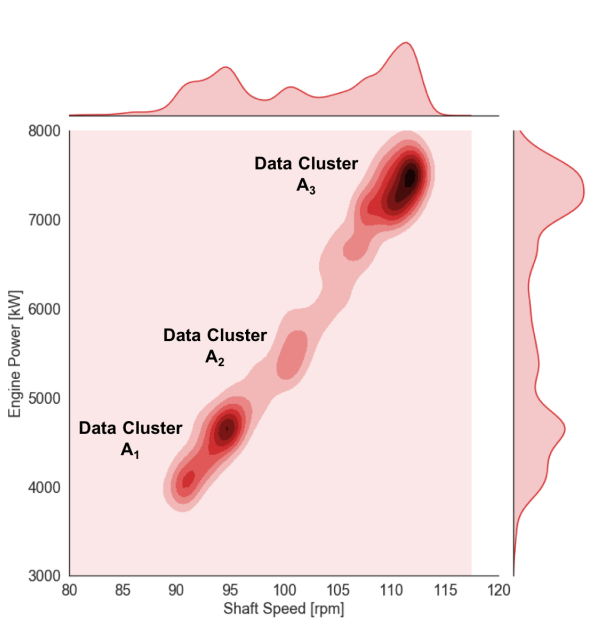

(a) KDE implementation.

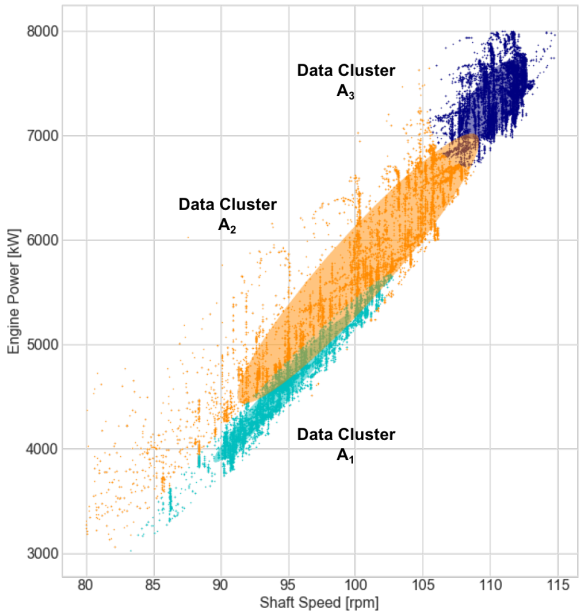

(b) GMMs implementation.

Figure 4.1: Engine data clustering. Figure from Paper I.

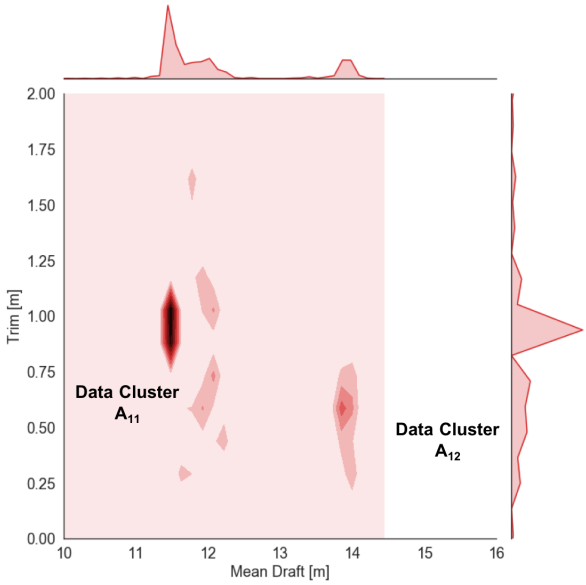

(a) KDE implementation.

(b) GMMs implementation.

Figure 4.2: Trim-draft data clustering with respect to data cluster A. Figure from Paper I.

vector shows a decrease in the ME power, thereby decreasing the ME fuel consumption. There is a trim-draft adjustment in this condition. A decrease in the relative wind direction and the relative wind speed can also be observed. It can be seen from the third singular vector that a decrease in the relative wind direction is caused by a decrease in the ship speed. Looking at the fourth top singular vector, the auxiliary power decreases, thus decreasing the auxiliary fuel consumption. The same correlation can also be seen for the ME power and the ME fuel consumption. The fifth singular vector reveals that a decrease in the auxiliary power leads to a decrease in the auxiliary fuel consumption.

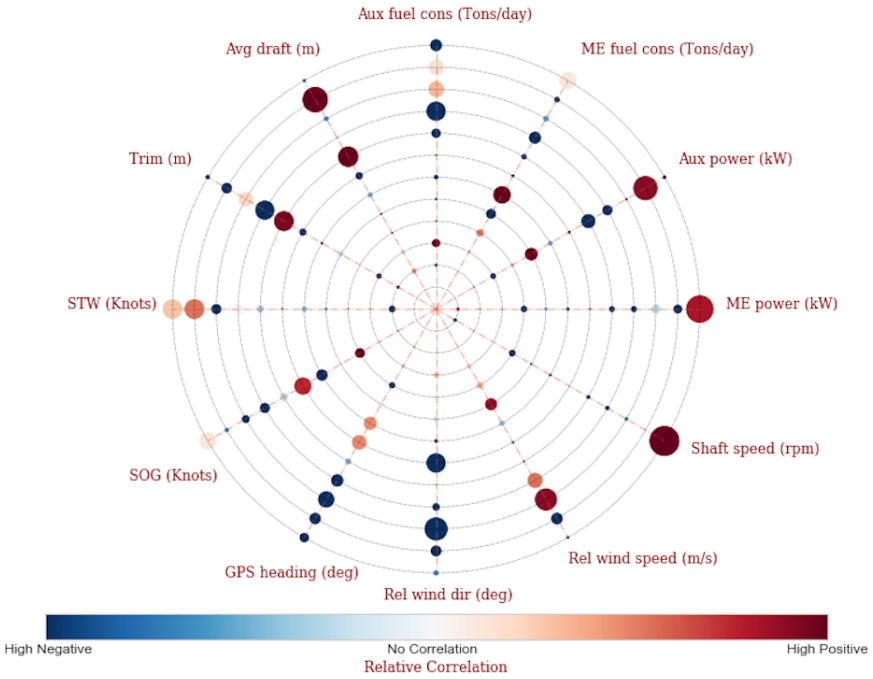

Figure 4.3: Visual analytics for data cluster A_{12} under trim-draft mode. Figure from Paper I.

As mentioned before, the bottom SVs express the least variance direction in the data. Therefore, the parameter correlations might be imprecise or anomalous in such SVs.

Contributions by the author

- The author developed the methodology together with the second co-author.
- The author carried out the implementation and experiments.
- The author prepared the original draft of this study.
- The author conducted subsequent revisions under the review of the second co-author.

Paper II: Advanced data analytics for ship performance monitoring under localized operational conditions

Paper II was built upon the work in Paper I with a more complete framework and thorough analysis on the localized operational conditions of the bulk carrier. The ADAF was developed by proposing a couple of data analytics coupling with domain knowledge, as illustrated in Figure 4.4. The following is a brief description of the ADAF.

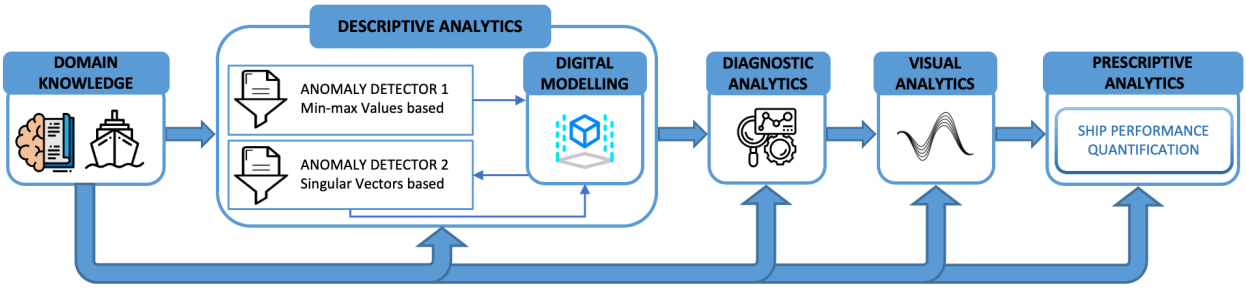

Figure 4.4: A representation of the ADAF. Figure from Paper II.

- Domain knowledge: It is of critical importance throughout the development of the ADAF. It relates to a set of specialized expertise from experts in the maritime domain. The power of ML models can only be harnessed with the help of such domain knowledge.
- Descriptive analytics: It is intended for digital modelling and data anomaly detection. The former is to uncover insights into the ship's localized operational conditions. The latter is to detect data anomalies.
- Diagnostic analytics: It suggests reasons why data anomalies are existing in the data set.
- Visual analytics: It produces visual representations of the relative correlations among parameters.
- Prescriptive analytics: It yields a selected KPI (i.e. key performance indicator) for ship performance quantification.

Figure 4.5 displays a general representation of what it is meant by the ship's localized operational conditions. Here the relationships between engine modes and trim-draft modes can be observed. Presumably, there are engine modes, e.g., A, B, C, etc., represented by clusters A, B, C, etc. Trim-draft modes may be found under such engine modes, represented by sub-clusters. An example of this is trim-draft modes, e.g., A_1, A_2, A_3, etc. represented by sub-clusters, e.g., A_1, A_2, A_3, etc..

Uncovering such localized operational conditions was undertaken under the descriptive analytics including the digital modelling and two data anomaly detectors. Figure 4.6 is an illustration of

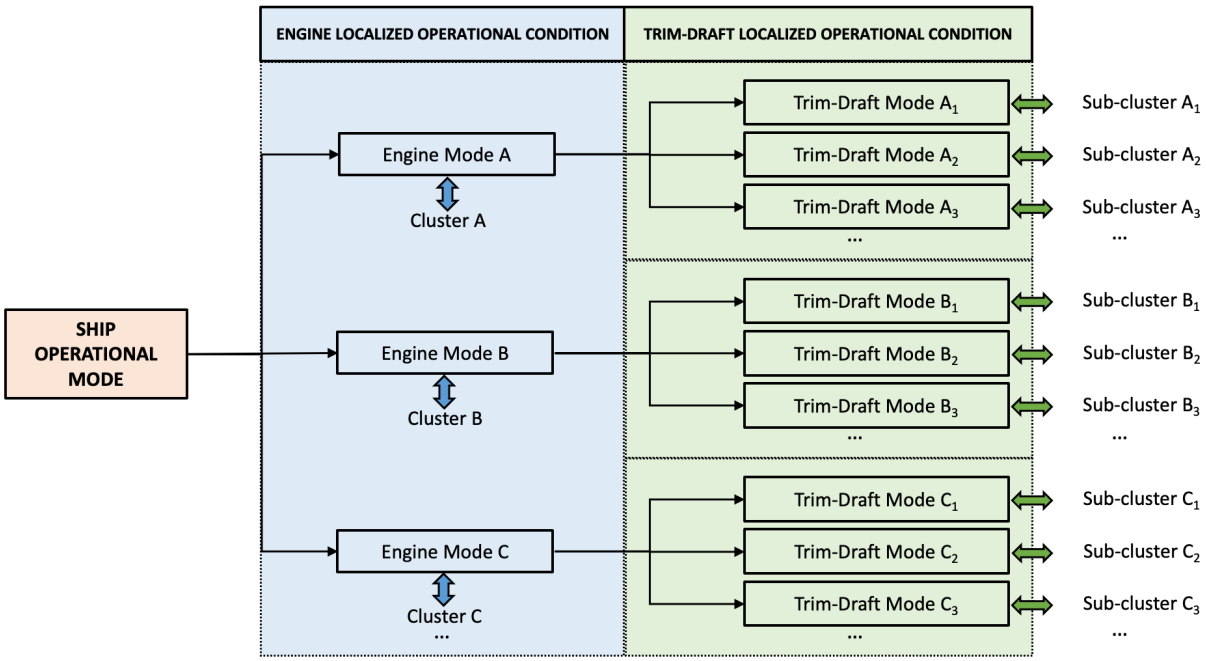

Figure 4.5: A hierarchical diagram of the ship's localized operational conditions. Figure from Paper II.

the digital modelling presented in the right-handed coordinate system. The digital model on the left illustrates data clusters A, B, and C representing engine modes. The structure of each data cluster is demonstrated by its SVs, for example, SVs of cluster A are $Z_{A,1}$, $Z_{A,2}$, and $Z_{A,3}$. The digital model on the right shows sub-clusters A_1, A_2, and A_3, projected onto another subspace, representing trim-draft modes with respect to cluster A. Another important observation from this figure is the existence of data outliers and data anomalies. While the former was addressed by the first anomaly detector based on minimum-maximum values, the latter was addressed by the second anomaly detector based on SVs.

In the first place, under the first data anomaly detector, proper ranges of the parameters in the data set were set by the domain knowledge, as presented in Table 4.3. Afterwards, the digital modelling was constructed. At this point, the KDE and GMMs methods for engine data clustering were implemented. As can be seen from Figure 4.7 that three data clusters of engine operational conditions, i.e., clusters A, B, and C, was discovered. Such clusters were visualized in a 3-dimensional space, as illustrated in Figure 4.8. It arrived at an answer that the ship was operating in three engine modes. While clusters A and C are the two main engine modes, cluster B was thought to be a transient mode of the engine.

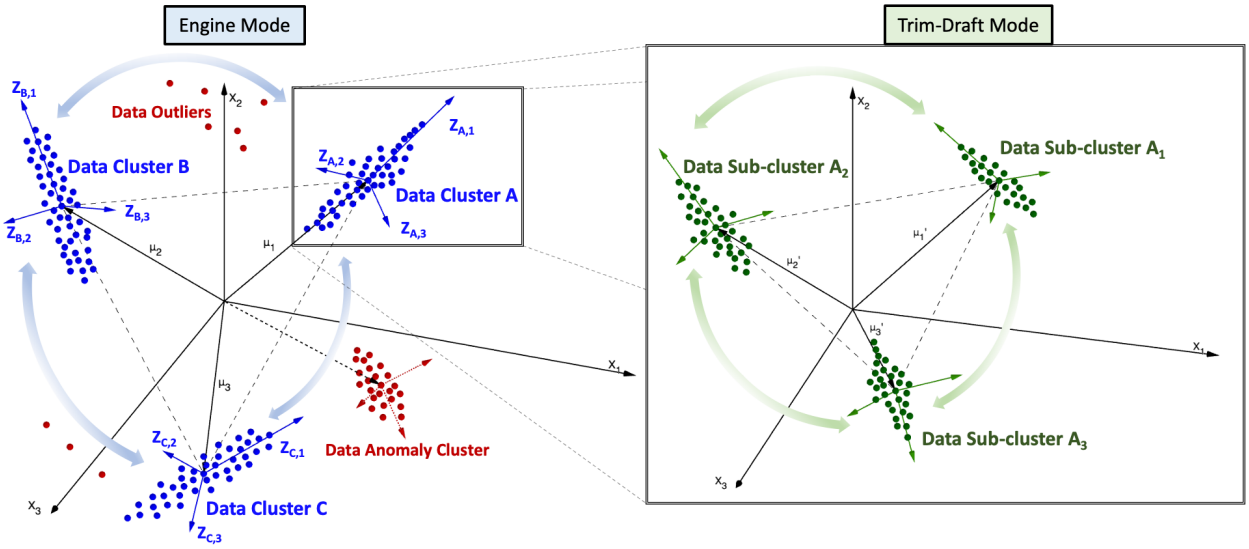

Figure 4.6: A representation of the digital models. Figure from Paper II.

Table 4.3: Minimum-maximum values of ship performance and navigation parameters

Parameter	Min value	Max value
Auxiliary (Aux) fuel consumption (cons) [Ton/day]	1	8
Main Engine (ME) fuel consumption (cons) [Ton/day]	1	40
Auxiliary (Aux) power [kW]	100	850
Main Engine (ME) power [kW]	3000	8000
Shaft speed [rpm]	80	120
Relative (Rel) wind speed [m/s]	0	25
Relative (Rel) wind direction (dir) [deg]	0	360
Course [deg]	0	360
Speed over ground (SOG) [Knots]	3	20
Speed through water (STW) [Knots]	3	20
Trim [m]	-2	4
Average (Avg) draft [m]	0	15

In the second place, the second data anomaly detector was capable of detecting data anomalies with the help of SVD. As indicated previously, the bottom singular vector contains the least significant information of each data cluster. In this respect, it was used as the principal axe for projecting data onto a new subspace. Figure 4.9 demonstrates the projection of data cluster A on the subspace represented by the bottom singular vector Z_{12}. Data anomalies were detected based on proper thresholds, i.e., -3σ and 3σ, (σ is the standard deviation of the data distribution). Any data points located beyond such thresholds were considered anomalies. Such data points were collated and analyzed in a time-series chart with all parameters of the data set. As shown in Figure 4.10, anomalous behaviors of interconnected parameters are identified. By way of illustration, the first

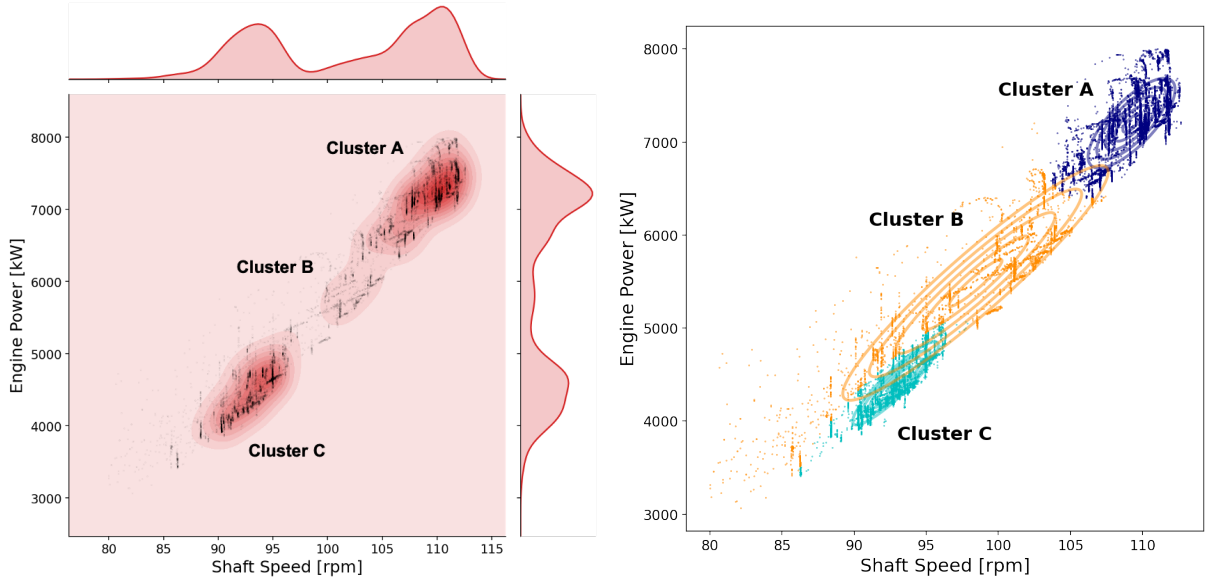

(a) KDE implementation.

(b) GMMs implementation.

Figure 4.7: Engine data clustering. Figure from Paper II.

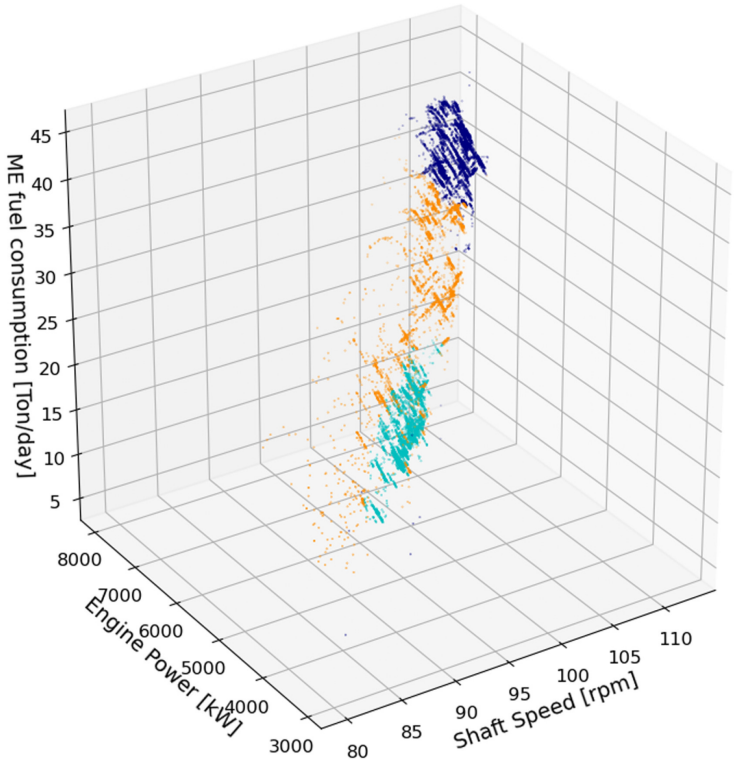

Figure 4.8: Engine data clustering in a 3-dimensional space. Figure from Paper II.

data anomaly (DA 1) shows a strange relationship between the ME power and the speed through water (STW). The second data anomaly (DA 2) demonstrates unreasonable dropping points in the ME fuel consumption and the STW. The same anomalous behavior can also be seen in the third data anomaly (DA 3). Table 4.4 reports the number of anomalies found in other data clusters. As indicated in this study, a possible explanation for such data anomalies might be attributed to sensor faults and/ or abnormal events in the ship's system.

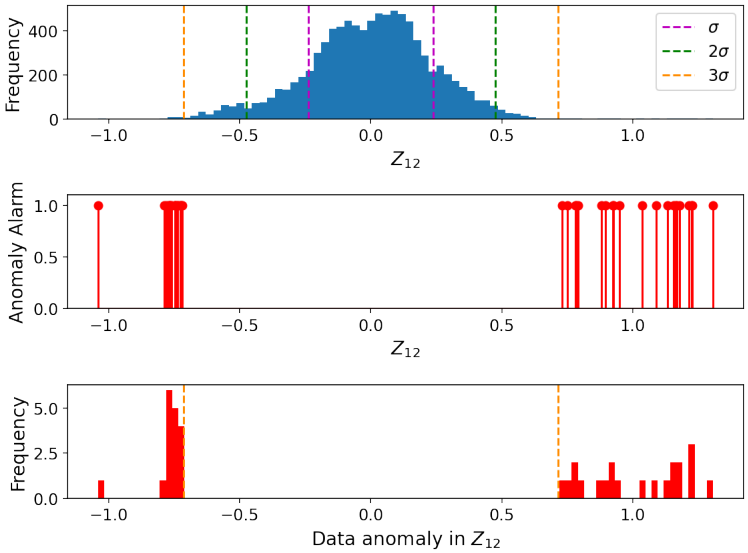

Figure 4.9: Data anomaly detection in the bottom singular vector. Figure from Paper II.

Table 4.4: Number of identified data anomalies using the second anomaly detector. Table from Paper II.

Cluster	No of identified data anomalies	Ratio* (%)
A	38	0.41
B	37	1.08
C	48	0.81

* The ratio (%) indicates the number of identified anomalies per the number of data points in the respective cluster

Further clustering analysis of trim-draft data revealed several sub-clusters with respect to the respective data clusters, as depicted in Figure 4.11 (i.e., sub-clusters A_1, A_2, A_3, and A_4), Figure 4.12 (i.e., sub-clusters B_1, B_2, B_3, and B_4), and Figure 4.13 (i.e., sub-clusters C_1, C_2, C_3, and C_4) respectively. Such sub-clusters are trim-draft modes under the identified engine modes.

Regarding the number of underlying components (i.e. clusters) applied to the GMMs method, some experiments using the BIC and the AIC were performed. Figure 4.14a shows the BIC and AIC

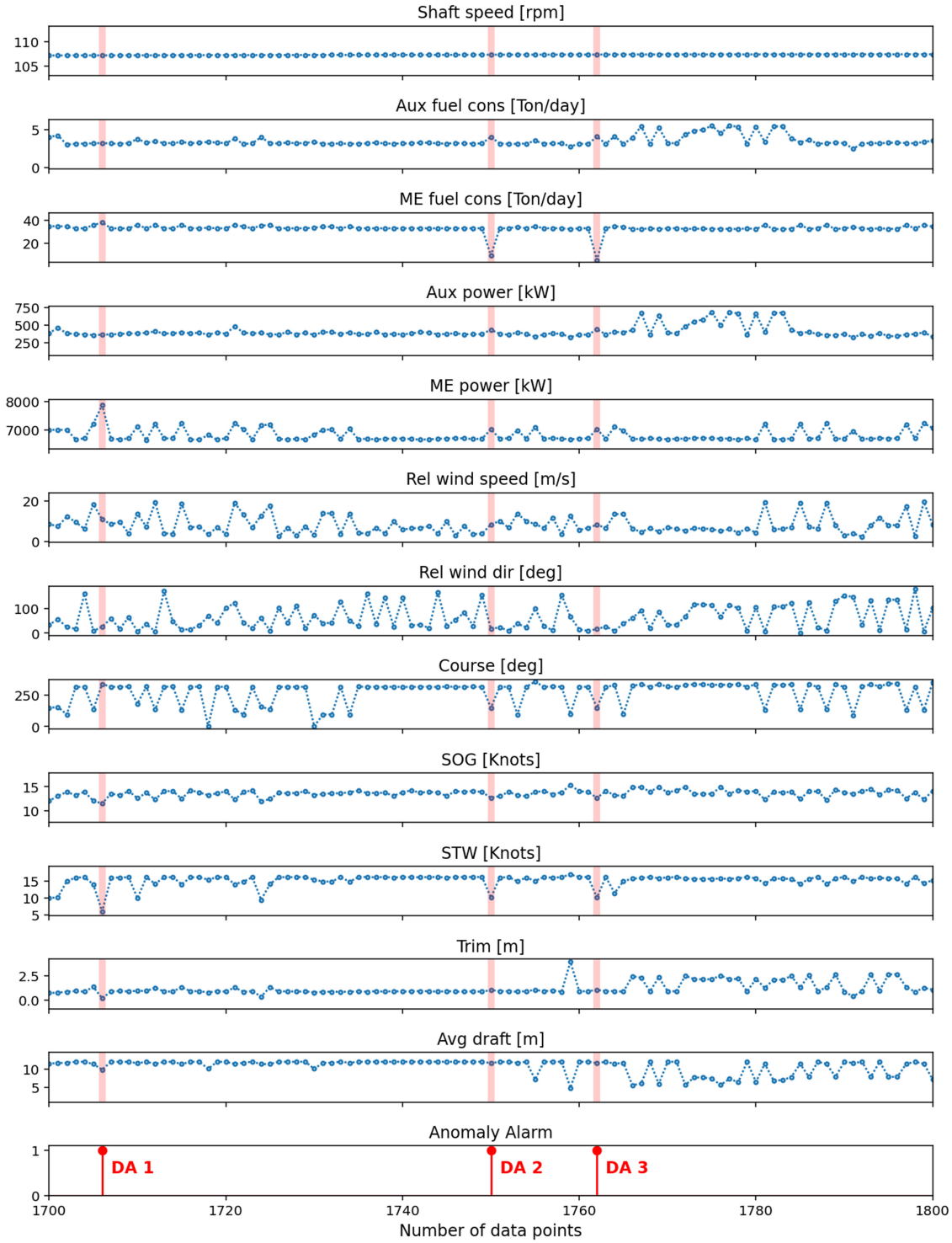

Figure 4.10: Data anomaly detection in the time-series plot. Figure from Paper II.

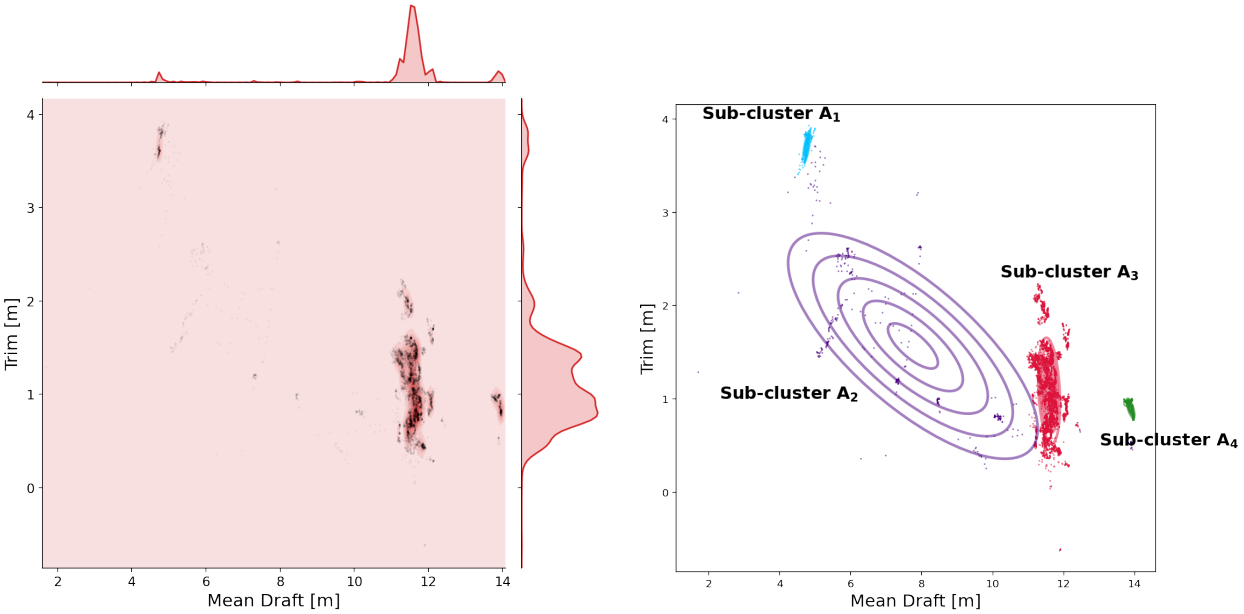

(a) KDE implementation. (b) GMMs implementation.

Figure 4.11: Trim-draft data clustering with respect to data cluster A. Figure from Paper II.

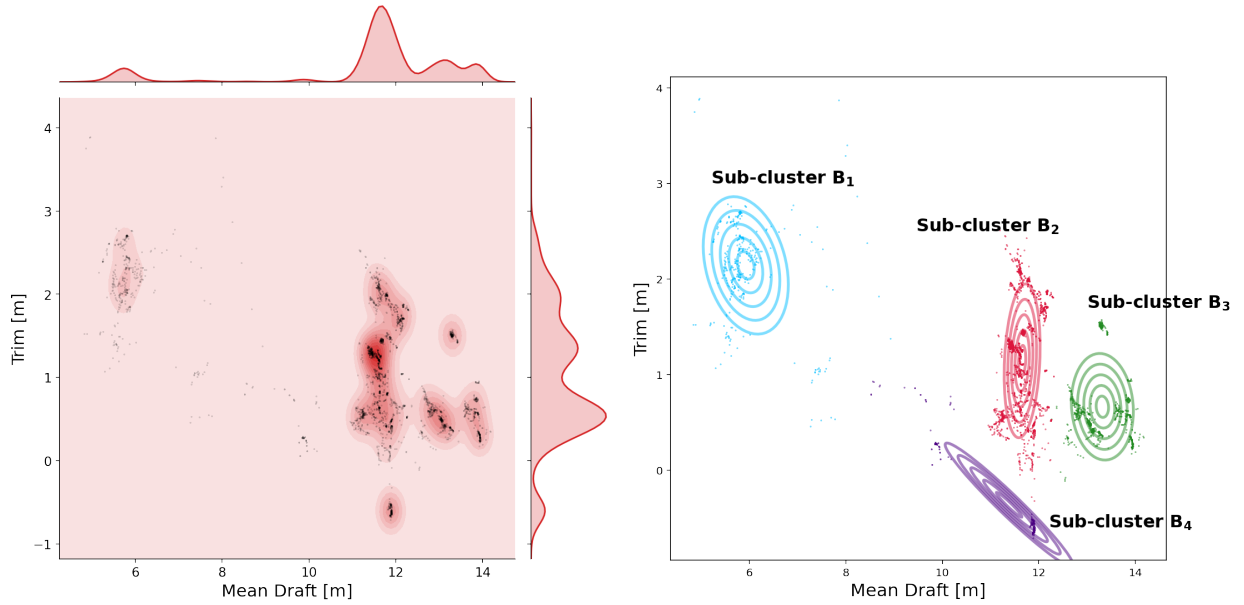

(a) KDE implementation. (b) GMMs implementation.

Figure 4.12: Trim-draft data clustering with respect to data cluster B. Figure from Paper II.

results from engine data. It is required to find the number of components K with the lowest BIC and AIC values. However, the results did not give a sensible answer for K in this case. Several

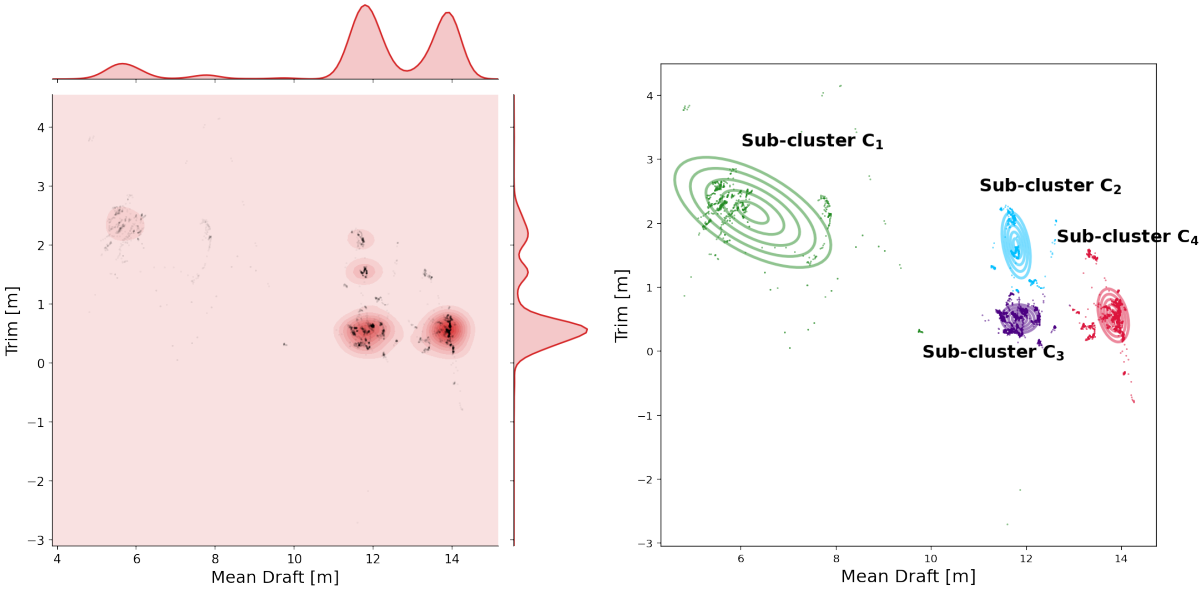

(a) KDE implementation.

(b) GMMs implementation.

Figure 4.13: Trim-draft data clustering with respect to data cluster C. Figure from Paper II.

attempts were also made to find the number of components K with respect to trim-draft data, as presented in Figure 4.14b, Figure 4.14c, and Figure 4.14d. It was found that the optimal number of components K could not be identified in these experiments. Instead, the most likely number of components was assigned by the domain knowledge.

Similar to the approach presented in Paper I, visual analytics constructed a graphic representation of the relative correlations among parameters within a sub-cluster (i.e. a trim-draft localized operational conditions). Figure 4.15 illustrates this point clearly. Generally, based on high singular values, meaningful relative correlations can be discovered in the top SVs. Looking at Figure 4.15c in which the parameter correlations of sub-cluster A_3 are depicted, in the top singular vector, there is an increase in both the shaft speed and the ME power that leads to an increase in the ME fuel consumption. In the same condition, the Auxiliary power is decreased, therefore, the Auxiliary fuel consumption is also decreased. It can also be seen that the Average draft is decreased. In the second singular vector, an adjustment of the Trim and the Average draft might result in an increase in the STW and the speed over ground (SOG). The third singular vector shows that an increase in the Auxiliary fuel consumption is caused by an increase in the Auxiliary power. As can be seen from the fourth singular vector, there is a decrease in the STW that leads to a significant increase in the Relative wind direction. The fifth singular vector shows that a decrease in the Auxiliary fuel consumption is attributed to a decrease in the Auxiliary power. The trim in this condition is increased. Turning to the sixth singular vector, there is an increase in the STW together with an increase in the Relative wind direction. There is also an adjustment of the trim-draft in the same condition. On the other hand, having low singular values, the bottom singular vectors may

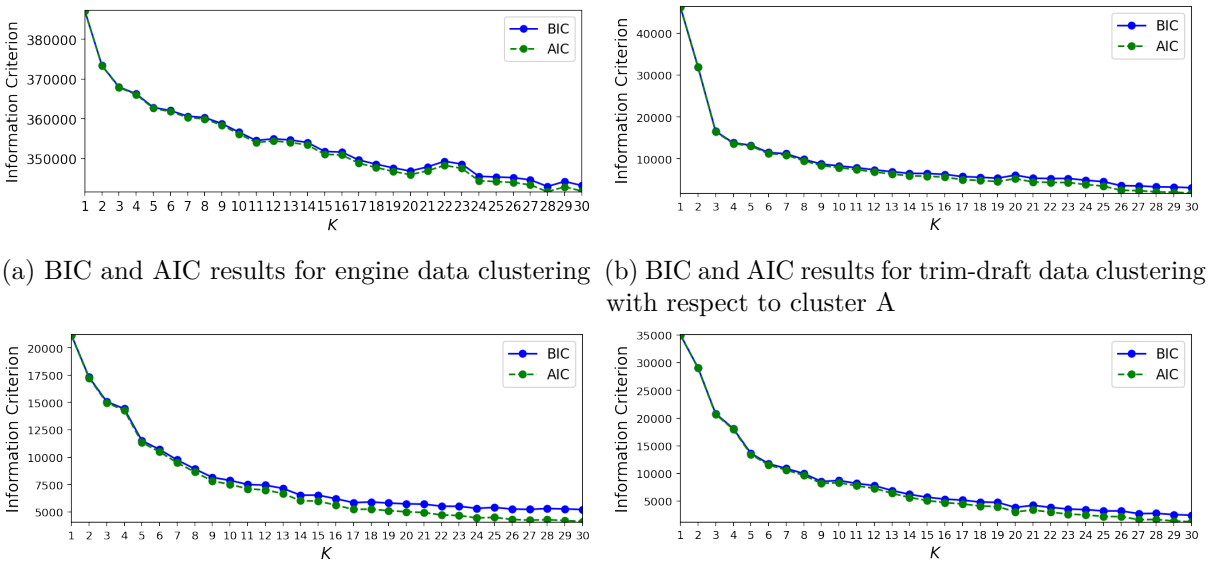

(a) BIC and AIC results for engine data clustering

(b) BIC and AIC results for trim-draft data clustering with respect to cluster A

(c) BIC and AIC results for trim-draft data clustering with respect to cluster B

(d) BIC and AIC results for trim-draft data clustering with respect to cluster C

Figure 4.14: BIC and AIC results. Figure from Paper II.

provide insignificant information about the parameter correlations. Results of such analytics for other sub-clusters were believed obtainable using a similar way of explanation.

In terms of prescriptive analytics, a KPI (i.e key performance indicator) was proposed to quantify the ship's performance. The KPI was accomplished in the form of the ship performance index SPI which can be defined as

$$SPI_i = \frac{FC_i}{D_i} \tag{4.1}$$

Consider

$$FC_i = FC_{avg,i} \times t_i \tag{4.2}$$

$$D_i = STW_{avg,i} \times t_i \tag{4.3}$$

where FC is the main engine fuel consumption [Ton], FC_{avg} is the average main engine fuel consumption [Ton/day], D is the traveled distance [NM], t is the time traveled [day], STW_{avg} is the average speed through water [NM/h], i indicates the i^{th} localized operational condition.

Hence, Equation (4.1) can be expressed as

$$SPI_i = \frac{FC_{avg,i}}{24\, STW_{avg,i}} \tag{4.4}$$

The unit of the SPI_i is [Ton/NM].

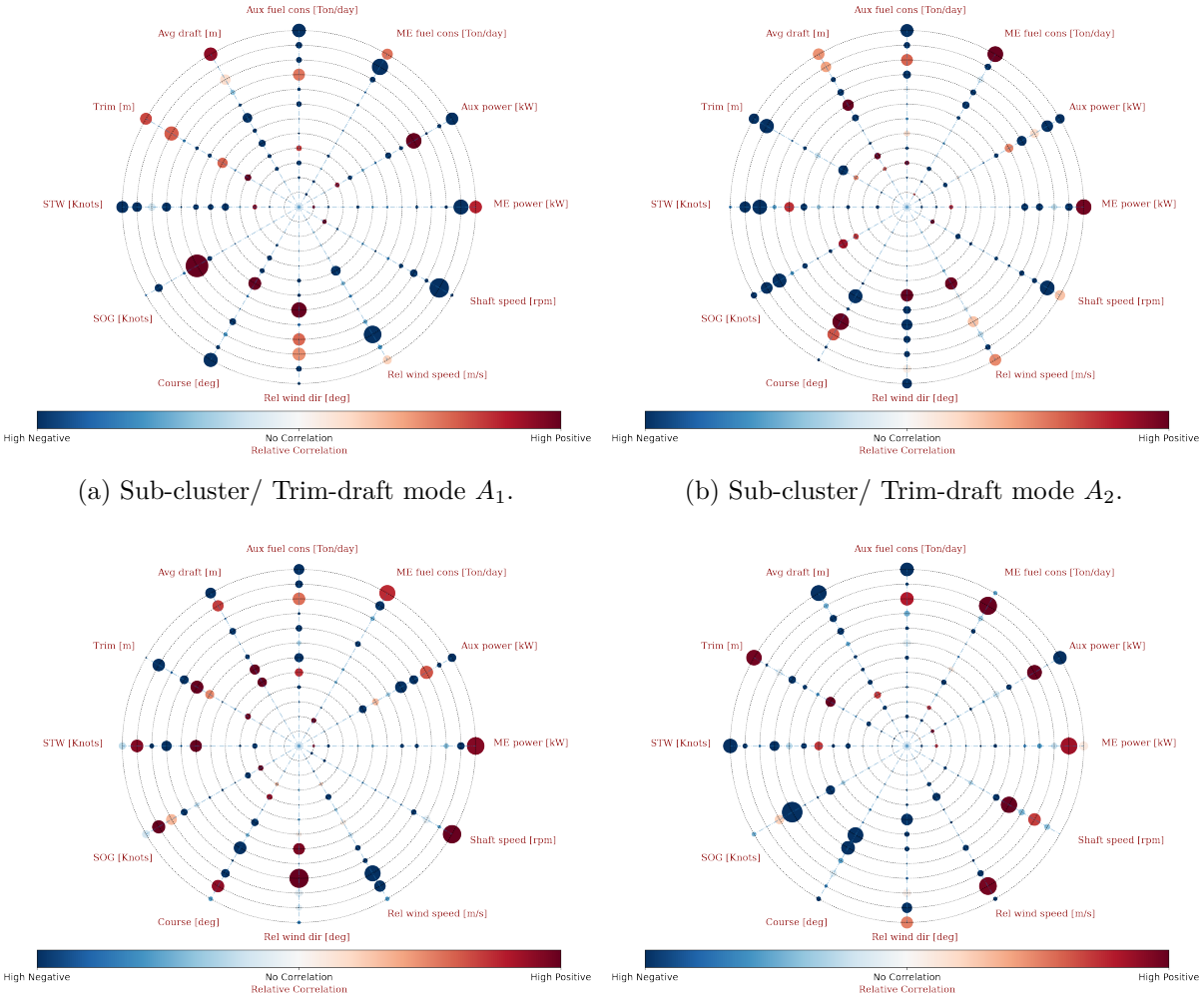

(a) Sub-cluster/ Trim-draft mode A_1.

(b) Sub-cluster/ Trim-draft mode A_2.

(c) Sub-cluster/ Trim-draft mode A_3.

(d) Sub-cluster/ Trim-draft mode A_4.

Figure 4.15: Visual analytics of data cluster A under trim-draft modes. Figure from Paper II.

The SPI was applied to each of the ship's localized operational conditions (i.e., engine and trim-draft modes) in order to identify the best performance mode. The resulting $SPIs$ are reported in the Table 4.5. It was concluded that trim-draft mode C_1 (with the lowest SPI value) is the best performance mode of the bulk carrier.

Table 4.5: SPI results for ship performance quantification. Table from Paper II.

Cluster (Engine Mode)	Sub-cluster (Trim-draft Mode)	SPI [Ton/NM]
A	A_1	0,0797
	A_2	0,1030
	A_3	0,1121
	A_4	0,1468
B	B_1	0,0936
	B_2	0,0992
	B_3	0,1080
	B_4	0,0805
C	C_1	0,0699
	C_2	0,0728
	C_3	0,0748
	C_4	0,0753

Contributions by the author

- The author developed the methodology together with the second co-author.
- The author carried out the implementation and experiments.
- The author prepared the original draft of this study.
- The author conducted subsequent revisions under the review of the second co-author.

4.2 LCCF for an innovative dual-fuel engine technology under uncertainties

In this section, the development of the LCCF for assessing the life-cycle cost performance of the dual-fuel engine compared with that of a conventional, is presented. The LCCF was applied to a case study pertaining to a bulk carrier with the deadweight of 7600 [t], and the Length-Over-All (LOA) of 112 [m]. It is assumed that the bulk carrier, using the diesel engine, will be retrofitted with the dual-fuel engine. Table 4.6 shows the specifications of these engines.

It would be useful at this stage to present the specific assumptions in the LCCA conducted in this thesis.

- The period of analysis (i.e. the expected lifespan of the engine) in the LCCA is 20 years. This is in line with those of earlier studies (H. Wang et al., 2019).
- In the construction phase, the engine delivery costs are not considered. A possible explanation

Table 4.6: Specifications of two engines. Table from Paper III, IV.

Specification	Diesel Engine	Dual-fuel Engine
Cylinder configuration	8L32	8V31DF
No of cylinder	8	8
Cylinder bore [mm]	320	310
Power per cylinder [kW]	580	600
Power [kW]	4640	4800
RPM	750	750
Fuel type	MGO	ULSD (in disesel mode) LNG (in gas mode)

MGO: Marine Gas Oil; ULSD: Ultra Low Sulphur Diesel.

for this is that these costs can be the same for these engines. Additionally, the installation costs of fuel systems (i.e. the MGO tank system for the diesel engine and the LNG tank system for the dual-fuel engine) are not included.

- In the maintenance phase, the costs of handling LNG storage facilities are not taken into account.
- The external costs due to air pollution from the iron and steel-making processes in the construction phase are omitted. This is due to the fact that the CO_2 emissions from such processes are considerably less, in comparison with the CO_2 emissions from fuel combustion in the operation phase.
- The external costs attributed to air pollution from the demolition or recycling process in the end-of-life phase are not included.

Before proceeding to present the research outcomes gained from Paper III and Paper IV, it is necessary to recall the cost components included in the LCCA, as previously discussed in Section 3.2.2.

4.2.1 Construction costs

To improve the readability of this thesis, the EBS for construction cost comparison between these engines is repeated, as shown in Table 4.7. The construction costs for the diesel engine and the dual-fuel engine were obtained after a discussion with the engine manufacturer (Wärtsilä, 2021b).

4.2.2 Operation costs

As previously mentioned in Section 3.2.2, in the case of internal costs, the term 'operation costs' is used to refer to fuel costs. A more detailed account of calculating the fuel costs is given as follows.

Table 4.7: A general Engine Breakdown Structure (EBS). Table from Paper IV.

2nd Level	3rd Level	Cost	
		Diesel Engine	Dual-fuel Engine
Main components & systems	Engine Basement		
	Camshaft & Valve Mechanism		
	Fuel Injection System		
	Turbocharging & Scavenging System		
	Ancillary System		
	Automation System		
	Low-value Parts		
	Exhaust Gas Cleaning System*		N/A
	Total	989K	1,200K

* Selective Catalytic Reduction (SCR) technology for NO_x reduction. The SCR cost for the diesel engine was adopted from the International Association for Catalytic Control of Ship Emissions to Air (IACCSEA) (IACCSEA, n.d.). SCR is not required for the dual-fuel engine. Other costs were obtained from the engine manufacturer (Wärtsilä, 2021b).
Unit K = 1000 €.

Table 4.8 displays the operational profile of the case ship with the diesel engine. In this table, the SFOC and SLOC were properly calibrated according to the engine load, which varies in different engine modes. This can be achieved by doing interpolation/ extrapolation based on the reference values, as presented in Table 4.9 (Wärtsilä, n.d.). The annual FOC and the annual LOC were calculated with the help of Equation (3.17) and Equation (3.18) respectively, as shown in Section 3.2.2.

Table 4.8: The case ship's operational profile operating the diesel engine. Table from Paper IV.

Operation Mode	Annual Hours [h/y]	Speed [Knot]	%	Power [kW]	Engine Load [%]	SFOC [g/kWh]	Annual FOC [t/y]	SLOC [g/kWh]	Annual LOC [t/y]
Port	1200	0	14%	0	0	0	0	0	0
Manoeuvring	100	0	1%	846.7	18.2%	192.5	16.3	0.06	0.01
Engine Mode 1	300	18.1	3%	3139.6	67.7%	181.0	170.5	0.24	0.22
Engine Mode 2	7100	15.3	82%	1720.9	37.1%	185.0	2261.1	0.13	1.59
Total	8700						2447.8		1.81

The relationship between the engine load and the relative SFOC can be plotted, as depicted in Figure 4.16. For the curve presented in this figure, the SFOC is a non-linear function of the engine load. The minimum of this function at a specific engine load denotes the required optimal way of operating the engine. Ideally, reducing fuel oil consumption should be around the minimum of engine load for achieving optimum results in terms of fuel consumption and engine performance. For

Table 4.9: Reference values for the SFOC & SLOC of the diesel engine. Table from Paper III, IV.

Engine Load [%]	SFOC [g/kWh]	SLOC [g/kWh]
100	184.7	0.35
85	181	
75	180.6	
50	181.9	

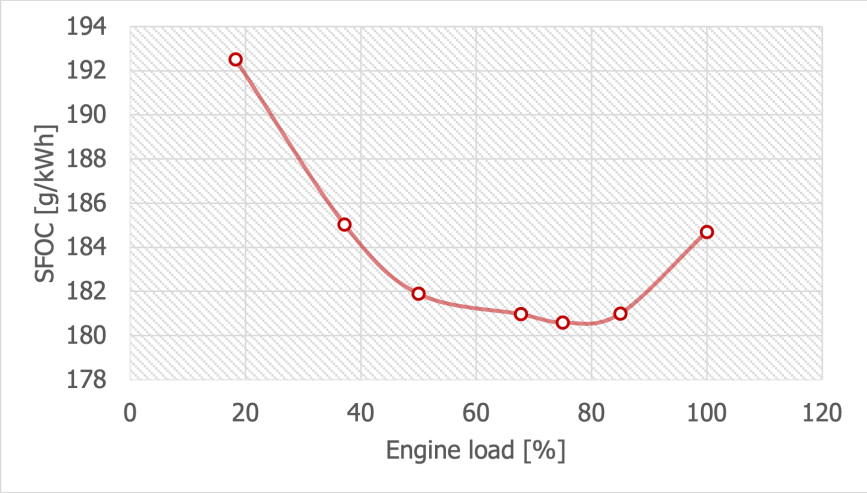

Figure 4.16: SFOC-engine load relation curve of the diesel engine. Figure from Paper IV.

a medium sized four-stroke diesel engine from Wärtsilä, the required engine load is approximately 80% (Jalkanen et al., 2012).

Table 4.10 presents a similar operational profile, applying for the dual-fuel engine under the following assumptions:

- In 'Manoeuvring', the dual-fuel engine operates in the diesel mode with Ultra Low Sulphur Diesel (ULSD).
- In 'Engine Mode 1' and 'Engine Mode 2', the dual-fuel engine operates in the gas mode with LNG.

As mentioned earlier, in the diesel mode, the dual-fuel engine operates according to the conventional diesel engine. The SFOC, the SLOC, the annual FOC and the annual LOC of the dual-fuel engine were obtained in a similar manner of what has been done for the diesel engine.

In the gas mode, there is a pilot injection with a small amount of diesel fuel integrated into the main fuel injection system. The SPFC and the annual PFC calculations can also be done by adopting the same approach for the diesel engine. Apart from that, it is necessary to quantify the SFGC and the annual FGC. The actual SFGC under different engine modes were determined by means of

interpolation/ extrapolation of the reference values presented in Table 4.11. Before doing that, the calorific value for LNG was used for converting the heat rate to the reference SFGC. The annual FGC was calculated by using Equation (3.19), as mentioned in Section 3.2.2.

The relative SFOC curve of the dual-fuel engine in the diesel mode is shown in Figure 4.17. It is required to have the relative engine load around its minimum point to reduce fuel oil consumption and enhance engine performance. Figure 4.18 depicts the relative SFGC curve and the relative SPFC of the dual-fuel engine in the gas mode. As can be seen from this figure, the SFGC variations between different engine loads are marginal.

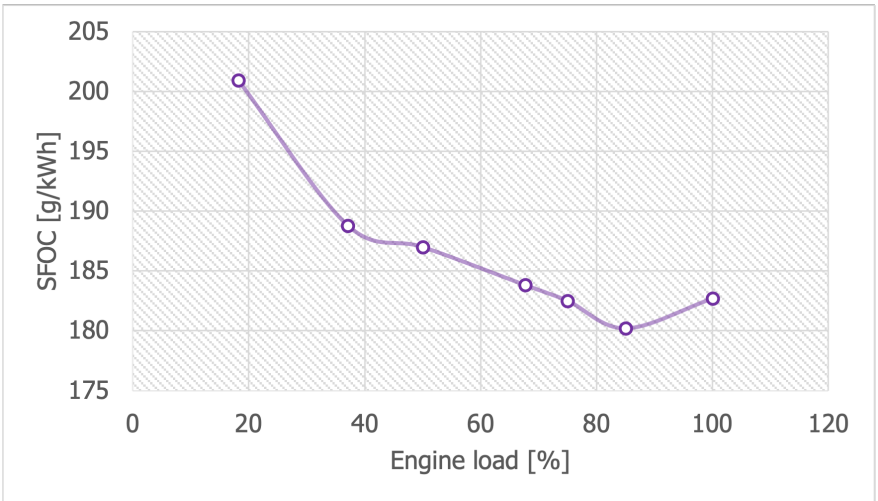

Figure 4.17: SFOC-engine load relation curve of the dual-fuel engine in the diesel mode. Figure from Paper IV.

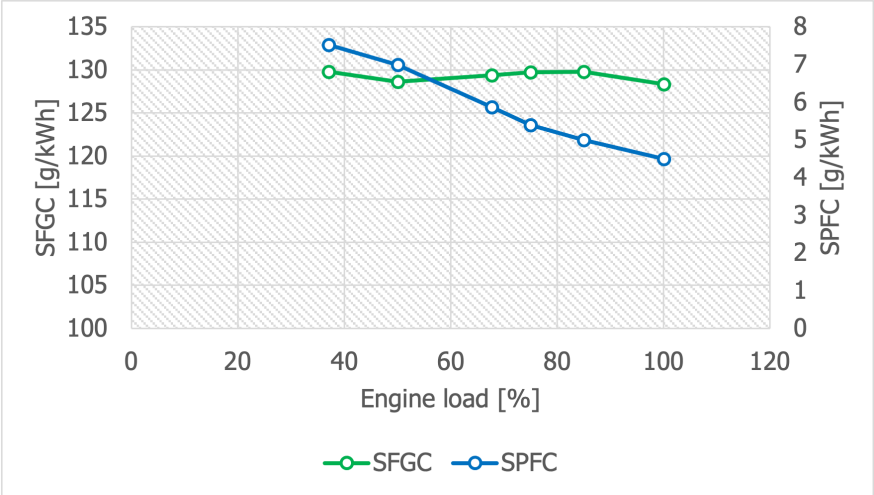

Figure 4.18: SFGC/ SPFC-engine load relation curves of the dual-fuel engine in the gas mode. Figure from Paper IV.

Table 4.10: The case ship's operational profile operating the dual-fuel engine. Table from Paper IV.

Operation Mode	Annual Hours [h/y]	Speed [Knot]	%	Power [kW]	Engine Load [%]	SFOC [g/kWh]	Annual FOC [t/y]	SLOC [g/kWh]	Annual LOC [t/y]	SFGC [g/kWh]	Annual FGC [t/y]	SPFC [g/kWh]	Annual PFC [t/y]
Port	1200	0	14%	0	0	0	0	0	0	0	0	0	0
Manoeuvring	100	0	1%	873.6	18.2%	200.9	17.6	0.08	0.01	131.1	N/A	N/A	N/A
Engine Mode 1	300	18.8	3%	3249.6	67.7%	183.8	N/A	0.30	0.30	129.4	126.2	5.9	5.7
Engine Mode 2	7100	15.9	82%	1780.8	37.1%	188.8	N/A	0.17	2.11	129.8	1641.1	7.5	95.1
Total	8700						17.6		2.42		1767.3		100.9

Table 4.11: Reference values for the SFOC, SLOC, SPFC & SFGC of the dual-fuel engine. Table from Paper III, IV.

Engine Load [%]	SFOC [g/kWh]	SLOC [g/kWh]	SPFC [g/kWh]	Heat Rate [kJ/kWh]	SFGC [g/kWh]
100	182.7	0.45	4.5	7058	128.3
85	180.2		5.0	7138	129.8
75	182.5		5.4	7134	129.7
50	187.0		7.0	7076	128.7

The calorific value for LNG: 55000 [kJ/kg] is used to convert the heat rate into the SFGC.

4.2.3 Carbon emissions costs

As noted in Section 3.2.2, the carbon emissions costs are due to air pollution from the operation phase. Given the carbon tax development under MBMs, such costs are included in the LCCA by simulating several carbon pricing scenarios. The annual CO_2 emissions emitted during fuel combustion can be calculated with the help of Equation (3.20) and the carbon emission conversion factor C_F presented in Table 4.12.

Table 4.12: Carbon emission conversion factor C_F (IMO, 2020)

Type of fuel	C_F [t-CO2/t-Fuel]
MGO	3.20600
ULSD	3.15104
LNG	2.75000

4.2.4 Maintenance costs

As explained in Section 3.2.2, the maintenance costs consist of the following costs:

- The labor costs for doing the maintenance tasks.
- The costs of part replacement.

4.2.5 End-of-life values

As noted in Section 3.2.2, the end-of-life values of the engines are the benefits that can be calculated from the benefits gained from recycling the engine materials. Table 4.13 displays the main metal materials used in the engines while Table 4.14 shows the weights of these engines.

Table 4.13: Metal material content of the engines & the benefits of recycling. Table from Paper III, IV.

Material	Weight ratio [%]	Benefits of recycling [€/kg]
Steel	16	0.25
Cast iron	80	0.25
Aluminium	2	0.7
Cooper	2	6.35

Source: Wärtsilä, (Greengate Metals, n.d.).

Table 4.14: Engine weights. Table from Paper III, IV.

Criteria	Diesel Engine	Dual-fuel Engine
Weight [t]	43.6	58.9

Source: (Wärtsilä, 2020; Wärtsilä, 2021b).

Paper III: Life-Cycle Cost Analysis on a Marine Engine Innovation for Retrofit: A Comparative Study

Paper III is a background study comparing the life-cycle cost performances between the studied engines. In order to achieve this, this paper proposed the LCCF consisting of several steps, as shown in Figure 4.19.

The LCCF was found to be successful in providing an economic KPI (i.e. the NPC) for the life-cycle cost comparison. The LCCF was conducted under the following fuel price scenarios between LNG and MGO. The fuel prices were obtained from real public databases (Global Maritime Hub, 2021; Ship & Bunker, 2021).

- Scenario 1: Low price differential between LNG and MGO (110%).
  - LNG price: 561.1 [€/t]
  - MGO price: 508.1 [€/t]
- Scenario 2: High price differential between LNG and MGO (180%).
  - LNG price: 938.3 [€/t]
  - MGO price: 515.8 [€/t]

The ULSD price and the lubricating oil price remain unchanged in these scenarios as follows.

- ULSD price: 576.8 [€/t]
- Lubricating oil price: 2300 [€/t]

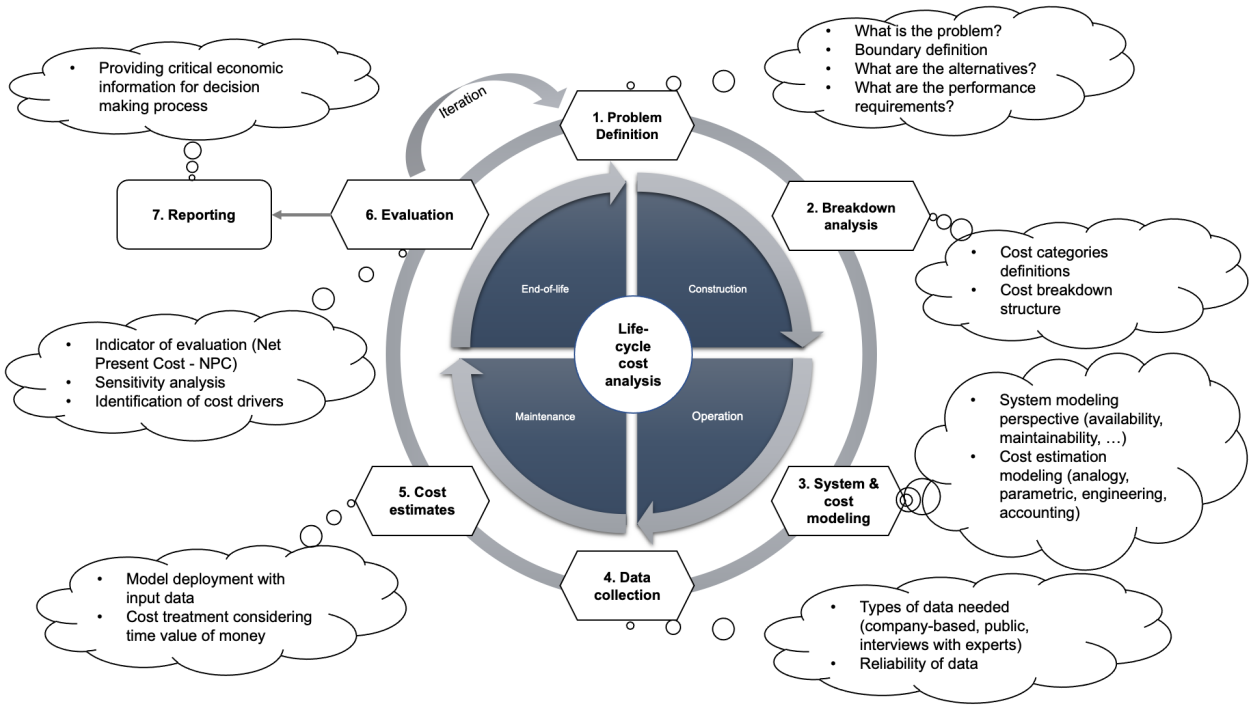

Figure 4.19: The proposed LCCF. Figure from Paper III.

Within these scenarios, the cost results in present value terms are summarized in Table 4.15, Figure 4.20, Table 4.16, and Figure 4.21 respectively. In terms of the maintenance costs, only the labor costs were included in this study. The part replacement costs were excluded because of data unavailability at the time being of this study. Results from the first scenario highlighted that the dual-fuel engine has a lower NPC than the diesel engine. However, in the second scenario, i.e. an extreme scenario with the high gas price, the results run contrary to the first scenario. Therefore, it was concluded that the dual-fuel engine is a cost-effective technology except for the high fuel price differential scenario.

However, it was revealed that irrespective of fuel prices, there is a potential for CO_2 emission reduction of 33% by using the dual-fuel engine, in comparison with the diesel engine, as shown in Table 4.17.

Table 4.15: Cost results in scenario 1. Table from Paper III.

Present value	Diesel Engine	Dual-fuel Engine
Construction costs	989K	1,200K
Operation costs	19,209K	16,450K
Maintenance costs	365K	399K
End-of-life value	10K	14K
NPC	20,553K	18,035K

Unit K = 1000 €
Discount rate = 2.5%

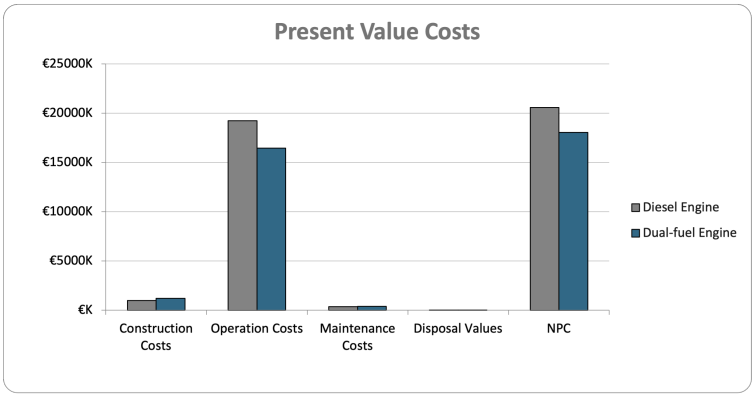

Figure 4.20: Results of scenario 1. Figure from Paper III.

Table 4.16: Cost results summary in scenario 2. Table from Paper III.

Present value	Diesel Engine	Dual-fuel Engine
Construction costs	989K	1,200K
Operation costs	19,498K	26,717K
Maintenance costs	365K	399K
End-of-life value	10K	14K
NPC	20,842K	28,303K

Unit K = 1000 €
Discount rate = 2.5%

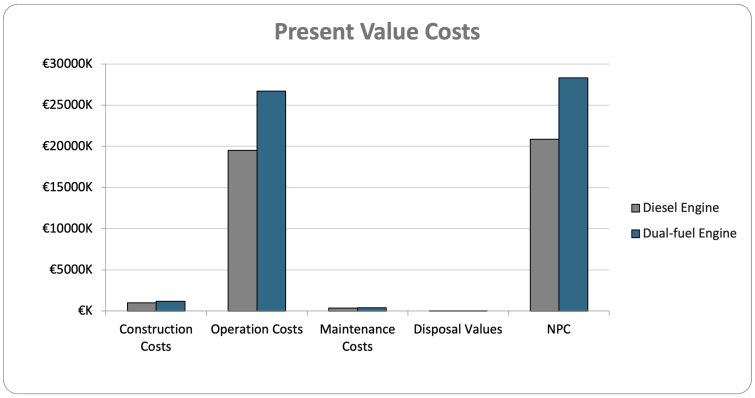

Figure 4.21: Results of scenario 2. Figure from Paper III.

Table 4.17: CO_2 emissions during 20 years operation of these engines. Table from Paper III.

Engine	Diesel engine	Dual-fuel engine
Amount per 20 years [Ton]	154,963	103,684
Percentage reduction	N/A	33%

Contributions by the author

- The conceptualization was conceived under the EU-funded SeaTech project (seatech2020.eu).
- The author developed the methodology.
- The author carried out the implementation and experiments.
- The author prepared the original draft of this study.
- The author conducted subsequent revisions under the review of the second co-author, the third co-author and the fourth co-author.

Paper IV: Life-cycle cost analysis of an innovative marine dual-fuel engine under uncertainties

Paper IV was built upon the work in Paper III to enhance the LCCF with an engineering build-up approach taking into account uncertainties. The enhanced LCCF featuring steps for conducting the LCCA integrating the ISO 15686-5 standard with a thorough examination of the engines' main components and systems is presented in Figure 4.22. The proposed LCCF transcended the internal boundary by including the external costs, i.e. carbon emission costs due to air pollution from the operation phase. For this reason, the LCCF was applied to two cases: the base case and the case with carbon pricing considering the development of carbon tax.

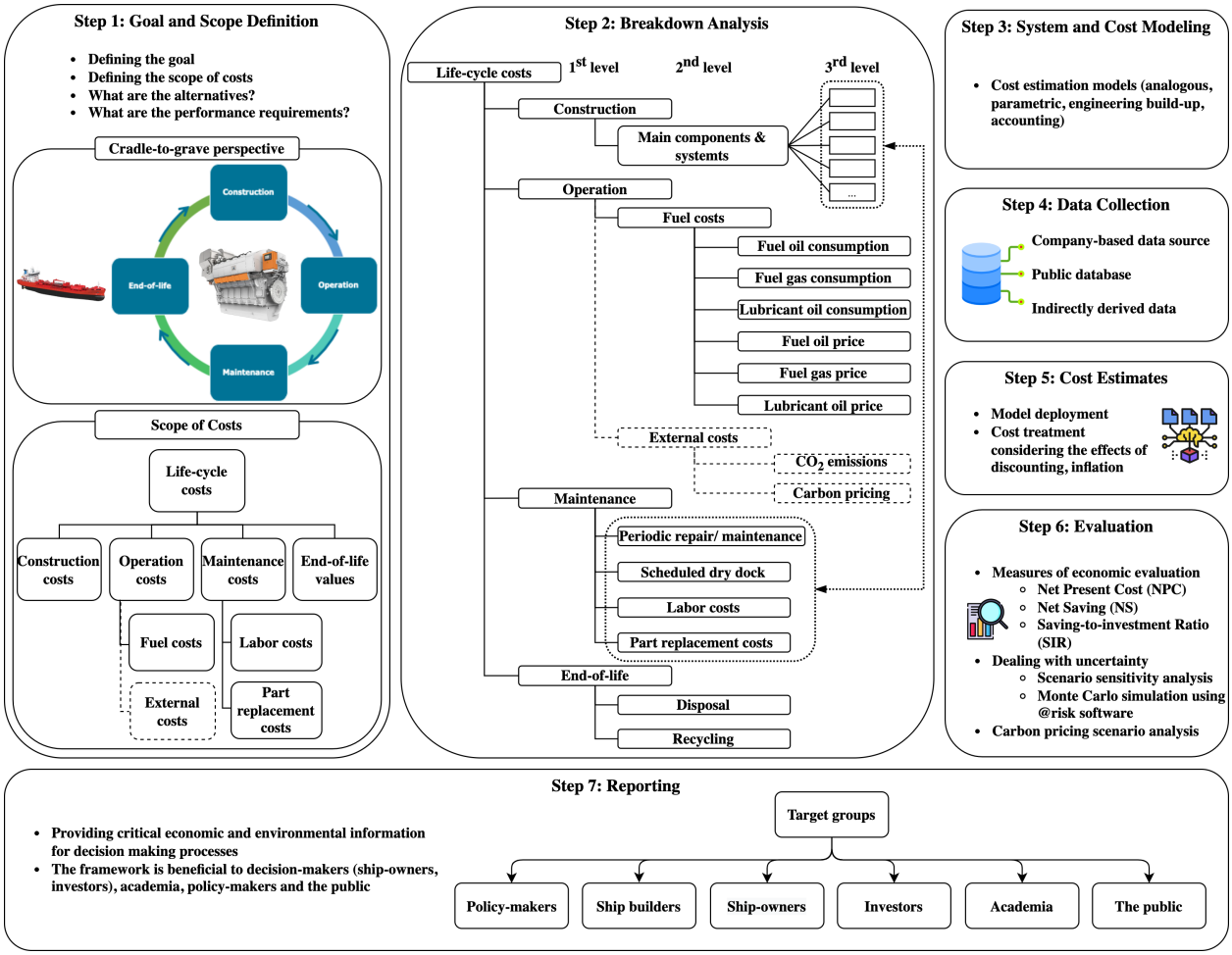

Figure 4.22: The proposed LCCF. Figure from Paper IV.

As far as the base case is concerned, fuel prices from real public databases are given as follows. These prices are consistent with the first scenario, as previously discussed in Paper III.

- LNG price: 561.1 [€/t]

- MGO price: 508.1 [€/t]
- ULSD price: 576.8 [€/t]
- Lubricating oil price: 2300 [€/t]

A summary of the cash flows of the cost components accumulated throughout 20 years is demonstrated in Table 4.18. The results for the maintenance costs presented in this table were strengthened with the part replacement costs that had not been included in Paper III. Furthermore, the maintenance costs were accounted for inflation with the inflation rate of 3.1%. All future cash flows were discounted back to present value by using an appropriate discount rate. Choosing the appropriate discount rate is based on the type of cost. For internal costs, it is closely connected with the cost of borrowing. With regard to the private sector, it can be anywhere from 5 to 15%, depending on the required return on investment (Hunkeler et al., 2008). In terms of publicly funded projects, it is normally falling into the range of 3-5%(Langdon, 2007). The chosen discount rate in this study is 5% because it is related to the private sector. It can be seen from Table 4.18 that the operation costs have the highest proportion of the total life cycle costs of these engines. The dual-fuel engine is prone to higher construction costs and maintenance costs. However, it has a better cost performance in terms of the operation costs compared to the diesel engine.

Table 4.18: Summary of the LCC appraisal in the base case. Table from Paper IV.

Cost Category	20-year Cash Flow: Diesel Engine		20-year Cash Flow: Dual-fuel Engine	
	Non-discounted Costs	Discounted Costs	Non-discounted Costs	Discounted Costs
Construction costs	989K	989K	1,200K	1,200K
Operation costs	24,960K	15,553K	21,308K	13,277K
Maintenance costs	4,614K*	2,678K	5,050K*	2,940K
Labour costs	697K*	411K	720K*	425K
Part replacement costs	3,917K*	2,267K	4,330K*	2,515K
End-of-life value	17K	6K	22K	8K

* Inflated values with the inflation rate of 3.1%.
Unit K = 1000 €, Discount rate $r = 5\%$.

For life-cycle cost comparison, several measures of economic performance, i.e. economic KPIs, were provided within the LCCF, as shown in Table 4.19. Given the above-mentioned fuel price scenario, it is apparent that the dual-fuel engine is more cost-effective than the diesel engine because of having a lower NPC (17,409K versus 19,213K) and the NS greater than zero. The cost-effectiveness of the dual-fuel engine was underlined with the SIR result of 4.95. This means that the dual-fuel engine will yield an average return of €4.95 for every €1 invested.

Dealing with the uncertainties in this study is two-fold. In the first place, sensitivity analyses of the NPC against changes in fuel prices and the discount rate were conducted. In this respect, different

Table 4.19: Measures of economic performance in the base case. Table from Paper IV.

Measure of Economic Performance	20-year Economic Calculations (Discounted Costs)	
	Diesel Engine	Dual-fuel Engine
Net Present Cost (NPC)	19,213K	17,409K
Net Saving (NS)	-	1,804K
Saving-to-ratio (SIR)	-	4.95

Unit K = 1000 €.
Discount rate $r = 5\%$.

future price scenarios were defined where the prices of LNG and MGO were varied in order to find the break-even point.

- The first sensitivity is to vary the prices of LNG and MGO to find at which price the decision will be made between these engines.
  - The rise of LNG price: Figure 4.23 demonstrates the increase in the LNG price while the MGO price is kept unchanged. An inspection of these scenarios revealed that the dual-fuel engine loses the competitive advantage in the high gas price scenarios, particularly from the point where the LNG price increases by 14.6%, of 643 [€/t], which is equal to 1.3 the MGO price.

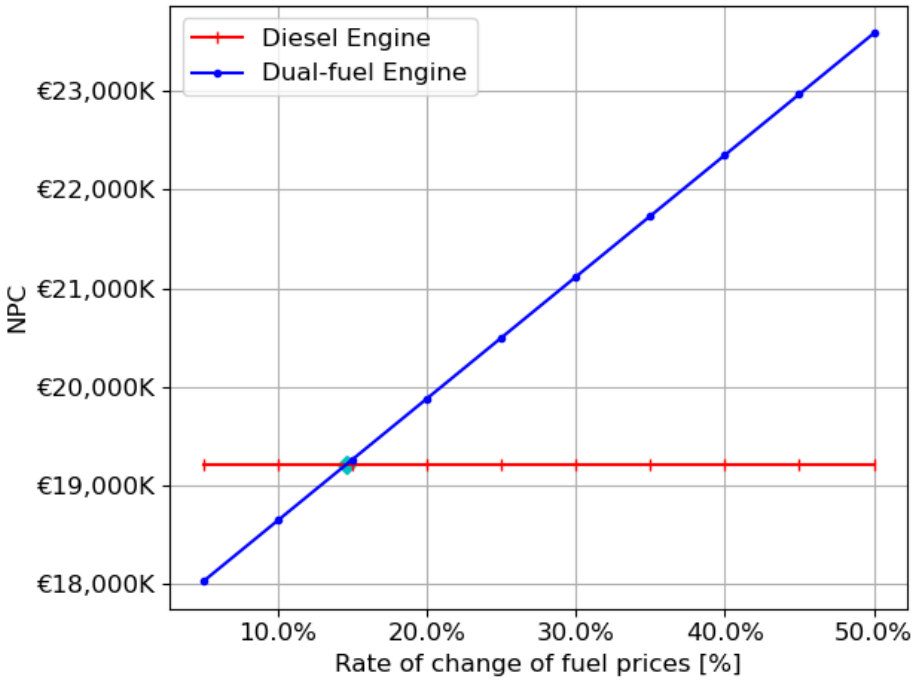

Figure 4.23: Rising LNG price and steady MGO price scenarios. Figure from Paper IV.

– The slump of MGO price: In these scenarios, the MGO price is dropping and the LNG price remains constant. Figure 4.24 shows that the crossover point occurs when the MGO price decreases by 11.6%, of 449 [€/t], which is equal to 0.8 the LNG price. Therefore, when the MGO price is less expensive than the crossover point, the dual-fuel engine is more competitive than the diesel engine.

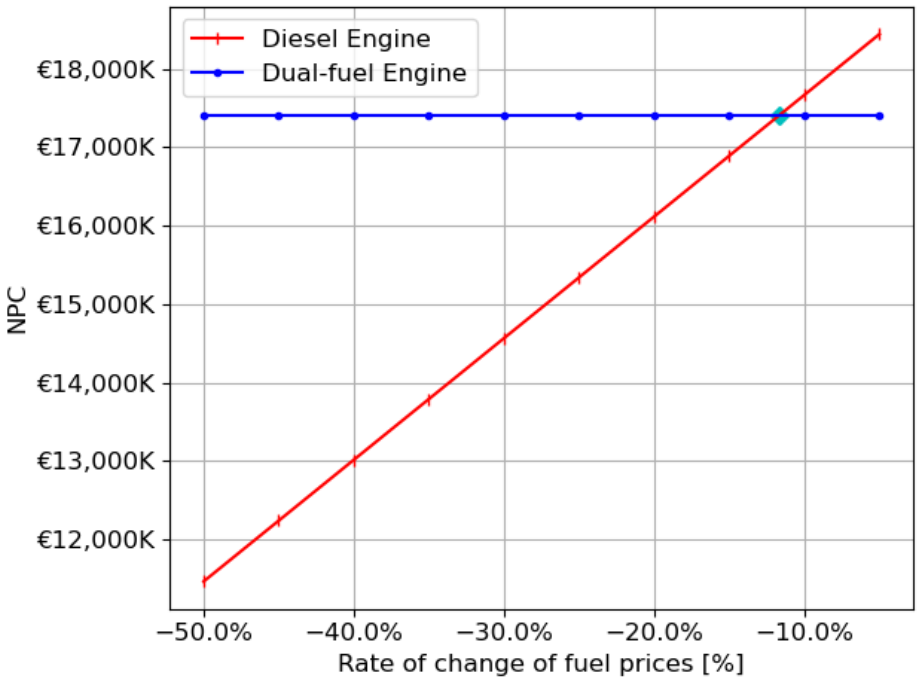

Figure 4.24: Steady LNG price and decreasing MGO price scenarios. Figure from Paper IV.

- The second sensitivity is to vary the discount rate from 1 to 10%. It is apparent from Figure 4.25 that higher discount rates lead to lower NPCs and there is no effect of discount rate on the competitiveness of the dual-fuel engine against the diesel engine.

In the second place, by performing a Monte Carlo simulation using the @RISK software, a reasonable estimate of uncertainty for the NPCs of these engines can be made. In this respect, the effect of simultaneous changes in uncertainties (i.e. uncertain variables) can be evaluated. Several uncertain variables were introduced into the model as triangular distributions. They are fuel prices, the discount rate, the inflation rate, the annual operating hours and the hourly wages, as presented in Table 4.20. Triangle distributions are generally preferred if the variable is suspected to be normally distributed but the uncertainty is rather large. If the uncertainty is rather large, a normal distribution seems to focus very little on the ends of the distribution, which is unexpected. Another significant aspect of triangle distributions is that they are better at handling asymmetry than to normal ones (Emblemsvåg, 2003). It should be noted that the minimum, most likely and maximum of fuel prices variables were obtained from a real public database (Ship & Bunker, 2021).

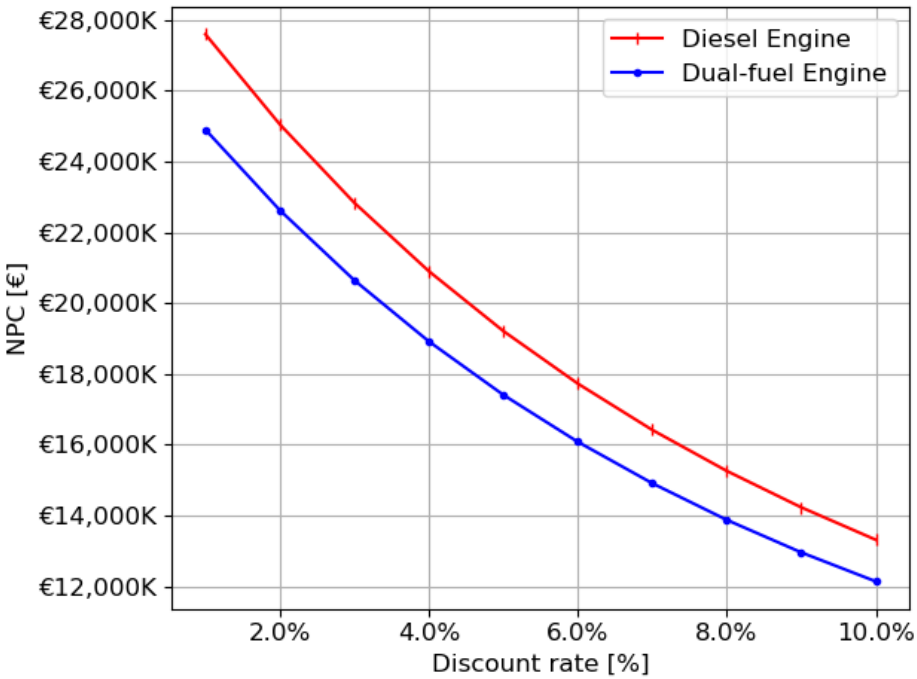

Figure 4.25: Scenarios of discount rate fluctuations. Figure from Paper IV.

Table 4.20: Triangular distributions of variables. Table from Paper IV.

Variable	(Min, Most Likely, Max)
MGO price [€/t]	(383.2, 469.4, 541.9)
LNG price [€/t]	(360.2, 482.2, 687.8)
Discount rate [%]	(1, 5, 10)
Inflation rate [%]	(1, 3.1, 5)
Annual operating hours [h/y]	(5500, 7500, 8760)
Hourly wages [€/h]	(20, 30, 46.9)

Figure 4.26 depicts the results of the Monte Carlo simulation with 10,000 iterations. It was found that dual-fuel engine gives a lower NPC with 68.6% of its cost range less than €26.7 million. The cost range for the diesel engine having the higher NPC was found between €26.7 and €29.8 million with the probability of 62%. It was concluded that the dual-fuel engine is appropriately superior to the diesel engine.

Furthermore, by using the @RISK software, it was identified from Figure 4.27 that fuel prices are the most significant cost contributor to the NPCs of these engines.

It should be borne in mind that fuel prices obtained from the real public database for conducting the LCCA in this study reflect the current high fuel price situation where the LNG price is higher than the MGO price. It is an abnormal situation and the LNG price is expected to be normalized

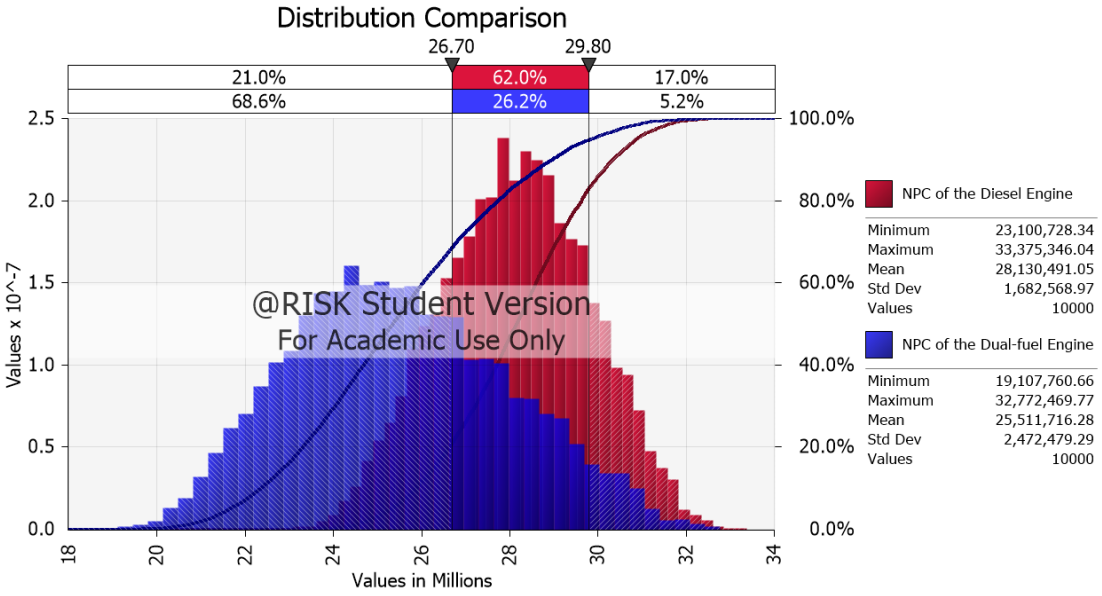

Figure 4.26: Overlay graph of the NPC of the diesel engine and the NPC of the dual-fuel engine. Figure from Paper IV.

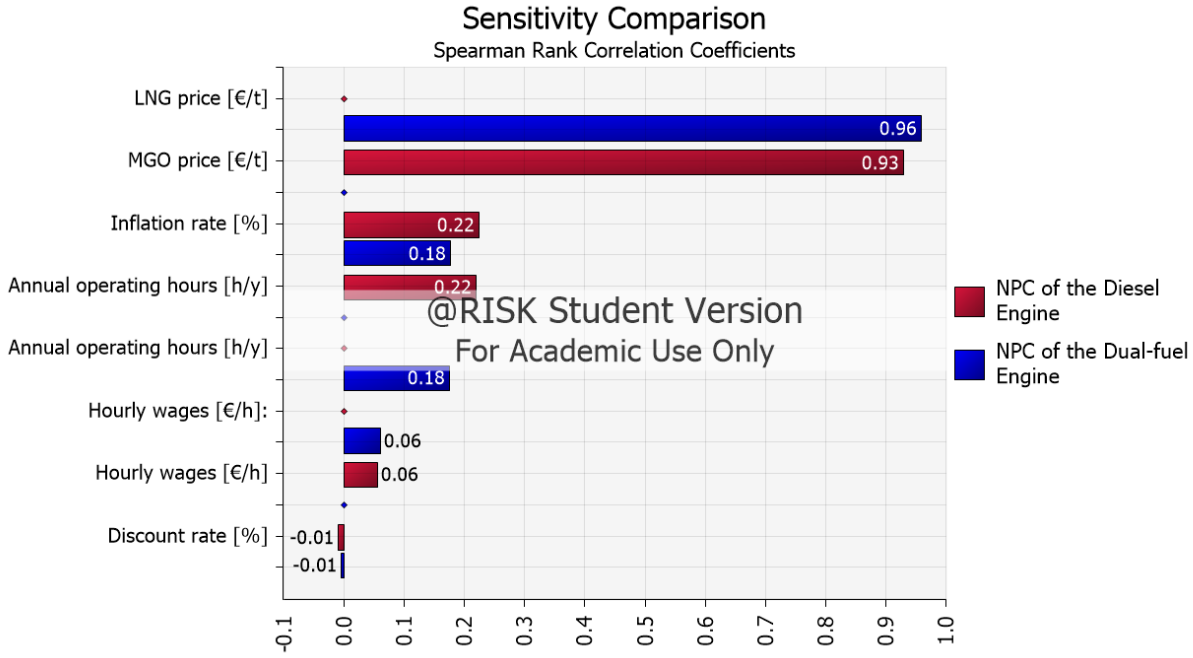

Figure 4.27: Sensitivity chart. Figure from Paper IV.

in the near future (The Loadstar, 2021). Another important aspect of using the dual-fuel engine is that it offers flexibility to ship owners based on fuel cost and availability.

For the case of carbon pricing, the carbon emission costs incurred from the operation phase were included in the LCCA. A lower discount rate should be used when considering a long time period of the social impact due to CO_2 emissions. Therefore, a chosen discount rate of 3.5% was applied for discounting back the future carbon emission costs into present value costs (Smith, 2021). Several carbon pricing scenarios were considered by adapting data gathered from World Energy Outlook 2021 (WEO2021) (OECD, 2021), as presented in Table 4.21. Such data are applied to the EU region in 2030, 2040, and 2050 correspondingly. Figure 4.28 demonstrates the annual carbon prices from 2022 to 2050. It should be noted that the carbon price for 2022 was set at zero because MBMs (i.e. IMO MBMs or EU ETS) have not been enforced in the shipping industry yet. Other annual carbon prices were determined by interpolation.

Table 4.21: CO_2 price scenarios. Table from Paper IV.

Scenario	Price (€/t-CO_2)		
	2030	2040	2050
STEPS	57.46	66.3	79.56
SDS	106.08	150.28	176.8
NZE	114.92	181.22	221

Source: OECD (2021).
STEPS: Stated Policies Scenario, SDS: Sustainable Development Scenario, NZE: Net Zero Emissions by 2050.

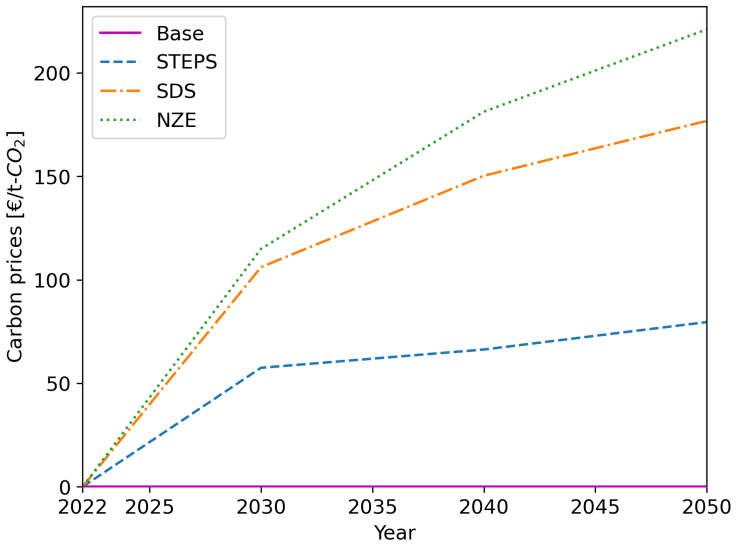

Figure 4.28: Carbon pricing scenarios. Figure from Paper IV.

The potential impact of carbon pricing on the life cycle cost performances of the studied engines was analyzed by performing a scenario analysis. As shown in Table 4.22 and Figure 4.29, the results of this analysis indicated that if MBMs are implemented, higher carbon pricing scenarios lead to higher NPCs. However, the dual-fuel engine gives lower NPCs in all carbon pricing scenarios. The results broadly support the work of other studies linking MBMs with the cost-effectiveness of emissions reduction technologies (Lagouvardou et al., 2022).

Furthermore, this study confirmed earlier findings from Paper III, showing a CO_2 emissions reduction potential of 33% when opting for the dual-fuel engine compared to the diesel engine, as shown in Table 4.23. This is corresponding to 52,291 [t] of CO_2 would be eliminated during the life-cycle of operating the engines.

Table 4.22: Measures of economic performance in carbon pricing scenarios. Table from Paper IV.

Scenario	NPC		NS
	Diesel Engine	Dual-fuel Engine	
STEPS	30,487K	24,927K	5,560K
SDS	42,585K	32,994K	9,591K
NZE	46,261K	35,446K	10,815K

Unit K = 1000 €.
Discount rate $r = 5\%$, inflation rate $I = 5\%$.
Discount rate for calculating the carbon emissions costs $r^{'} = 3.5\%$

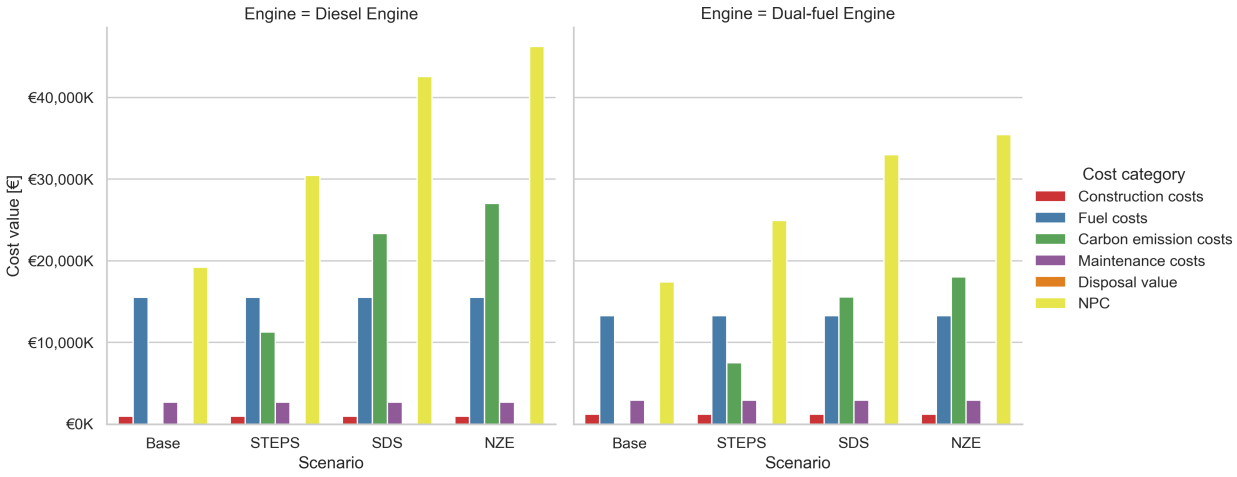

Figure 4.29: Results of 20-year discounted costs under carbon pricing scenarios. Figure from Paper IV.

Table 4.23: 20-year CO_2 emissions in operation. Table from Paper IV.

Criteria	Diesel Engine	Dual-fuel Engine
Total CO_2 emissions [t]	156,954	104,663
Amount saving [t]		52,291
Percentage reduction [%]		33%

Contributions by the author

- The conceptualization was conceived under the EU-funded SeaTech project (seatech2020.eu).
- The author developed the methodology.
- The author carried out the implementation and experiments.

- The author prepared the original draft of this study.
- The author conducted subsequent revisions under the review of the second co-author, the third co-author.

Chapter 5

Discussion

This chapter gives an in-depth discussion on the research outcomes. The first section reflects on the research findings of this thesis by reviewing the research aim and objectives formulated in Chapter 1. The second section ties together the novelty of this thesis. The third section includes a discussion on the limitations of this thesis. The final section explains the connection between the ADAF and the LCCF.

5.1 Fulfillment of the research aim and objectives

The main aim of this thesis is to contribute to the enhancement of the performance of a ship from both the operational efficiency and life-cycle economic perspectives. This was accomplished by addressing the research question and subsequent research objectives raised in Chapter 1, as depicted in Figure 1.1. In this regard, the thesis was directed towards developing an integrated data analytics framework encompassing the ADAF and the LCCF. The fulfillment of the research objectives with respect to the appended papers is presented in Table 5.1. The level of fulfillment is represented by the degree of the '+' symbol with '++' indicating the complete fulfillment. The way the objectives were accomplished is discussed in greater depth as follows.

Table 5.1: Fulfillment of research objectives in the appended papers.

	RO1 (i)	RO1 (ii)	RO1 (iii)	RO1 (iv)	RO1 (v)	RO2 (i)	RO2 (ii)	RO2 (iii)	RO2 (iv)	RO2 (v)
Paper I	+	+		+						
Paper II	++	++	++	++	++					
Paper III						+	+	+		++
Paper IV						++	++	++	++	++

RO1 (i) Provide the ADAF with a number of data analytics approaches together with domain knowledge for ship performance quantification.

The completion of this objective was based on the development of the ADAF, including components such as several analytics and the domain knowledge. The ADAF was initially proposed in Paper I and then further improved in Paper II, as detailed in Section 4.1. The flow of the ADAF in Paper II is depicted in Figure 4.4. The ADAF includes the domain knowledge, the descriptive analytics, the diagnostic analytcis, the visual analytics, and the prescriptive analytics, providing a methodological approach for data handling workflow. Under the descriptive analytics, two data anomaly detectors were proposed to deal with abnormal data pre-processing to detect data outliers and anomalies. The descriptive analytics was proposed with the development of the digital models using improved data. The diagnostic analytics was provided to identify the likely causes for the detected anomalies. The visual analytics was proposed to offer graphic representations as regards the relative correlations among parameters in the data set. Finally, the prescriptive analytics was proposed to quantify the ship's performance with respect to its operational conditions. The development of the ADAF addresses the gap in the literature for a comprehensive ship performance monitoring framework taking into account the operational conditions on a local scale. The important role of the domain knowledge should be highlighted in the ADAF, providing firm guidance for other analytics components.

RO1 (ii) Investigate the ship's localized operational conditions, including its main engine modes and associated trim-draft modes.

This objective was achieved through the development of the digital modelling in Paper I and Paper II, as elaborated in Section 4.1. The digital modelling includes engine and trim-draft models, as illustrated in Figure 4.6. Such models respectively represent the localized operational conditions with regard to engine and trim-draft modes. The relationship between these modes is illustrated in Figure 4.5. The implementation of such models was achieved with the help of the KDE and the GMMs methods for data clustering. It was uncovered that the selected ship was operating in three engine modes, denoted by three data clusters. Furthermore, under each of the engine modes, several trim-draft modes were explored, denoted by sub-clusters. The novel aspect of the digital modelling is that it revealed the ship's operational conditions from a localized perspective, allowing the observation in hindsight.

RO1 (iii) Detect data anomalies existing in the data set for improving data quality.

This objective was completed in Paper II via the descriptive analytics with two data anomaly detectors, as discussed in Section 4.1. The first data anomaly detector, based on the domain knowledge, was able to identify data outliers beyond a given minimum-maximum range of the parameters in the data set. The second data anomaly detector, based on SVD, discovered data anomalies after the construction of the digital modelling with three data clusters in engine modes. In this respect, data anomalies in the respective clusters were found, as reported in Table 4.4. Combining the domain knowledge with the SVD-based solution, the detection of data anomalies fills the gap in the literature in which data veracity has been overlooked in the maritime research domain.

RO1 (iv) Identify the relative correlations among ship performance and navigation parameters.

This objective was fulfilled in Paper I and Paper II through the visual analytics as discussed in Section 4.1, and visually depicted in Figure 4.3 and Figure 4.15 correspondingly. Meaningful information from the data set was extracted by examining the structure of each data cluster or sub-cluster, represented by its top SVs. The novelty of the visual analytics is to generate insights into the relative correlations of the parameters in a high dimensional space. Few researchers have addressed the problem of visualization of high dimensional data in the literature.

RO1 (v) Derive an operational efficiency key performance indicator (KPI), i.e. the ship performance index (SPI), for ship performance quantification in order to identify the best performance trim-draft mode under the engine modes.

This objective was attained in Paper II by offering the ship performance index SPI for ship performance quantification. Within the available information of the data set, the SPI was defined as the average main engine fuel consumption per nautical mile [Ton/NM], as expressed in Equation 4.1. The creation of the SPI provides with the capability of evaluating the ship performance in its localized operational conditions. As such, by using the resulting SPI, trim-draft mode C_1 appeared to be the best performance mode, as detailed in Table 4.5. The SPI could conceivably be a representative of an operational efficiency KPI that is relevant within the shipping sector.

RO2 (i) Provide a methodological procedure with an engineering build-up approach for conducting the life-cycle cost analysis.

This objective was accomplished by developing the LCCF, which integrates the ISO 15686-5 standard with an engineering build-up cost estimation model, as proposed in Section 4.2 and demonstrated in Figure 4.19 which was taken from Paper III. This framework was further enhanced in Paper IV, as depicted in Figure 4.22. First of all, the cost components, including the internal and external costs, were defined. Afterwards, such costs were further classified into local costs based on a breakdown analysis. At this point, a thorough investigation into the engines' main components and system up to the third level was conducted. There is a link between the third levels of the construction phase and the maintenance phase. In this respect, the maintenance costs were calculated on the basis of the parts of the engines' main components and systems under recommended maintenance intervals. Given the high level of detail under an engineering build up approach, gathering data required a great deal of effort. Subsequently, a cost model was developed taking into account the effects of discounting and inflation. The life-cycle cost comparison was carried out by proposing some economic KPIs, such as the Net Present Cost (NPC), the Net Saving (NS), and the Saving-to-Investment Ratio (SIR). Furthermore, the uncertainties were thoroughly treated by performing sensitivity analyses and the Monte Carlo simulation. In addition, the impact of MBMs on the life-cycle cost performances of the engines was examined under a carbon pricing scenario analysis.

RO2 (ii) Compare the life-cycle cost performance of the dual-fuel engine with that of a conventional diesel engine by considering several economic KPIs, including the Net Present Cost (NPC), the Net

Saving (NS), and the Saving-to-Investment Ratio (SIR).

This objective was completed by employing the cost model to compute the NPC, the NS and the SIR of each engine for comparison, as elaborated in Section 4.2. While Paper III involved computing the NPC, Paper IV provided supplemental measures including the NS and the SIR. The results of such measures (i.e. economic KPIs) are presented in Table 4.15 and Table 4.16 which were extracted from Paper III. Paper IV formed a detailed picture of these results, as presented in Table 4.19. Within the given fuel price setting, the dual-fuel engine appears to be a competitive technology in comparison with the diesel engine because of having a lower NPC, the NS greater than zero and the SIR greater than 1.0.

RO2 (iii) Deal with uncertainties by conducting sensitivity analyses and a Monte Carlo simulation.

This objective was achieved in Paper IV through the sensitivity analyses and the Monte Carlo simulation. As discussed in Section 4.2, Paper III conducted the sensitivity analysis with only two fuel price scenarios. Paper IV simulated various scenarios to allow for the uncertainties and to test how pessimistic and optimistic variations across a range of uncertainties can affect the NPCs of the engines. The first sensitivity is fuel prices and the analysis was done by varying the prices of LNG and MGO, as shown in Figure 4.23 and Figure 4.24 which were taken from Paper IV. By doing this, the indicative thresholds for the competitiveness of the dual-fuel engine versus the diesel engine can be identified. When the LNG price becomes more expensive, i.e. increases by 14.6%, the dual-fuel engine starts to be less competitive than the diesel engine. The second sensitivity is to vary the discount rate, as shown in Figure 4.25. Such analysis revealed that the dual-fuel engine is more cost-effective than the diesel engine, irrespective of changes in the discount rate.

In terms of the Monte Carlo simulation, it is capable of introducing the uncertainties into the model by triangular distributions and assessing the impact of combined changes of the uncertainties at the same time. The results showed an adequate degree of confidence when switching to the dual-fuel engine, as depicted in Figure 4.26. Moreover, the results revealed that fuel prices are the most dominant cost driver, as demonstrated in Figure 4.27.

RO2 (iv) Assess the implications of MBMs on the life-cycle cost performances of the studied engines.

The fulfillment of this objective was gained in Paper IV by attaching the carbon emission costs to the cost model, as detailed in Section 4.2. To do so, foreseeable carbon pricing scenarios adapted from WEO2021 were considered, as visually demonstrated in Table 4.21 and Figure 4.28. A carbon pricing scenario analysis was carried out to evaluate and compare the NPC and the NS under the respective scenarios, as presented in Table 4.22 and depicted in Figure 4.29. It was found that there are substantial increases in the carbon emission costs and the NPCs in higher carbon price scenarios. However, the dual-fuel engine is still more cost-effective than the diesel engine with lower NPCs in all scenarios. The results are suggestive of a link between MBMs and the cost competitiveness of emissions reduction technologies.

RO2 (v) Derive an environmental KPI from the environmental impact (EI) of switching over to the dual-fuel engine.

This objective was achieved in Paper III and Paper IV by quantifying and comparing the CO_2 emissions released from the life-cycle of operating the studied engines, as mentioned in Section 4.2. This was done by considering Equation (3.20) and the carbon emission conversion factor C_F provided in Table 4.12. An environmental KPI was derived through the estimation of the potential emissions saving by applying the dual-fuel engine, as presented in Table 4.17 and 4.23 respectively. It was concluded that the potential CO_2 emissions reduction could be 33% when opting for the dual-fuel engine compared to the diesel engine.

5.2 Research novelty

The novelty of this thesis stems from the integrated data analytics framework developed for enhancing both the environmental and economic performance of a vessel via the combination of ML/DA approaches and the life-cycle cost approach. Keeping in line with the stated research aim and the associated research objectives as demonstrated in Figure 1.1, two distinct frameworks were developed: the ADAF and the LCCF. Each of them has theoretical, industrial and policy implications on maritime decarbonization, as summarized in Figure 5.1. Having attempted to find solutions aligned with the IMO's regulatory measures towards maritime decarbonization, the ADAF has the potential to fall under the operational measure category while the LCCF could be taken advantage of in order for ship owners to take retrofitting actions on innovative technologies (i.e. technical measures) for regulatory compliance and emission profile improvement. More details on the novelties of this thesis will be given below.

As regards the ADAF, as outlined in Bui and Perera (2021), there are many related studies in the literature applying similar methods, i.e. using ML models. However, many of them have used artificial neural networks (ANNs) which are considered 'black-box' methods. Moreover, data anomaly detection has been overlooked in the investigated areas in the maritime research domain. In addition, the visual relationships among factors affecting fuel consumption in a high-dimensional space have not been dealt with in depth. Furthermore, studies that integrate domain knowledge into ML models are rather scarce. Another noticeable gap is that research to date has not yet conducted to explore and monitor ship performance under the local operational conditions. The established ADAF addresses the aforementioned gaps by offering a novel understanding of the operational conditions of a selected ship at the local level (i.e. engine and trim-draft modes). Several outcomes derived from the ADAF include a number of data analytics coupled with the domain knowledge for the investigation of the ship's localized operational conditions, the detection of data anomaly, the identification of the relative correlations among parameters, and the creation of an operational efficiency KPI (i.e. the SPI) for ship performance quantification. The findings emerged from the ADAF add to the rapidly expanding field of fault detection, diagnostics of ship systems, ship performance and condition monitoring towards operational energy efficiency.

Given the data-driven nature of the ADAF, it can potentially be applied to various applications. With technological advancements and digitalization transformation towards Shipping 4.0, an example of this application is digital twins. Digital twins are developed from digital models to replicate ship monitoring systems. In this respect, all useful sensor data regarding the ship's operating conditions, weather conditions and more are gathered and processed by a digital copy to produce valuable insights. Such insights are then applied back to the original physical monitoring systems to improve operational decision-making via performance monitoring, diagnostics and corrective actions. Therefore, the findings generated through the ADAF are of interest to ship owners and operators who strive for enhancing energy efficiency during ship operation. In this regard, they will benefit from data analytics tools and the operational efficiency KPI that advise them at which engine/ trim-draft mode will necessary energy-efficient manners such as eco-maneuvering be made, for example, operating the engine in the load range with the lowest specific fuel consumption. This could potentially be applied across the fleet management operations for further energy efficiency improvement and comparison.

In terms of the LCCF, Mondello, Salomone, Saija, Lanuzza, and Gulotta (2021) pointed out a need for adapting the ISO 15686-5 standard for conducting LCCA rather than using the ISO 14040/14044 standards which are designed for life-cycle environmental assessment. As detailed in Bui, Perera, and Emblemsvåg (2022), a number of studies using the LCC method have been undertaken in order to evaluate the economic impacts of technological alternatives and ship propulsion systems. Despite this interest, little research has been undertaken to examine the life-cycle cost performance of a marine dual-fuel engine from the retrofitting perspective with a complete account of such an engine with respect to its main components and systems. Moreover, most LCC studies in the maritime research domain have not treated the inherent uncertainty in much detail. In this respect, these studies have tended to focus on deterministic approaches (e.g. sensitivity analysis) which do not allow for the probabilities of different outcomes. With these gaps in mind, in the LCCF, a methodological procedure for performing LCCA was developed and applied to the dual-fuel engine and the diesel engine for life-cycle cost comparison by using a set of economic KPIs (i.e. the NPC, NS and SIR). This was achieved by encompassing the ISO 15686-5 standard and an engineering build-up approach with data collected from numerous sources. The theoretical implication of the LCCF is that it represents a comprehensive examination of the whole main components and systems of the studied engines.

Another novel aspect of the LCCF is the in-depth analysis of the inherent uncertainties which were conducted by the sensitivity analyses and the Monte Carlo simulation. The sensitivity analyses were performed to model the effects of varying key uncertain variables (i.e. fuel prices and the discount rate) one at a time to identify the break-even point that leads to the preferred selection of one engine over the other. The Monte Carlo simulation, considered a probabilistic approach, has the capability to evaluate the impacts of combined changes in uncertain variables simultaneously. In this respect, the probabilities of having the NPCs of the engines were revealed.

Furthermore, the LCCF provided not only the economic KPIs, i.e. the NPC, NS and SIR, but also an environmental KPI, i.e. the environmental impact (EI) of switching over to the dual-fuel engine. In this respect, the dual-fuel engine could offer a 33% reduction of CO_2 emissions in comparison with the diesel engine. The EI results derived from the LCCF have a practical implication for the EEXI and CII compliance. As detailed in Section 2.2, the EEXI and CII were adopted by the IMO in June 2021 and will take effect from 2023 onwards. The EEXI formula takes the simplest form as follows (Baldi & Coraddu, 2022)

$$EEXI = \frac{CO_2 emissions}{TransportWork} \tag{5.1}$$

The current metric to calculate the CII is the Annual Efficiency Ratio (AER) which can be expressed as (Baldi & Coraddu, 2022)

$$AER = \frac{\sum_j C_j}{DWT \times D_j} \tag{5.2}$$

where for each voyage j the C_j is the CO_2 emissions, D_j is the distance traveled, DWT is the deadweight (i.e. the ship's cargo-carrying capacity).

Given the EI results, if the selected bulk carrier is retrofitted with the dual-fuel engine, it is compliant with the EEXI (i.e. having the attained EEXI lower than the required EEXI). Furthermore, the ship will achieve a better CII rating on an annual basis. However, concerns have arisen which question the effectiveness of the CII and call for improvement (Norton, PE, Merrill, Brouwer, & Correa, 2022; S. Wang, Psaraftis, & Qi, 2021). One of the reasons emerged from such concerns is that the CII assumes the ship is always loaded with its DWT capacity - a fixed value.

The final novelty of the LCCF is that it has been one of the first investigations to thoroughly examine the impacts of MBMs on the life-cycle cost competitiveness of emissions abatement technologies (i.e. the dual-fuel engine). Having several carbon pricing scenarios simulated, the correlation between the adoption of emissions reduction technologies (e.g. the dual-fuel engine) and the potential introduction of MBMs was identified. This implies that MBMs are needed to promote carbon emissions reduction in shipping linked to future energy technologies.

Therefore, the findings gained from the LCCF add to a growing body of literature on shipping investment appraisals and LCCA in the maritime context. In addition, the findings should be of value to ship-owners wishing to make retrofitting decisions on innovative emissions reduction technologies for EEXI compliance in order to improve their environmental footprint and remain attractive. Investors and lenders are another target group that could benefit from the outcomes of the LCCF. In this respect, they are in search of investment opportunities to provide capital for the right technologies.

Taken together, with various KPIs derived from the integrated data analytics framework, the overall

novelty of this thesis is that it marks the first attempt to incorporate ML/DA approaches and the life-cycle cost approach into a single study for enabling better decision-making with respect to ship performance monitoring and investment decisions on an innovative emissions reduction technology (i.e. the dual-fuel engine).

<table>
<tr><td rowspan="5">Research Question</td><td rowspan="5">Aim</td><td>RO</td><td>Paper</td><td>Main Points</td><td>Implications</td></tr>
<tr><td rowspan="2">RO1</td><td>Paper I
Background study</td><td>• Develop a preliminary framework for a cost-effective and energy efficient shipping
• Digital modelling for identifying the ship localized operational conditions (engine and trim-draft modes) via data clustering
• Visual analytics for identifying the relative correlations among parameters in the data set</td><td rowspan="2">Theoretical:
• The findings add to the rapidly expanding field of fault detection, diagnostics of ship systems, and ship performance monitoring
Industrial:
• The findings are of interest to ship owners and operators who strive for enhancing energy efficiency during ship operation
• The findings could potentially be applied across the fleet management operations for further energy efficiency improvement.</td></tr>
<tr><td>Paper II</td><td>• Develop the ADAF encompassing a set of data analytics and the domain knowledge
• Digital modelling for identifying the ship localized operational conditions (engine and trim-draft modes) via data clustering
• Descriptive analytics for detecting data anomalies in the data set
• Visual analytics for identifying the relative correlations among ship performance and navigation parameters in the data set
• Prescriptive analytics for deriving an operational efficiency KPI, i.e. the SPI, for ship performance quantification in order to find the best performance trim-draft mode under the engine modes</td></tr>
<tr><td rowspan="2">RO2</td><td>Paper III
Background study</td><td>• Develop the LCCF for comparing the life-cycle cost performance of the dual-fuel engine with that of a conventional diesel engine
• NPC as an evaluation indicator
• The dual-fuel engine is found to be more cost-effective than the diesel engine except for the high fuel price differential scenario.
• The dual-fuel engine has the potential for CO_2 emission reduction of 33%</td><td rowspan="2">Theoretical:
• The findings add to a growing body of literature on shipping investment appraisals and LCCA in the maritime context
Industrial:
• The findings should be of value to ship-owner wishing to make retrofitting decisions on innovative emissions reduction technologies
• Investors and lenders could benefit from the findings to support decision-making
Policy:
• MBMs are required to promote carbon emissions reduction through the use of future energy technologies</td></tr>
<tr><td>Paper IV</td><td>• Enhance the LCCF framework proposed in Paper III
• Compare the life-cycle cost performance of the dual-fuel engine with that of a conventional diesel engine under uncertainties
• NPC, NS and SIR as economic KPIs
• Within a given fuel price scenario, the dual-fuel engine is appears to be a competitive technology in comparison with the diesel engine
• However, the competitiveness of the dual-fuel engine is prone to higher gas price scenarios
• There is an adequate degree of confidence when adopting the dual-fuel engine in the default setting of fuel prices
• Fuel prices are identified as the most dominant cost driver
• In all carbon pricing scenarios simulated, the dual-fuel engine is still more cost-competitive than the diesel engine
• EI as an environmental KPI: a 33% reduction in CO_2 emissions is confirmed when applying the dual-fuel engine</td></tr>
</table>

Figure 5.1: Research implications related to objectives

5.3 Limitations

A number of potential limitations need to be noted regarding this thesis. In light of the established ADAF, the LCCF and the subsequent findings, the limitations in each framework need to be acknowledged.

As far as the ADAF is concerned, its implementation was showcased through a case study of one selected ship. The findings derived from the ADAF would have been improved with the inclusion of other ships for comparison purposes. If that is the case, the ADAF could be useful for fleet optimization with regard to emission performance and energy efficiency. However, obtaining commercial data from shipping companies can always be challenging for the research community. An additional limitation of the ADAF is the lack of the ship's loading conditions in the data set. Recall the resulting SPI findings presented in Section 4.1.

$$SPI_i = \frac{FC_i}{D_i} \implies SPI_i = \frac{FC_{avg,i}}{24\ STW_{avg,i}} \tag{5.3}$$

The SPI is an expression of the ship's average main engine fuel consumption per nautical mile [t/NM]. When it comes to energy efficiency improvement, it is required to reduce the carbon intensity (i.e. carbon generated per transport work). The IMO's Energy Efficiency Operational Index (EEOI), which is a voluntary monitoring tool, is defined as the ratio of the CO_2 emissions per the actual cargo carried and the distance traveled [t-CO_2/(t-cargo×NM)]. Therefore, the SPI findings need to be interpreted cautiously due to the absence of the ship's loading conditions (i.e. cargo data). This underlines the difficulty of getting such data because they are considered sensitive.

Regarding the LCCF, it has certain limitations in terms of excluding the external costs due to air pollution resulting from the construction phase (i.e. mainly from the iron and steel-making processes) and the end-of-life phase (i.e. from the disposal process). The findings generated from the LCCF would have been enhanced with such cost data for a socio-economic impact assessment. Furthermore, the maintenance cost for handling LNG tanks was not considered. Another source of limitation is the possibility of having a higher installation cost of the LNG tank system for the dual-fuel engine compared to that of the MGO tank system for the diesel engine. Due to time constraints and commercial reasons, such data were not included in the LCCF.

Furthermore, it is generally understood that the so-called 'methane slip' can be occurred when the dual-fuel engine is running in the gas mode with LNG as main fuel. Methane slip refers to unburned methane released into the atmosphere when LNG is burned. Methane is regarded as a highly potent GHG with a global warming potential more many times than that of CO_2 (IPCC, 2014). However, according to the engine manufacturer (i.e. Wärtsilä), methane slip reduction on LNG-fuelled ships has been improved thanks to technological advancements (Huhmarsalo, Mannelin, & Puputti, 2021). Furthermore, in the case of carbon pricing under the LCCF, carbon prices obtained from WEO2021 are also applied to methane (Bui et al., 2022). It is also important to stress that the dual-fuel

engine can run on bio-LNG which further reduce CO_2 emissions. However, a discussion on the use of bio-LNG lies beyond the scope of this thesis.

5.4 The connection between the ADAF and the LCCF

It has been assumed that the selected ship will be retrofitted with the dual-fuel engine. However, as mentioned in Section 5.3, the lack of the loading conditions (i.e. cargo data) from the ADAF added caution when the LCCF was conducted. For this reason, in the LCCF, the dual-fuel engine was compared with another diesel engine with the same number of cylinders for a fair comparison, as shown in Table 4.6.

Nonetheless, it is believed that there is a direct connection between the ADAF and the LCCF, as depicted in Figure 5.2. In this regard, from each identified engine mode (i.e. represented by data clusters A, B, and C) from the ADAF, the annual operating hours and the loading conditions can be extracted and then fed into the operation phase of the LCCF for calculating the operation costs (i.e. fuel costs). It is important to note that the loading conditions (i.e. cargo data) are represented as a function of the engine loads. Therefore, if the loading conditions are given, the engine loads can be found.

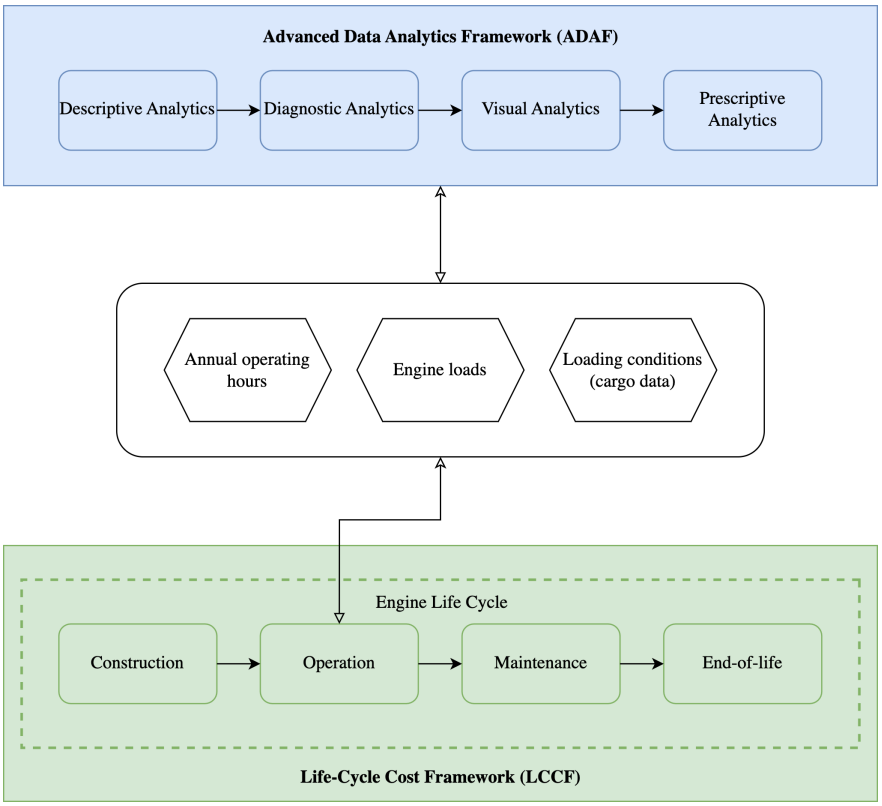

Figure 5.2: The connection between the ADAF and the LCCF

Chapter 6

Conclusions

This final chapter concludes the thesis by presenting concluding remarks and providing an outlook for future work.

6.1 Concluding remarks

The shipping industry is undergoing a revolutionary transition, driven by the regulatory and commercial drivers as mentioned in Section 2.2. Such transition is demanding a basket of solutions that accord with the IMO's technical and operational measures. From the technical perspective, retrofitting existing ships with state-of-the-art technologies should be one of the top priorities considering the vast number of ships on the waters. In terms of the operational perspective, stepping up employment of digital tools by utilizing AI, ML and DA techniques can help to lower emissions during ship operations. The overarching aim of this thesis was to help ship-owners leverage digitalization with ML and DA techniques for quantifying the performance of a selected ship while retrofitting the ship with an innovative emissions reduction technology, i.e. the dual-fuel engine, taking into account the total life cycle cost impact of such an engine. This was accomplished by developing an integrated data analytics framework combining the ADAF and the LCCF with ML/DA and life-cycle cost approaches.

The established ADAF includes the development of a number of data analytics approaches including the descriptive, diagnostic, visual and prescriptive analytics along with the domain knowledge. The findings gained from the ADAF have identified the ship's localized operational conditions, i.e. engine and trim-draft modes, represented by clusters and sub-clusters respectively. The second major finding is that a number of data anomalies under the respective clusters were detected for data quality improvement. The findings have also shown the relative correlations among the investigated parameters. One of the more significant findings emerged from the ADAF is that an operational KPI, i.e. the SPI, was derived for quantifying the ship's performance attached to each of the respective conditions. In this respect, trim-draft mode C_1 was found to be the best performance

mode. The findings have theoretical implications with extended knowledge regarding fault detection, diagnostics of ship systems and ship performance monitoring in the current literature. In terms of industrial implications, the findings are beneficial to ship-owners and ship operators interested in improving their operational energy efficiency.

By encompassing the ISO-15685 and an engineering build-up approach, the LCCF has proven to be a comprehensive methodological procedure to perform LCCA. Via the implementation of the LCCF using several economic KPIs (i.e., the NPC, NS and SIR), it has been revealed that the dual-fuel engine is an economically viable technology compared to a traditional diesel engine under a given fuel price scenario. However, the sensitivity analyses have shown that the cost-effectiveness of the dual-fuel engine is prone to higher gas prices. Within the default setting of fuel prices, the Monte Carlo simulation has shown an adequate degree of confidence when applying the dual-fuel engine. Furthermore, fuel prices have emerged as the dominant factor that impacts the total life cycle costs of the studied engines. In response to current discussions on MBMs, the carbon pricing scenario analysis has confirmed the relevance of the potential enforcement of MBMs to the cost-effectiveness of emission abatement technologies. It has also demonstrated that the dual-fuel engine is still more cost-competitive than the diesel engine. Irrespective of fuel price and carbon pricing scenarios, the dual-fuel has an environmental impact (EI) which can conceivably result in a 33% reduction in CO_2 emissions compared to the diesel engine. The findings make a theoretical contribution to the current literature on LCCA and shipping investment appraisals. Furthermore, the findings are particularly relevant for ship-owners in their engine retrofitting decision-making for regulatory compliance. Investors might also find value from the findings for their decision-making. From a policy perspective, the findings have important implications for developing MBMs to promote the use of future emissions reduction technologies.

Overall, this thesis is one of the first studies utilizing ML/DA approaches coupled with the life-cycle cost approach to derive various KPIs (i.e., the SPI, NPC, NS, SIR and EI) for enhancing the environmental and life-cycle economic performance in shipping.

6.2 Recommendations for future work

The developed ADAF, with several data analytics approaches contained within, is a major area of interest within the fields of fault detection, ship systems diagnostics and ship performance monitoring. Future research directions that can further extend the respective fields are suggested below:

- A future study investigating the area of data anomaly detection would be interesting. This can be done by adopting several approaches such as probabilistic-based, distance-based, clustering-based or reconstruction-based models (Tan, Steinbach, Karpatne, & Kumar, 2019).
- Another possible area of future research would be data recovery using ML techniques.
- The prospect of being able to carry out a comparative study with more available data sets

from other ships serves as an incentive for future research.

- Regarding the absence of the loading conditions (i.e. cargo data), the research on the ADAF can be further extended with some assumptions on such conditions. This can be validated with the help of crew-members onboard. In this way, several engine modes found from the ADAF can be further studied under the loading conditions and environmental conditions. In this respect, further investigation can be conducted on the linkage between the SPI findings and the CII.

The findings derived from the LCCF suggest the following directions for future research:

- The findings from the LCCF would be enhanced if more cost data could be gathered such as installation costs of fuel tank systems (MGO for the diesel engine and LNG for the dual-fuel engine) and the cost of handling LNG tanks in the maintenance phase.
- Further research is needed to account for the external costs from the construction and end-of-life phases to carry out a socio-economic assessment.
- Further research should be undertaken to assess the environmental impacts of the dual-fuel engine using the life-cycle assessment approach.
- As ship owners and operators are exploring technological solutions that reduce fuel usage and emissions in response to the drivers for decarbonization, LCCA is an intriguing area that could be usefully explored in further research on techno-economic assessment of future energy technologies.
- More research is required to conduct LCCA considering the aspect of the circular economy.

Bibliography

Akaike, H. (1974, December). A new look at the statistical model identification. *IEEE Transactions on Automatic Control*, *19*(6), 716–723. doi: 10.1109/TAC.1974.1100705

Andersson, K. (2022, January). Chapter 1 - The shipping industry and the climate. In F. Baldi, A. Coraddu, & M. E. Mondejar (Eds.), *Sustainable Energy Systems on Ships* (pp. 3–25). Elsevier. doi: 10.1016/B978-0-12-824471-5.00007-4

Ayodele, T. (2010, February). Types of Machine Learning Algorithms.. doi: 10.5772/9385

Balcombe, P., Brierley, J., Lewis, C., Skatvedt, L., Speirs, J., Hawkes, A., & Staffell, I. (2019, February). How to decarbonise international shipping: Options for fuels, technologies and policies. *Energy Conversion and Management*, *182*, 72–88. doi: 10.1016/j.enconman.2018.12.080

Baldi, F., & Coraddu, A. (2022, January). Appendix B - Towards halving shipping GHG emissions by 2050: The IMO introduces the CII and the EEXI. In F. Baldi, A. Coraddu, & M. E. Mondejar (Eds.), *Sustainable Energy Systems on Ships* (pp. 513–517). Elsevier. doi: 10.1016/B978-0-12-824471-5.00028-1

Bishop, C. (2006). *Pattern Recognition and Machine Learning*. New York: Springer-Verlag.

Bouman, E. A., Lindstad, E., Rialland, A. I., & Strømman, A. H. (2017, May). State-of-the-art technologies, measures, and potential for reducing GHG emissions from shipping – A review. *Transportation Research Part D: Transport and Environment*, *52*, 408–421. doi: 10.1016/j.trd.2017.03.022

Bourboulis, S., Krantz, R., & Mouftier, L. (2022, May). *Alternative fuels: Retrofitting ship engines.* https://www.globalmaritimeforum.org/news/alternative-fuels-retrofitting-ship-engines.

Brunton, S. L., & Kutz, J. N. (2019). *Data-Driven Science and Engineering: Machine Learning, Dynamical Systems, and Control*. Cambridge: Cambridge University Press. doi: 10.1017/9781108380690

Brynolf, S., Baldi, F., & Johnson, H. (2016). Energy Efficiency and Fuel Changes to Reduce Environmental Impacts. In K. Andersson, S. Brynolf, J. F. Lindgren, & M. Wilewska-Bien (Eds.), *Shipping and the Environment : Improving Environmental Performance in Marine Transportation* (pp. 295–339). Berlin, Heidelberg: Springer. doi: 10.1007/978-3-662-49045-7_10

Bui, K. Q., Ölçer, A. I., Kitada, M., & Ballini, F. (2021, February). Selecting technological alternatives for regulatory compliance towards emissions reduction from shipping: An inte-

grated fuzzy multi-criteria decision-making approach under vague environment. *Proceedings of the Institution of Mechanical Engineers, Part M: Journal of Engineering for the Maritime Environment*, *235*(1), 272–287. doi: 10.1177/1475090220917815

Bui, K. Q., & Perera, L. P. (2021, September). Advanced data analytics for ship performance monitoring under localized operational conditions. *Ocean Engineering*, *235*, 109392. doi: 10.1016/j.oceaneng.2021.109392

Bui, K. Q., Perera, L. P., & Emblemsvåg, J. (2022, December). Life-cycle cost analysis of an innovative marine dual-fuel engine under uncertainties. *Journal of Cleaner Production*, *380*, 134847. doi: 10.1016/j.jclepro.2022.134847

Carlo, R., Marc, B. J., Fuente, S., Suarez de la, Smith, T., & Søgaard, K. (2020, January). *Aggregate investment for the decarbonisation of the shipping industry.* UMAS.

Cheremisinoff, N. P. (2016). *Pollution control handbook for oil and gas engineering.* Hoboken, New Jersey: John Wiley & Sons, Inc.

DNV. (2021). *Maritime Forecast to 2050* (Tech. Rep.). Author.

DNV. (2022). *Maritime Forecast to 2050* (Tech. Rep.). Author.

Emblemsvåg, J. (2003). *Life-cycle costing: Using activity-based costing and Monte Carlo methods to manage future costs and risks.* Hoboken, N.J: Wiley.

Eurostat. (2022a, March). *Hourly labour costs.* https://ec.europa.eu/eurostat/statistics-explained/index.php?title=Hourly_labour_costs.

Eurostat. (2022b). *Inflation in the euro area.* https://ec.europa.eu/eurostat/statistics-explained/index.php?title=Inflation_in_the_euro_area.

Global Maritime Hub. (2021, June). *Bunker Prices Weekly Outlook – Week 24.* https://globalmaritimehub.com/bunker-prices-weekly-outlook-week-24.html.

Greengate Metals. (n.d.). *UK Scrap Metal Prices 2021, Manchester - Greengate Metals Scrap Yard.* https://www.greengatemetals.co.uk/scrapmetal/prices.

Halim, R. A., Kirstein, L., Merk, O., & Martinez, L. M. (2018, July). Decarbonization Pathways for International Maritime Transport: A Model-Based Policy Impact Assessment. *Sustainability*, *10*(7), 2243. doi: 10.3390/su10072243

Huhmarsalo, M., Mannelin, M., & Puputti, H. (2021, May). *Fueling the future: Delivering fuel efficiency and cutting greenhouse gas emissions through methane slip reduction.*

Hunkeler, D., Lichtenvort, K., & Rebitzer, G. (Eds.). (2008). *Environmental life cycle costing.* Pensacola, Fla. : Boca Raton: SETAC ; CRC Press.

IACCSEA. (n.d.). *Marine SCR - a proven and viable technology.* https://www.iaccsea.com/faq/marine-scr/.

IMO. (2011). *Inclusion of regulations on energy efficiency for ships in MARPOL Annex VI* (Tech. Rep.). London, UK: International Maritime Organization (IMO).

IMO. (2014). *Third IMO GHG Study 2014* (Tech. Rep.). London, UK: International Maritime Organization (IMO).

IMO. (2018). *Initial IMO Strategy on Reduction of GHG Emissions from Ships. IMO Resolution MEPC.304(72)* (Tech. Rep.). London, UK: International Maritime Organization (IMO).

IMO. (2020). *Fourth IMO GHG Study 2020* (Tech. Rep.). London, UK: International Maritime Organization (IMO).

IMO. (2021a, June). *Further shipping GHG emission reduction measures adopted.* https://imopublicsite.azurewebsites.net/en/MediaCentre/PressBriefings/pages/MEPC76.aspx.

IMO. (2021b). *IMO's work to cut GHG emissions from ships.* https://www.imo.org/en/MediaCentre/HotTopics/Pages/Cutting-GHG-emissions.aspx.

IMO. (2022). *Marine Environment Protection Committee (MEPC) - 78th session, 6-10 June 2022.* https://www.imo.org/en/MediaCentre/MeetingSummaries/Pages/MEPC-78th-session.aspx.

IPCC. (2014). *Climate Change 2013 – The Physical Science Basis: Working Group I Contribution to the Fifth Assessment Report of the Intergovernmental Panel on Climate Change.* Cambridge: Cambridge University Press. doi: 10.1017/CBO9781107415324

Isermann, R. (2006). Fault detection with limit checking. In R. Isermann (Ed.), *Fault-Diagnosis Systems: An Introduction from Fault Detection to Fault Tolerance* (pp. 95–110). Berlin, Heidelberg: Springer. doi: 10.1007/3-540-30368-5_7

ISO. (2017, July). *ISO 15686-5:2017 Buildings and constructed assets — Service life planning — Part 5: Life-cycle costing.* International Organization for Standardization (ISO).

Jalkanen, J.-P., Johansson, L., Kukkonen, J., Brink, A., Kalli, J., & Stipa, T. (2012, March). Extension of an assessment model of ship traffic exhaust emissions for particulate matter and carbon monoxide. *Atmospheric Chemistry and Physics*, *12*(5), 2641–2659. doi: 10.5194/acp-12-2641-2012

Kneifel, J., & Webb, D. (2022, May). *NIST Handbook 135 Life-Cycle Costing Manual for the Federal Energy Management Program.* National Institute of Standards and Technology U.S. Department of Commerce.

Lagouvardou, S., & Psaraftis, H. N. (2022, January). Implications of the EU Emissions Trading System (ETS) on European container routes: A carbon leakage case study. *Maritime Transport Research*, *3*, 100059. doi: 10.1016/j.martra.2022.100059

Lagouvardou, S., Psaraftis, H. N., & Zis, T. (2022, May). Impacts of a bunker levy on decarbonizing shipping: A tanker case study. *Transportation Research Part D: Transport and Environment*, *106*, 103257. doi: 10.1016/j.trd.2022.103257

Langdon, D. (2007, May). *Life Cycle Costing (LCC) as a contribution to sustainable construction: A common methodology* (Final Report). Brussels: European Commission.

Metzger, D. (2022, March). Market-based measures and their impact on green shipping technologies. *WMU Journal of Maritime Affairs*, *21*(1), 3–23. doi: 10.1007/s13437-021-00258-8

Mondello, G., Salomone, R., Saija, G., Lanuzza, F., & Gulotta, T. M. (2021, September). Life Cycle Assessment and Life Cycle Costing for assessing maritime transport: A comprehensive literature review. *Maritime Policy & Management*, *0*(0), 1–21. doi: 10.1080/03088839.2021.1972486

Norton, S., PE, J. H., Merrill, K., Brouwer, I., & Correa, L. (2022, May). *A Perspective on IMO Efficiency Measures: Opportunities for Improvement* (Tech. Rep.). Blue Sky Maritime Coalition.

OECD. (2021). *World Energy Outlook 2021.* Paris: Organisation for Economic Co-operation and Development (OECD).

Ölçer, A. I. (2018). Introduction to Maritime Energy Management. In A. I. Ölçer, M. Kitada, D. Dalaklis, & F. Ballini (Eds.), *Trends and Challenges in Maritime Energy Management* (pp. 1–12). Springer International Publishing. doi: 10.1007/978-3-319-74576-3_1

Palmejar, E., & Chubb, N. (2022). *The Learning Curve: The state of artificial intelligence in maritime* (Tech. Rep.). Thetius - Lloyd's Register.

Perera, L. P. (2016, January). Marine Engine Centered Localized Models for Sensor Fault Detection under Ship Performance Monitoring. *IFAC-PapersOnLine*, *49*(28), 91–96. doi: 10.1016/j.ifacol.2016.11.016

Pyle, D. (1999). *Data Preparation for Data Mining* (1st ed.). San Francisco, CA, USA: Morgan Kaufmann Publishers Inc.

Ricardo Energy & Environment. (2022, January). *Technological, Operational and Energy Pathways for Maritime Transport to Reduce Emissions Towards 2050* (Tech. Rep. No. ED13389- Issue Number 6).

Rödger, J.-M., Kjær, L. L., & Pagoropoulos, A. (2018). Life Cycle Costing: An Introduction. In M. Z. Hauschild, R. K. Rosenbaum, & S. I. Olsen (Eds.), *Life Cycle Assessment: Theory and Practice* (pp. 373–399). Cham: Springer International Publishing. doi: 10.1007/978-3-319-56475-3_15

Ronen, D. (2011, January). The effect of oil price on containership speed and fleet size. *Journal of the Operational Research Society*, *62*(1), 211–216. doi: 10.1057/jors.2009.169

Schinas, O., & Bergmann, N. (2021, January). The Short-Term Cost of Greening the Global Fleet. *Sustainability*, *13*(16), 9439. doi: 10.3390/su13169439

Schwarz, G. (1978, March). Estimating the Dimension of a Model. *The Annals of Statistics*, *6*(2). doi: 10.1214/aos/1176344136

Shell. (2020). *Decarbonising Shipping: Setting Shell's Course* (Tech. Rep.). Shell International B.V.

Sherif, Y. S., & Kolarik, W. J. (1981, January). Life cycle costing: Concept and practice. *Omega*, *9*(3), 287–296. doi: 10.1016/0305-0483(81)90035-9

Ship & Bunker. (2021). *World Bunker Prices.* https://shipandbunker.com/prices.

Silverman, B. W. (2017). *Density Estimation for Statistics and Data Analysis.* New York: Routledge. doi: 10.1201/9781315140919

Smith, C. (2021, March). *Government investment programmes: The 'green book'.* https://lordslibrary.parliament.uk/government-investment-programmes-the-green-book/.

Stopford, M. (2009). *Maritime economics* (3rd ed ed.). London ; New York: Routledge.

Tan, P.-N., Steinbach, M., Karpatne, A., & Kumar, V. (2019). *Introduction to data mining* (Second edition ed.). NY NY: Pearson.

The Loadstar. (2021, September). *Carriers watch as price of LNG 'transition fuel' sails past the cost of diesel.* https://theloadstar.com/carriers-watch-as-price-of-lng-transition-fuel-sails-past-the-cost-of-diesel/.

The World Bank. (n.d.). *Inflation, consumer prices (annual %).*

https://data.worldbank.org/indicator/FP.CPI.TOTL.ZG.

UNCTAD. (2021, November). *Review of Maritime Transport 2021* (Tech. Rep.).

Wang, H., Oguz, E., Jeong, B., & Zhou, P. (2019, May). Life cycle and economic assessment of a solar panel array applied to a short route ferry. *Journal of Cleaner Production*, *219*, 471–484. doi: 10.1016/j.jclepro.2019.02.124

Wang, S., Psaraftis, H. N., & Qi, J. (2021, December). Paradox of international maritime organization's carbon intensity indicator. *Communications in Transportation Research*, *1*, 100005. doi: 10.1016/j.commtr.2021.100005

Wärtsilä. (n.d.). *Engine Online Configurator — Wärtsilä.* https://www.wartsila.com/marine/engine-configurator.

Wärtsilä. (2020, December). *Wärtsilä 31DF Product guide.* Wärtsilä, Marine Business.

Wärtsilä. (2021a). *A discussion with the Project Manager on the construction costs of the studied engines.*

Wärtsilä. (2021b, March). *Wärtsilä 32 Product Guide.* Wärtsilä, Marine Business.

Zis, T. P. V., & Cullinane, K. (2020, May). The desulphurisation of shipping: Past, present and the future under a global cap. *Transportation Research Part D: Transport and Environment*, *82*, 102316. doi: 10.1016/j.trd.2020.102316

Part III

Appended Papers

Paper I

A Decision Support Framework for Cost-Effective and Energy-Efficient Shipping

Khanh Quang Bui and Lokukaluge Prasad Perera (2020)

Published in *Proceedings of the ASME 2020 39th International Conference on Ocean, Offshore and Arctic Engineering. Volume 6A: Ocean Engineering.* Virtual, Online. August 3–7, 2020. V06AT06A026. ASME.

https://doi.org/10.1115/OMAE2020-18368.

Paper II

Advanced data analytics for ship performance monitoring under localized operational conditions

Khanh Quang Bui and Lokukaluge Prasad Perera (2021)

Published in *Ocean Engineering, 235*, 109392.

https://doi.org/10.1016/j.oceaneng.2021.109392.

Ocean Engineering 235 (2021) 109392

Contents lists available at ScienceDirect

Ocean Engineering

journal homepage: www.elsevier.com/locate/oceaneng

Advanced data analytics for ship performance monitoring under localized operational conditions

Khanh Q. Bui [a,b,*], Lokukaluge P. Perera [a]

[a] Department of Technology and Safety, UiT The Arctic University of Norway, Tromsø, Norway
[b] Faculty of Navigation, Vietnam Maritime University, Hai Phong, Viet Nam

ARTICLE INFO

Keywords:
Big data analytics
Machine learning
Ship performance monitoring
Energy efficiency
Emission control
Data anomaly detection

ABSTRACT

Improving the operational energy efficiency of existing ships is attracting considerable interests to reduce the environmental footprint due to air emissions. As the shipping industry is entering into Shipping 4.0 with digitalization as a disruptive force, an intriguing area in the field of ship's operational energy efficiency is big data analytics. This paper proposes a big data analytics framework for ship performance monitoring under localized operational conditions with the help of appropriate data analytics together with domain knowledge. The proposed framework is showcased through a data set obtained from a bulk carrier pertaining the detection of data anomalies, the investigation of the ship's localized operational conditions, the identification of the relative correlations among parameters and the quantification of the ship's performance in each of the respective conditions. The novelty of this study is to provide a KPI (i.e. key performance indicator) for ship performance quantification in order to identify the best performance trim-draft mode under the engine modes of the case study ship. The proposed framework has the features to serve as an operational energy efficiency measure to provide data quality evaluation and decision support for ship performance monitoring that is of value for both ship operators and decision-makers.

1. Introduction

International shipping is an indispensable sector for the facilitation of global economy since it is responsible for about 80% of the total volume of global trade (UNCTAD, 2019). Furthermore, seaborne transportation is recognized as the most energy-efficient mode of cargo transport as regards energy use per unit transported. Nonetheless, considering its scale and current growth rate, the shipping industry is a major catalyst for global ecological change (Balcombe et al., 2019). According to the Fourth Greenhouse Gas (GHG) Study published by the International Maritime Organization (IMO), global anthropogenic emissions from shipping increased by approximately 10% from 2012 to 2018 (IMO, 2020). It is envisaged that shipping emissions will rise between 90% and 130% by 2050 relative to 2008 for long-term economic and energy scenarios. Therefore, shipping CO_2 emissions are increasing. By way of illustration, if the maritime sector had been treated as a country, it would have been the sixth largest CO_2 emitter in 2015 (Olivier et al., 2016).

Such environmental concerns have been acknowledged in a number of regulatory frameworks established by the IMO. GHG emissions from shipping are addressed by energy efficiency measures under Annex VI of the International Convention for the Prevention of Pollution from Ships (MARPOL). In response to the Paris agreement, the IMO set out an Initial IMO Strategy on reducing GHG emissions from ships, aiming at reducing the total annual GHG emissions by at least 50% by 2050, compared to 2008 levels. These increasingly stringent regulations have exerted pressure on the shipping industry to pursue possible avenues of reducing its environmental footprint (Perera et al., 2021). In order to achieve this, finding alternative fuel sources has been paid much attention in the industry. The search for the right future fuel is challenging since it is a multi-faceted problem where the evaluation of a pallet of different alternative options is influenced by multiple criteria, such as technical, economic, environmental, and social criteria (Bui and Perera, 2019; Bui et al., 2020). In addition to fuel changes, it is an orthodox norm that reducing fuel consumption or improving energy efficiency is an effective solution to reduce ship emissions due to the fact that GHG emissions from internal combustion engines are directly related to ship fuel consumption.

Energy efficiency improvement solutions are generally divided into technical and operational measures. The former refers to improvements made throughout the ship design phase, such as hull form optimization, air lubricant, propulsion efficiency devices, waste heat recovery

* Corresponding author at: Department of Technology and Safety, UiT The Arctic University of Norway, Tromsø, Norway.
E-mail addresses: khanh.q.bui@uit.no (K.Q. Bui), prasad.perera@uit.no (L.P. Perera).

https://doi.org/10.1016/j.oceaneng.2021.109392
Received 21 February 2021; Received in revised form 19 May 2021; Accepted 25 June 2021
Available online 8 July 2021

technology (Brynolf et al., 2016); the latter refers to measures including optimal handling of ships (e.g., trim and ballast optimization), voyage optimization (e.g., weather routing, slow steaming, just-in-time arrival), and good maintenance practices for engine, hull and propeller (Ölçer, 2018). It has been observed from the literature that there is still a large potential for increasing energy efficiency from operational practices, thereby reducing CO_2 emissions. For example, voyage optimization has the potential effect on CO_2 emissions reduction at the figure of up to 48% (Bouman et al., 2017). Nonetheless, technical support systems, ship performance monitoring systems are required to facilitate this practice (IMO, 2014; Viktorelius and Lundh, 2019).

It is a widely held view that the shipping industry is on its way to the fourth industrial revolution (as known as Shipping 4.0) (Rødseth et al., 2016). The transformational role of digitalization and the rise of Artificial Intelligence (AI) together with Machine Learning (ML) will exert tremendous impacts on all of the aspects of the industry. Internet of things (IoT) with the utilization of sensor technologies as well as data acquisition systems can produce a massive amount of sensor data, referred to as big data, which can be used for analysis and further insights on ship performance monitoring. Therefore, proper techniques are required to leverage big data to support increased energy efficiency during ship operation (Zaman et al., 2017; Sullivan et al., 2020). In this respect, big data analytics have emerged as a disruptive technology that can be an operational energy efficiency measure under the ship performance monitoring systems.

The last few years have witnessed a considerable growth in the number of data-driven studies on improving ship energy efficiency. Despite this interest, scant studies have applied big data analytics approach. In addition, several studies have failed to demonstrate significant advantages of domain knowledge in every step of data analysis workflow. The term "domain knowledge" means the domain-specific expertise of the field and it plays an important role in each step of a data analysis project, ranging from problem formulation, data collection, data pre-processing, modeling, to result interpretation. Therefore, the accuracy of data-driven models based on ML can be increased if domain knowledge is incorporated into such models.

Furthermore, concerns have arisen which call into question the quality of ship performance and navigation data. This problem is related to data veracity, which is one of the characteristics of big data, as known as 'the four V's of big data', including volume, velocity, variety, and veracity (Perera and Mo, 2017; Zaman et al., 2017). It should also be noted that knowledge and awareness of ship operators have been recognized as one of the energy efficiency gaps from the operational side (Kitada and Ölçer, 2015; Rasmussen et al., 2018).

Given the above-mentioned background, this paper aims to develop an advanced data analytics framework for ship performance monitoring under localized operational conditions, where domain knowledge is taken into account. The proposed framework will be able to serve as an operational energy efficiency measure to provide data quality evaluation and decision support for ship performance monitoring under the digitalization of the maritime industry.

The structure of this paper is organized as follow. Section 2 reviews the literature on ship's operational energy efficiency and data anomaly detection. The proposed methodology is described in Section 3. Results of the proposed methodology are reported in Section 5. The conclusions are drawn in Section 6.

2. Literature review

2.1. Ship's operational energy efficiency

On the question of improving operational energy efficiency, more attention in the literature has been given to the prediction of ship fuel consumption or engine power. In this regard, statistical models were deployed in several studies (Erto et al., 2015; Sasa et al., 2015). However, these parametric methods may have bias problems due to their assumptions on data distributions. Additionally, they have failed to cope with complicated and non-linear data (Yan et al., 2020; Soner et al., 2018). Therefore, ML models have been widely developed to overcome these problems. In this context, a number of studies implemented ML models such as artificial neural networks (ANNs) (Petersen et al., 2012a,b; Bal Beşikçi et al., 2016; Farag and Ölçer, 2020; Karagiannidis and Themelis, 2021), regression models (Brandsæter and Vanem, 2018; Yan et al., 2020; Wang et al., 2018) and ensemble models (Soner et al., 2018; Gkerekos et al., 2019).

Engine speed optimization and trim optimization have also been gained attention in the literature in terms of improving operational energy efficiency. In this respect, there has been considerable interest in using big data analytics approach. Wang et al. (2017) made an attempt to achieve ship energy efficiency through a big data analysis based on Hadoop platform architecture. In this study, route division with regard to environmental factors was examined and speed optimization in different navigational segments of a route was investigated. Yan et al. (2018) proposed a big data analytics platform to analyze environmental factors for the purpose of optimizing engine speed for inland ships. This study applied the distributed parallel k-means clustering algorithm to obtain an elaborate route division and then find the optimal engine speed for the selected inland ship. Coraddu et al. (2017) employed a data analytics approach for fuel consumption prediction and trim optimization of a tanker. In this study, two gray box models were proposed as predictive models for the prediction of the fuel consumption. Based on these models, a trim optimization method of the tanker was developed. Lee et al. (2018) utilized weather archive big data to estimate the fuel consumption function for speed optimization in maritime logistics. In this study, they developed a decision support systems for minimizing fuel consumption while maintaining service level agreement by applying an optimization method called Particle Swarm Optimization.

It is probable that these ML-based studies have become the means to provide better prediction and decision support towards energy efficiency. Nonetheless, several studies have not treated domain knowledge in much detail. In this regard, Man et al. (2020) proposed an ethnographic method to identify operational challenges on using fuel monitoring systems. One of these challenges is the lack of effective analytical approaches for ship performance evaluation. This leads to a need for utilizing big data analytics in order to gain understanding of actual fuel consumption to achieve energy efficiency.

It has also been observed that many studies hold the view that ship speed is the major determinant for ship fuel consumption. Nonetheless, other factors including, among others, displacement, trim-draft conditions, loading conditions, environmental conditions, and navigation conditions also have impacts on ship fuel consumption (Tran, 2020; Yuan et al., 2017; Soner et al., 2019). It should be noted that these factors may pose a high dimensional challenge for data visualization as pointed out by Perera and Mo (2020).

2.2. Data anomaly detection

It is a self-evident fact that data collected from real-world sources are often impure. The so-called "garbage in – garbage out" (GIGO) refers to the fact that poor quality data input is associated with untrustworthy output (Pyle, 1999). This leads to the needs for methods that can be used for preparing quality data (i.e. data preprocessing) as a fundamental step during data analysis workflow (Zhang et al., 2003). Nevertheless, data quality awareness has yet to be reached its maturity in the maritime industry and a call for the industry to value and improve data quality. In addition, it is worth bearing in mind that the practicality of data quality cannot be done without considering domain knowledge.

In the literature, several taxonomies for data anomaly detection have been developed such as fault diagnosis, fault detection, and fault-tolerant control. Such taxonomies can be treated under decision support

systems and condition monitoring, aiming at enhancing reliability, safety, and energy efficiency of ship systems. Different approaches for the detection of possible faults in decision support systems of a container ship were proposed, i.e., the deployment of residuals and the generalized likelihood ratio (GLR) algorithm (Lajic and Nielsen, 2010), the deployment of Volterra theory (Lajic et al., 2009) and the deployment of a frequency domain-based model (Nielsen et al., 2012). Raptodimos and Lazakis (2018) proposed a method based on the integration of ANNs and Self Organising Maps (SOM) along with inter-clustering for data clustering and fault diagnosis of measurement data of physical parameters of a ship main engine cylinder. Vanem and Brandsæter (2019) deployed unsupervised learning techniques for data anomaly detection for sensor-based condition monitoring for a marine diesel engine.

Capezza et al. (2019) developed a model based on the combination of partial least squares (PLS) regression and prediction error control charts for monitoring of fuel consumption and diagnosis of faults. Lazakis et al. (2019) investigated the utilization of Support Vector Machine (SVM) for the detection of deviant and abnormal ship machinery conditions. Dalheim and Steen (2020) developed a data preparation toolbox for time series data in order to improve the quality of ship operation and performance analysis. Cheliotis et al. (2020) proposed a method based on Expected Behavior (EB) models in combination with Exponentially Weighted Moving Average (EWMA) control charts for early faults detection in the main engine of a ship. Karagiannidis and Themelis (2021) demonstrated that their proposed algorithms for replacing and cleaning data were be able to increase the accuracy of their produced ANN models.

2.3. Research contribution

The research studies reviewed in the previous section point to the following research drawbacks. First, the use of ANNs have been observed in several studies albeit its shortcomings. The most fundamental shortcoming of this approach has been clearly recognized as a 'black-box' approach and it is challenging to interpret behavior of the network. Second, the contribution of domain knowledge has received little attention within the context of maritime applications. Third, most of the studies reviewed have not been able to take into account correlations between factors contributing to ship fuel consumption in a high-dimensional data space. Fourth, data quality for ship operation and performance is still a neglected area in the maritime domain and few researchers have addressed this issue in the literature.

In order to overcome aforementioned drawbacks, this study proposes an advanced data analytics framework for ship performance monitoring. The novelty of this study is to utilize the proposed framework in order to quantify the performance of a selected ship in the context of its localized operational conditions (i.e., engine and trim-draft modes). As the novel contributions of this study, the proposed framework is be able to: (i) detect and isolate data anomalies existing in a given data set, (ii) investigate the ship's localized operational conditions, (iv) deal with numerous factors that have influences on the ship's performance in a high-dimensional data space, and (iii) to provide a KPI (i.e. ship performance indicator) for ship performance quantification.

3. Method

The proposed framework presented in this paper has been built upon a preliminary work as described in Bui and Perera (2020). Fig. 1 illustrates the overall architecture of the proposed framework with key aspects that can be listed as follows: domain knowledge, descriptive analytics, diagnostic analytics, visual analytics, and prescriptive analytics:

- Domain knowledge: is embedded in every step of the proposed framework. It refers to an understanding of the ship's localized operational conditions (i.e., engine and trim-draft modes), the reasoning behind conclusions in each data analytics. It also refers to the knowledge obtained from interactions with experts in the field of maritime transport (e.g., ship owners, ship operators, engine manufacturers).
- Descriptive analytics: this attempts to answer the question of 'What happened?'; it provides an understanding of what happened to the system. From this perspective, two anomaly detectors are proposed to detect and isolate data anomalies. Furthermore, digital modeling is proposed for the investigation of certain patterns of the ship's operational conditions through data clustering.
- Diagnostic analytics: this attempts to answer the question of 'Why did it happen?'; it reflects an understanding of why something happened to the system. From this perspective, the causes of data anomalies are identified.
- Visual analytics: this visualizes the improved data in order to identify the relative relationships or correlations among ship performance and navigation parameters under each of the localized operational conditions.
- Prescriptive analytics: this attempts to answer the question of 'What do we do?'. From this perspective, a selected KPI (i.e. key performance indicator) for ship performance quantification is provided.

3.1. Descriptive analytics

3.1.1. Digital modeling

What follows is an account of digital modeling which aims to provide insights into data properties with respect to the ship's localized operational conditions. For this reason, a digital model is formulated to gain a better understating of discrete data distributions in a high-dimensional space. Fig. 2 depicts the digital model which is an extended version of Perera and Mo (2020). The digital model is represented in the right-handed coordinate system of three parameters (i.e., X_1, X_2, X_3) of a selected data set. It is assumed in the digital model that there is an existence of several data clusters, i.e., A, B, C, which represent engine localized operational conditions. These data clusters are represented by vectors with their respective mean values, i.e., μ_1, μ_2, μ_3. Moreover, each of the data clusters contains several structural vectors in the form of singular vectors (SVs). For example, SVs of cluster $i, i = \{A, B, C\}$ are denoted as $Z_{i,1}$, $Z_{i,2}$, $Z_{i,3}$. Furthermore, Fig. 2 also pinpoints some arrows between the data clusters in the digital model. A probable explanation is that there are certain transient regions, representing the transition modes from an operational condition to another. It is necessary to be borne in mind that data outliers and data anomaly clusters can also be represented under the digital model. This is attributed to the data veracity that should be properly addressed. It is also of interest to further investigate other operational conditions, i.e. trim and draft conditions, within the respective data clusters. In this respect, the projection of the data cluster A onto another high dimensional space is shown in the window on the right-handed side of Fig. 2, where sub-data clusters with respect to trim and draft condition, i.e., A_1, A_2, A_3, can be explored.

A more detailed account of the ship's localized operational conditions can be observed in Fig. 3. In this regard, there are hierarchical relationships between engine operational conditions and trim-draft operational conditions. It can be assumed that there are several engine modes, e.g., engine mode A, B, C, etc. Such engine modes can be demonstrated by cluster A, B, C, etc. Several trim-draft modes can be further explored under each of these engine modes. For example, trim-draft modes A_1, A_2, A_3, etc. can be found under engine mode A. These trim-draft modes can be demonstrated by sub-clusters (e.g., sub-cluster A_1, A_2, A_3, etc.).

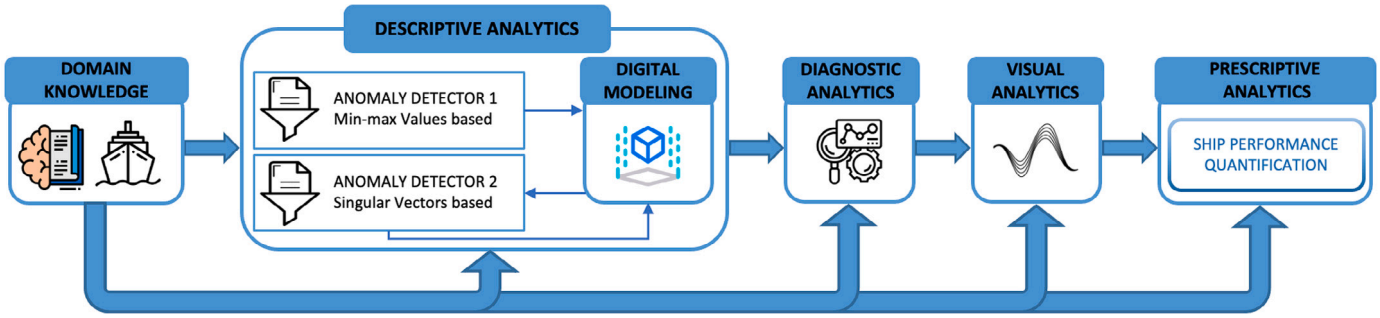

Fig. 1. A representation of the proposed framework.

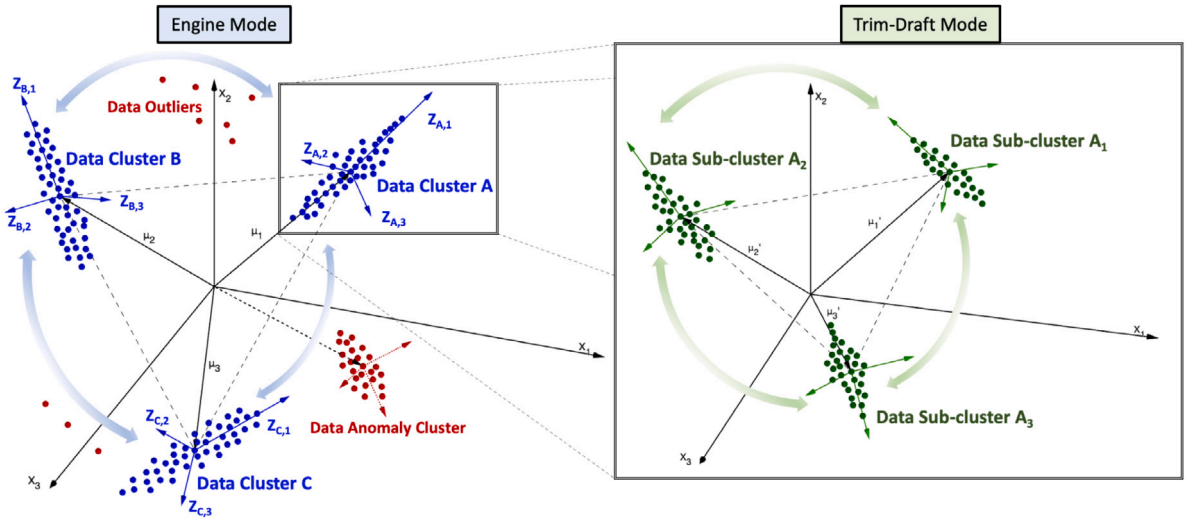

Fig. 2. A representation of the digital model.

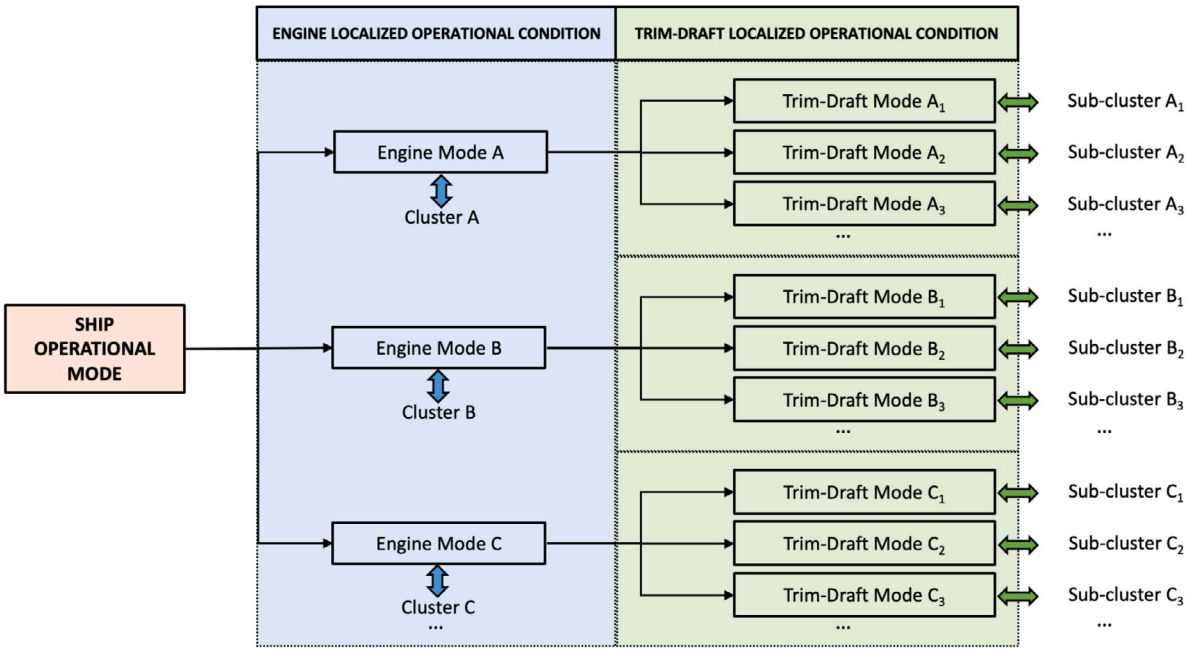

Fig. 3. Ship's localized operational conditions.

3.1.2. Kernel Density Estimation (KDE)

The investigation on the properties of the data can be done by KDE, a non-parametric density estimation method, which yields a smooth representation of the underlying probability density function of the data. Supposing a data set of observations $x = [x_1, x_2, x_3, \dots, x_N]$ with N samples are being drawn from an unknown probability density $p(x)$. We wish to estimate the shape of $p(x)$, the kernel density estimation at x is defined as follows (Bishop, 2006)

$$\hat{p}(x) = \frac{1}{Nh}\sum_{i=1}^{N}\phi\left(\frac{x - x_i}{h}\right) \tag{1}$$

where ϕ is a kernel function, which specifies the shape of the distribution placed at each point, h is a smoothing parameter called the bandwidth, which controls the size of the kernel at each point. The choice for ϕ in this study is the Gaussian kernel.

3.1.3. Gaussian Mixture Models (GMMs)

The following is a brief description of an unsupervised learning technique for data clustering. The technique is based on probability density estimation using GMMs and the Expectation–Maximization (EM) algorithm for distributing data into different clusters. The Gaussian distribution of a d-dimensional vector x is defined as (Bishop, 2006)

$$\mathcal{N}(x|\mu, \Sigma) = \frac{1}{(2\pi)^{d/2}\sqrt{|\Sigma|}} exp\left(-\frac{1}{2}(x-\mu)^T\Sigma^{-1}(x-\mu)\right) \tag{2}$$

where μ is a mean vector and Σ is a covariance matrix.

The probability given in a mixture of K Gaussians is defined as

$$p(x) = \sum_{k=1}^{K}\pi_k\mathcal{N}(x|\mu_k, \Sigma_k) \tag{3}$$

where each Gaussian density $\mathcal{N}(x|\mu_k, \Sigma_k)$ is called a component of the mixture with its mean vector μ_k and covariance Σ_k for the k^{th} Gaussian component, π_k is the prior probability of the k^{th} Gaussian; π_k is also defined as the mixing coefficients with the constraint that $\sum_{k=1}^{K}\pi_k = 1$

EM algorithm for Gaussian Mixtures

Fitting a mixture of Gaussians to data can be done by using the maximum likelihood and the EM algorithm. From Eq. (3), the log of the likelihood function is expressed as

$$ln\ p(X|\pi, \mu, \Sigma) = \sum_{n=1}^{N} ln\left(\sum_{k=1}^{K}\pi_k\mathcal{N}(x_n|\mu_k, \Sigma_k)\right) \tag{4}$$

Given a Gaussian mixture model, the EM algorithm is a powerful technique for maximizing this likelihood function with respect to the parameters, i.e., the means μ_k, the covariances of the components Σ_k and the mixing coefficients π_k.

- Step 1: Initialize μ_k, Σ_k, π_k, and evaluate the initial value of the log likelihood.
- Step 2 (Expectation step): Use the current values for parameters to evaluate the posterior probabilities, or the responsibilities $\gamma(z_{nk})$ which is taken by component k for explaining the observation of data point x_n

$$\gamma(z_{nk}) = \frac{\pi_k\mathcal{N}(x_n|\mu_k, \Sigma_k)}{\sum_{j=1}^{K}\pi_j\mathcal{N}(x_n|\mu_j, \Sigma_j)} \tag{5}$$

- Step 3 (Maximization step): Re-estimate the parameters using the current responsibilities

$$\mu_k^{new} = \frac{1}{N_k}\sum_{n=1}^{N}\gamma(z_{nk})x_n \tag{6}$$

$$\gamma_k^{new} = \frac{1}{N_k}\sum_{n=1}^{N}\gamma(z_{nk})(x_n - \mu_k^{new})(x_n - \mu_k^{new})^T \tag{7}$$

$$\pi_k^{new} = \frac{N_k}{N} \tag{8}$$

where

$$N_k = \sum_{n=1}^{N}\gamma(z_{nk}) \tag{9}$$

N_k can be interpreted as the effective number of points assigned to cluster k

- Step 4: Evaluate the log likelihood

$$ln\ p(X|\pi, \mu, \Sigma) = \sum_{n=1}^{N} ln\left(\sum_{k=1}^{K}\pi_k\mathcal{N}(x_n|\mu_k, \Sigma_k)\right) \tag{10}$$

and check for convergence of either the parameters or the log likelihood. If the convergence criterion is not satisfied, get back to Step 2.

3.1.4. Finding the optimal number of clusters

The GMMs for data clustering is an unsupervised learning technique in which the ground true class labels are not given in the data set. Consequently, the performance of the GMMs is constrained by finding the number of components K. In order to do this, several techniques exist. It may not possible to use the silhouette metric because it may not reliable if the clusters are not spherical or have different sizes, shapes and orientations. Instead, finding the model that minimizes a theoretical criterion information such as the Bayesian Information Criterion (BIC) or the Akaike Information Criterion (AIC) is considered. The BIC and the AIC are expressed as follows (Schwarz, 1978; Akaike, 1974).

$$BIC = ln\ (n)q - 2\ ln\ (\hat{L}) \tag{11}$$

$$AIC = 2q - 2\ ln\ (\hat{L}) \tag{12}$$

where n is the number of observations, q is the number of parameters learned by the model, $\hat{L}$ is the maximized value of the likelihood function of the model. The optimal number of components K (i.e. the number of clusters) is likely with the lowest BIC and AIC value.

3.1.5. Data anomaly detectors

In the section that follows, it is critical to investigate the quality of the data set before proceeding to deploy the digital modeling with further data analysis. For the purpose of such investigation, two data anomaly detectors are proposed, as illustrated in Fig. 4. First of all, the data set needs to go through the first data anomaly detector based on minimum–maximum values. In this regard, a limit check approach, as discussed by Isermann (2006) and Perera (2016), is adopted for the detection of data anomalies and/or outliers. The domain knowledge is required to define the minimum and maximum values of the parameters of the data set. These values represent the general range that the parameters can exist. If data points stay beyond one of the given minimum and maximum thresholds, they are indicating data outliers and will then be removed.

The second data anomaly detector will be executed when the digital modeling is constructed. If there are any anomalies detected, flag alarms will be given. Afterwards, these anomalies are isolated. It is noted that these outliers and anomalies acquired from the two data anomaly detectors are then stored in a data anomaly database for data recovery. However, dealing with the recovery process is beyond the scope of this study.

The second data anomaly detector is based on Singular Value Decomposition (SVD) (Brunton and Kutz, 2019). This is a numerically stable matrix decomposition method with versatile applications. Considering the following data set $X \in \mathbb{R}^{n\times m}$ where n is the number of

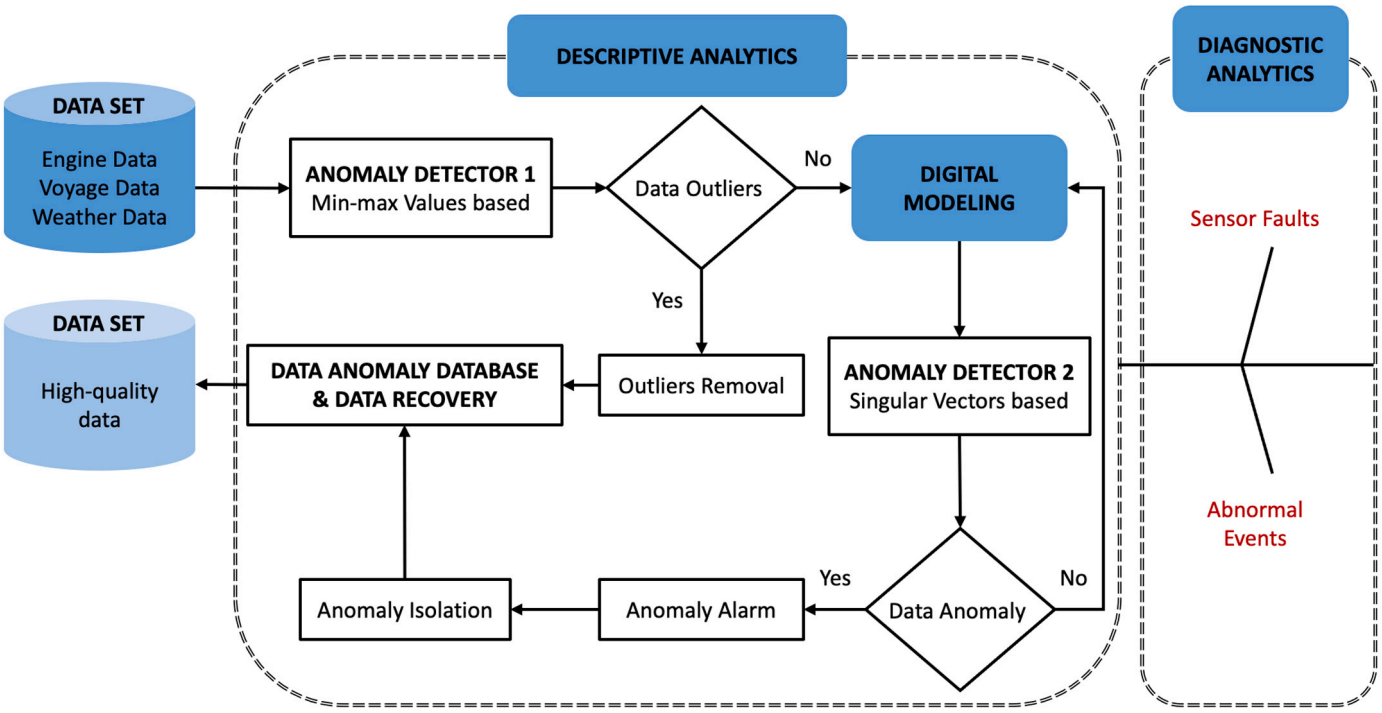

Fig. 4. Descriptive analytics architecture.

observations and m is the number of features (i.e. parameters) ($n > m$). The SVD formula can be expressed as follows.

$$X = U\Sigma V^T \tag{13}$$

where $U \in \mathbb{R}^{n\times n}$ is a square matrix with its column vectors are called the left-singular vectors. $V \in \mathbb{R}^{m\times m}$ is a square matrix with its column vectors are called the right-singular vectors. $\Sigma \in \mathbb{R}^{n\times m}$ is called the singular value matrix, consisting of singular values $\sigma_i, i = 1, \dots, m$. These singular values are ordered as $\sigma_1 \geqslant \sigma_2 \geqslant \dots \sigma_m \geqslant 0$.

An elegant interpretation of the SVD can be observed in the correlation matrix $X^T X$ (i.e. the normalized covariance matrix) as follows.

$$X^T X = V\hat{\Sigma}^2 V^T \implies X^T XV = V\hat{\Sigma}^2 \tag{14}$$

where $\hat{\Sigma} \in \mathbb{R}^{m\times m}$ is the square diagonal matrix with the singular values.

This interpretation provides some important advantages in using the SVD in this study. First, the SVD is able to construct optimal orthogonal expansions for projecting the original data set onto a linear subspace. In this respect, the columns of V (i.e. the right-singular vectors) can be used as principal axes for data projections. Therefore, the representation of the original data set can be constructed intuitively and meaningfully. Second, with the help of the SVD, the most important information of the data set can be extracted based on the hierarchical order of importance of the dominant features. This information can be observed in the top SVs. On the contrary, the least important information of the data set are accommodated in the bottom SVs. For this reason, data anomalies can be perceived in such bottom SVs. These anomalies can be understood as the parameter relationships that are deviated from the existing physical relationships of the parameters.

3.2. Visual analytics

As indicated previously, high-dimensional data may cause a difficulty for data visualization. In other words, it is not easy to have intuition about the structure of data clusters in a high-dimensional space. The visual analytics is therefore proposed in order to identify the relative correlations or relationships among parameters under the respective data clusters. In this regard, the SVD is performed and the

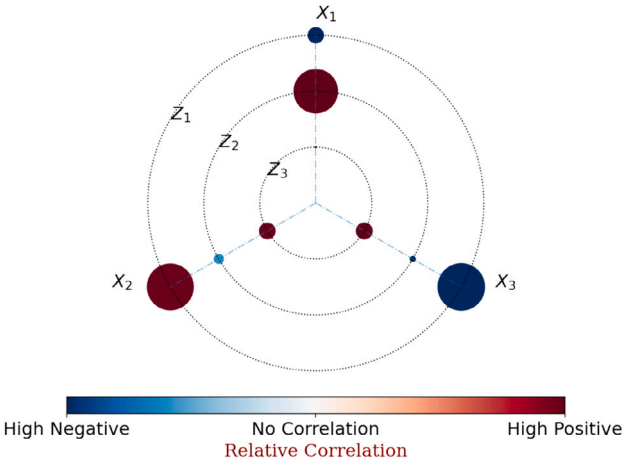

Fig. 5. Visual analytics on a high dimensional singular vector space.

structure of each data cluster is denoted by SVs. Fig. 5 illustrates this approach with three parameters (i.e., X_1, X_2 and X_3) in a high dimensional space as a general representation. Presumably, there are three SVs Z_1, Z_2 and Z_3, sorted in descending order (i.e. from the outermost circle to the innermost circle) associated with their singular values which represent the descending variance directions. Such variance information can be used to extract relevant correlations among parameters, as represented by colored circles in the SVs. The size of each colored circle expresses the significance (i.e. the strength) of the parameter correlation. The color of each colored circle expresses the positive/negative sign of the parameter correlation. When the colored circle is denoted in a large red circle, it means that there is a high positive correlation. When it is denoted in a large blue circle, it means that there is a high negative correlation. Taking the top singular vector Z_1 in Fig. 5 as an example, there is a significant increase in the parameter X_2 while there is a significant decrease in the parameter X_3. A decrease in the parameter X_1 can also be seen in this condition.

It should be noted that the top singular vector Z_1 represents the largest variance direction (i.e. the most information) of the data cluster while the bottom singular vector Z_3 represents the smallest variance direction (i.e. the least information) of the respective data cluster. For this reason, several correlations among parameters might be unclear in the bottom singular vector.

3.3. Prescriptive analytics

The section below proposes a selected KPI (i.e key performance indicator) for ship performance quantification. It is important to stress that this KPI is derived with respect to the availability of the ship performance and navigation parameters in the respective data set. The KPI is attached to each of the ship's localized operational conditions (i.e. represented by a cluster or a sub-cluster) in order to evaluate its performance. The resulting KPI for ship performance quantification can be expressed as

$$SPI_i = \frac{FC_i}{D_i} \tag{15}$$

where

$$FC_i = FC_{avg,i} \times t_i \tag{16}$$

$$D_i = STW_{avg,i} \times t_i \tag{17}$$

here SPI_i is the ship performance index of the ship's localized operational condition i, FC_i is the main engine (ME) fuel consumption (cons) [Ton], $FC_{avg,i}$ is the average ME fuel cons [Ton/day], D_i is the traveled distance [NM], t_i is the time traveled [day], and $STW_{avg,i}$ is the average speed through water (STW) [NM/h] under the respective localized operational condition i, correspondingly. For the sake of unit consistency, Eq. (15) can be rewritten as follows.

$$SPI_i = \frac{FC_{avg,i}}{24\ STW_{avg,i}} \tag{18}$$

It is noted that SPI_i [Ton/NM] is a representation of the ship's average ME fuel cons per nautical mile.

4. Data description and experimental settings

As an exemplification for the application of the proposed method, a ship performance and navigation data set was obtained from a bulk carrier. This is a time-series data set of 3 years with a sampling rate of 15 minutes. Table 1 shows several principal particulars of the selected ship while Table 2 demonstrates twelve parameters with respect to ship performance and navigation along with their minimum–maximum values.

The programming language used to analyze the data was Python with Jupyter Notebook 6.0.3 interface. It was running on a macOS computer, consisting of Intel Core i7 CPU 2.2 GHz with 6 Cores and 32 GB RAM. The computational complexity of training the GMMs depends on the number of observations n, the number of parameters m, the number of clusters K, and the constraints on the covariance matrices. Regarding the settings of the GMMs, it needs to be run several times in order to end up converging to the best solution. The number of initializations was set in this study is 10.

Table 1
Ship particulars.

Feature	Value [Unit]
Ship length	225 [m]
Beam	33 [m]
Gross tonnage	38.889 [N/A]
Deadweight at max draft	72.562 [Ton]
A 2-stroke main engine with maximum continuous rating (MCR)	7564 [kW]
Main engine - shaft rotational speed	105 [rpm]
Two auxiliary engines with MCR	850 [kW]
Auxiliary engines - shaft rotational speed	800 [rpm]
Fixed pitch propeller with 6.20 [m] in diameter and four blades	

Table 2
Ship performance and navigation parameters and their minimum–maximum values.

Parameter	Unit	Min value	Max value
Auxiliary (Aux) fuel consumption (cons)	[Ton/day]	1	8
Main Engine (ME) fuel consumption (cons)	[Ton/day]	1	40
Auxiliary (Aux) power	[kW]	100	850
Main Engine (ME) power	[kW]	3000	8000
Shaft speed	[rpm]	80	120
Relative (Rel) wind speed	[m/s]	0	25
Relative (Rel) wind direction (dir)	[deg]	0	360
Course	[deg]	0	360
Speed over ground (SOG)	[Knots]	3	20
Speed through water (STW)	[Knots]	3	20
Trim	[m]	−2	4
Average (Avg) draft	[m]	0	15

5. Results and discussion

5.1. Descriptive analytics

Regarding the deployment of the first data anomaly detector, it was found that several data points were unreasonable. For example, the values of trim were around −10 [m] or the values of the ME fuel (cons) were around 118 [Ton/day]. Based on the domain knowledge, these values were characterized as outliers and should be omitted. Therefore, threshold values, i.e. the minimum and maximum values of the navigation and performance parameters, were accordingly identified based on the domain knowledge, as shown in Table 2. The ranges for the engine power and the shaft speed were given by the engine manufacturer.

In the case of the digital modeling, Fig. 6 exemplifies the implementation of the KDE and the GMMs for engine data (i.e. shaft speed and engine power). In the first place, the KDE was constructed to gain insights into the number of components K for the GMMs. In this respect, the density estimation of the engine data can be approximately perceived as three components (i.e., cluster A, B, and C), as shown in Fig. 6a. Among of these, cluster A and C are the two main modes of the engine in operation while other data points are belonging to cluster B which could be attributed to a transient state of the engine. Therefore, by using the KDE as a representation guidance together with the domain knowledge, the number of components (i.e. the number of clusters) $K = 3$ was then be suggested for the GMMs. Fig. 6b illustrates the results of the deployment of the GMMs, capturing these three clusters as ellipsoid-shaped clusters, denoted in dark blue, orange and turquoise respectively. Therefore, it arrived at a conclusion that the selected ship was operating in three engine modes. The GMMs was further investigated in three-dimensional space where the ME fuel consumption, the shaft speed and the engine power were taken into consideration. As presented in Fig. 7, there are three clusters in relation to engine modes existing in the digital modeling.

When the digital modeling had been constructed, the deployment of the second data anomaly detector was carried out. As mentioned earlier, the bottom singular vector (i.e. Z_{12}) carries the least important information of the data set. Hence, it was used to detect anomalies for the second anomaly detector. Fig. 8 shows that data cluster A is projected onto a new subspace represented by Z_{12}. It should be noted that -3σ and 3σ (here σ is the standard deviation of the respective data distribution) were chosen as appropriate threshold values. If data points exceed these values, they are flagged as anomalies for this detector. In this regard, a number of anomalies are detected, as shown in the middle and the bottom plot of Fig. 8.

The identification of such anomalies was further investigated in Fig. 9, where all parameters are presented in a time-series format with respect to the number of data points. What stands out in this figure is that several anomalies are detected, denoted by the red pulses and

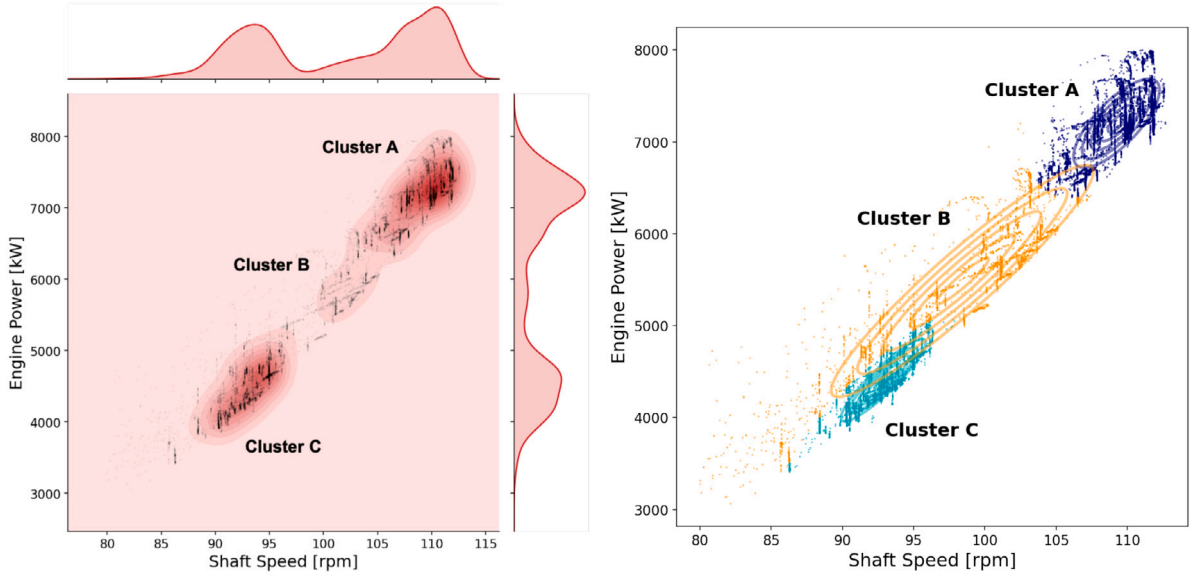

(a) KDE implementation. (b) GMMs implementation.

Fig. 6. Engine data clustering.

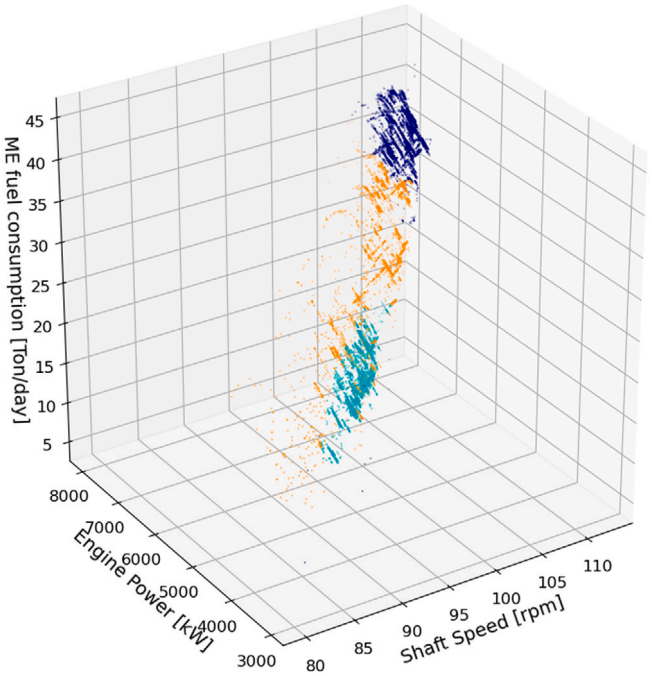

Fig. 7. Engine data clustering in three-dimensional space.

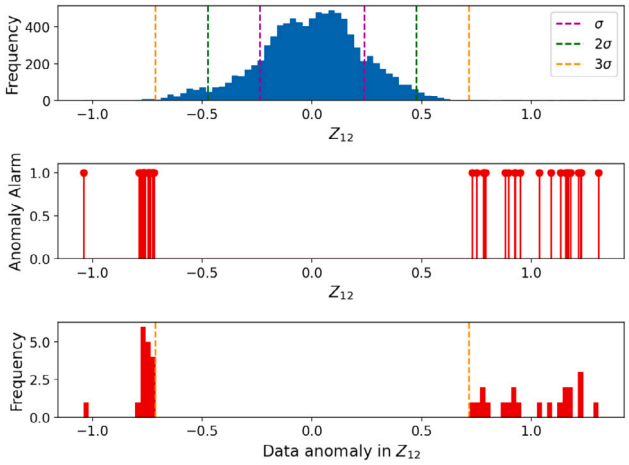

Fig. 8. Data anomaly detection in the bottom singular vector Z_{12}.

Table 3
Number of identified data anomalies using the SVs-based detector.

Cluster	No of identified data anomalies	Ratio[a] (%)
A	38	0.41
B	37	1.08
C	48	0.81

[a]The ratio (%) indicates the number of identified anomalies per the number of data points in the respective cluster.

the anomaly alarms are accordingly raised. It should be borne in mind that the shaft speed, arranged in ascending order in the first plot, is a basis for the detection of such anomalies. It is also important to bear in mind that the operation of other on-board systems, including hotel systems, is completely independent of the main engine in some situations. Therefore, any variations in the Auxiliary (Aux) fuel cons or the Aux power do not have any effects on the actual ME fuel consumption in such situations. In the first anomaly point (DA 1), there are some sudden changes with respect to the ME power and the STW. In the second anomaly point (DA 2), there are falling points in the ME fuel cons and the STW. Similar strange behaviors can also be observed with respect to the ME fuel cons and the STW in the third anomaly point (DA 3). This approach was further adopted to cluster *B* and cluster *C*. Table 3 presents the number of anomalies identified by this detector in the respective clusters. The most likely causes of identified data anomalies existing in the data set are sensor faults and/or abnormal events. These causes draw conclusions for the diagnostic analytics.

Perhaps the most interesting aspect of the descriptive analytics is the exploration of the ship's localized operational conditions. As was pointed out previously, the selected ship was operating in three engine modes, represented by cluster *A*, *B* and *C*. Each of these engine modes has different trim-draft modes which can be represented by sub-clusters. To further examine this, the deployment of the KDE and the

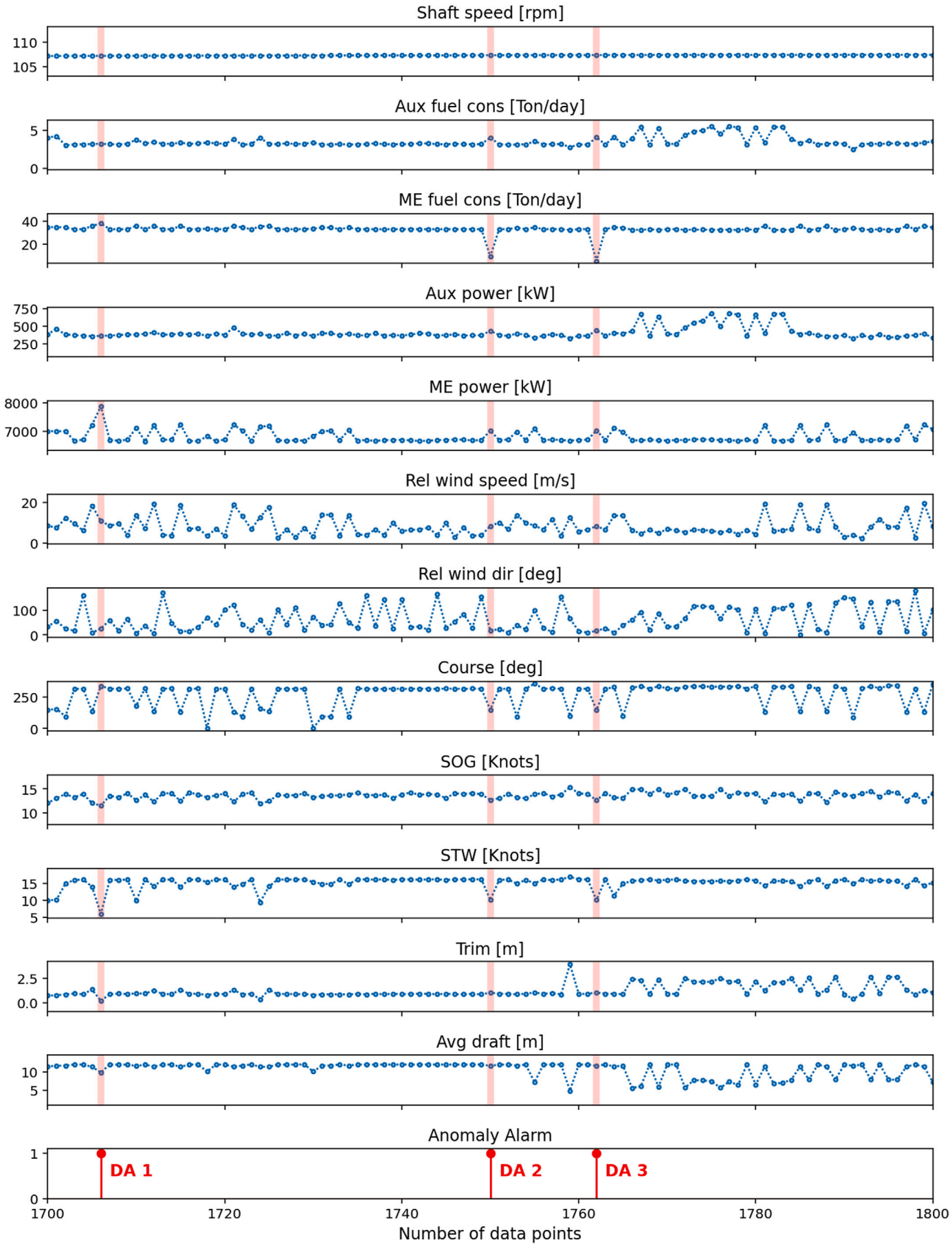

Fig. 9. Data anomaly detection in the time-series plot.

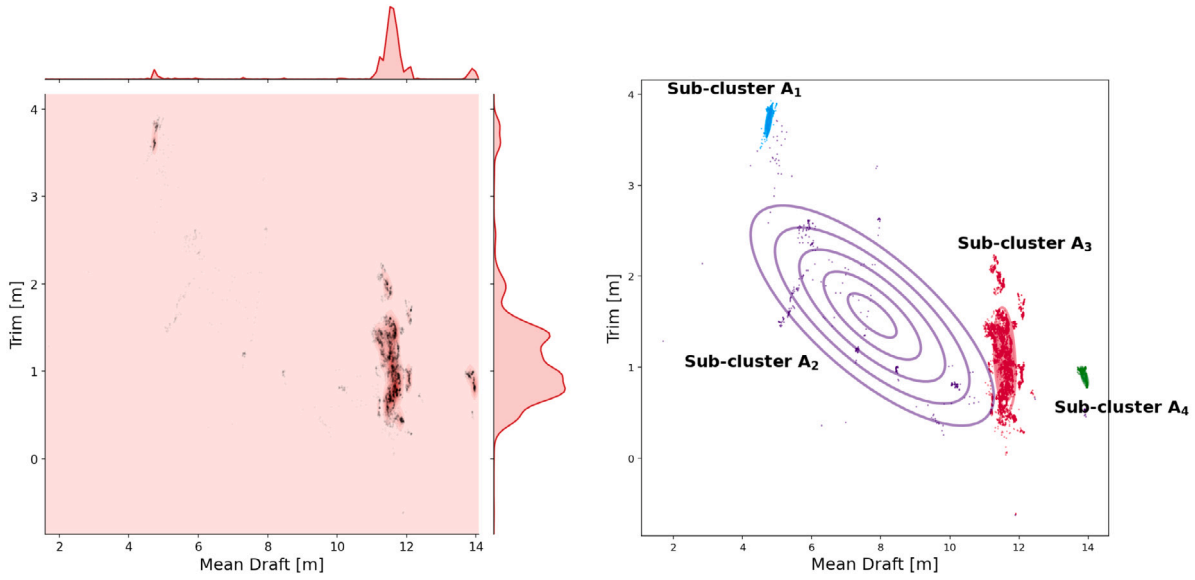

(a) KDE implementation. (b) GMMs implementation.

Fig. 10. Trim-draft data clustering with respect to data cluster *A*.

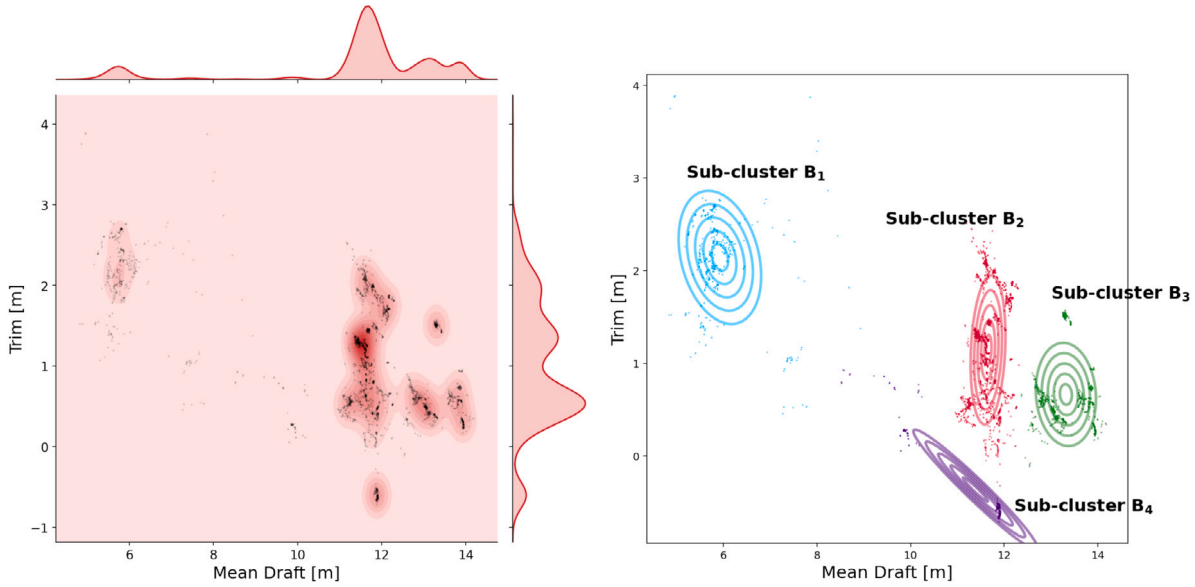

(a) KDE implementation. (b) GMMs implementation.

Fig. 11. Trim-draft data clustering with respect to data cluster *B*.

GMMs for trim-draft data was carried out under each of these engine modes. The domain knowledge also occupied a role in determining the number of sub-clusters in these cases. Fig. 10 indicates there are four sub-clusters A_1, A_2, A_3, and A_4, representing trim-draft modes with respect to cluster A. It can be seen from Fig. 11 that there are four sub-cluster B_1, B_2, B_3, and B_4, (i.e. trim-draft modes) with respect to cluster B. Fig. 12 reports four sub-clusters C_1, C_2, C_3, and C_4 (i.e. trim-draft modes) with respect to cluster C.

5.2. Finding the optimal number of clusters

As mentioned earlier, an important factor by which the GMMs can be evaluated is finding the optimal number of clusters K. This can be done by calculating the BIC and the AIC. The results on the BIC and the AIC of the engine data (i.e., shaft speed and engine power) are shown in Fig. 13. It can be seen from this figure that the BIC and the AIC results do not give an optimal position for K. If there are many components K in the GMMs, it will increase the probability of over-fitting. Therefore, in this case, the BIC and the AIC results are inconclusive. The domain knowledge can play a crucial role in this case. After consulting with the ship owner who provided us the data set, they confirmed that the ship was operating in three engine modes. This is in line with what we determined before.

Further experiments on the BIC and the AIC were also performed for trim-draft data, as shown in Figs. 14, 15, 16. It can be observed from these figures that the results on the BIC and the AIC in all cases are also inconclusive. Therefore, in this study, the domain knowledge regarding the engine operational modes and the trim-draft operational modes should be directly embedded into the GMMs in order to identify

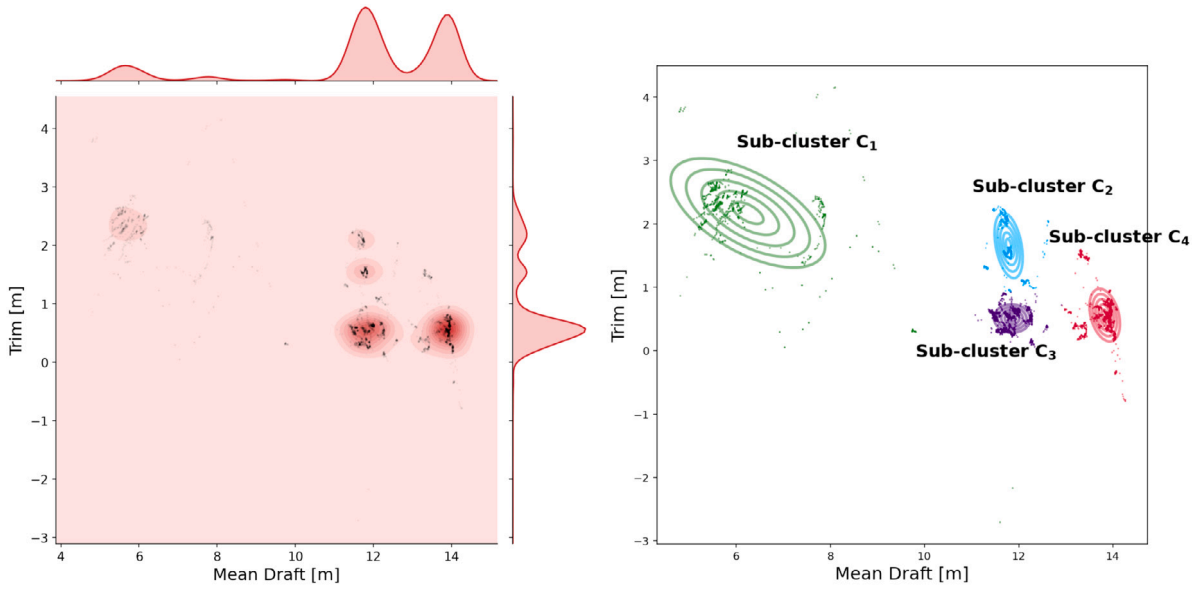

(a) KDE implementation. (b) GMMs implementation.

Fig. 12. Trim-draft data clustering with respect to data cluster C.

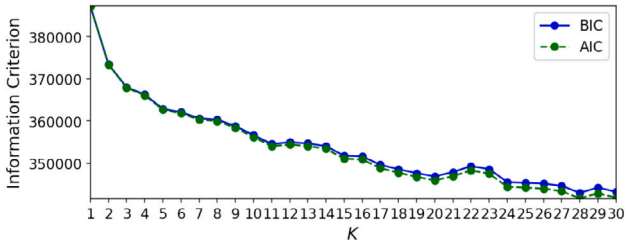

Fig. 13. BIC and AIC results for engine data clustering.

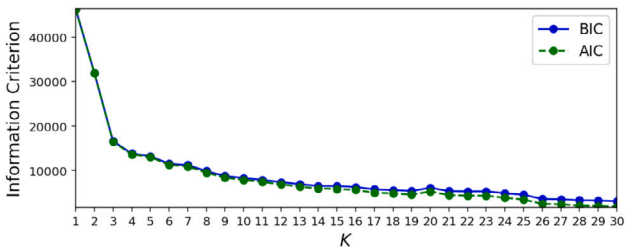

Fig. 14. BIC and AIC results for trim-draft data clustering with respect to cluster A.

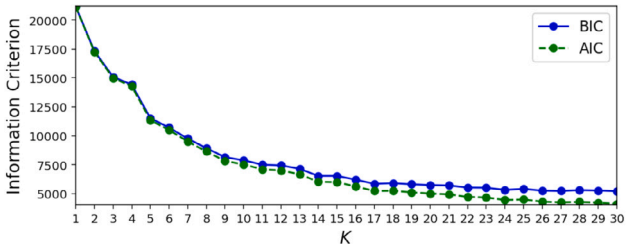

Fig. 15. BIC and AIC results for trim-draft data clustering with respect to cluster B.

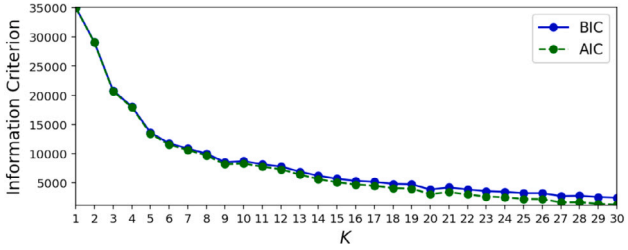

Fig. 16. BIC and AIC results for trim-draft data clustering with respect to cluster C.

possible data clusters. By doing this, the accuracy of the digital model can be improved.

5.3. Visual analytics

As explained earlier, the purpose of the visual analytics is to reveal the relative correlations among parameters under a cluster or a sub-cluster. The results on the visual analytics of data cluster A under trim-draft modes (i.e. represented by sub-cluster A_1, A_2, A_3, and A_4) are illustrated in Fig. 17. The results on this analytics of sub-cluster A_3 was selected for the purpose of illustration. Fig. 17c is revealing in several ways. The top singular vector shows an increase in the Shaft speed and an increase in the ME power, thus the ME fuel cons also increases. It can also be found that a decrease in the Aux power leads to a decrease in the Aux fuel cons. The Average (Avg) draft is also decreased in this condition. Turning to the second singular vector, there is an adjustment of the Trim and the Avg draft, thereby increasing the STW and the speed over ground (SOG). The third singular vector demonstrates that an increase in the Aux fuel cons is attributed to an increase in the Aux power. It can be observed from the fourth singular vector that an decrease in the STW may cause a considerable increase in the Rel wind direction. The fifth singular vector indicates that a decrease in the Aux fuel cons stems from a decrease in the Aux power. It can also be seen in this situation that the Trim is increased. The sixth singular vector shows that there is an increase in the STW along with an increase in the Rel wind direction. Besides, a trim-draft adjustment can be observed. It is noted that the bottom singular vectors have low singular values. As a result of this, the correlations among parameters are unclear or there are no realistic correlations that can be observed in

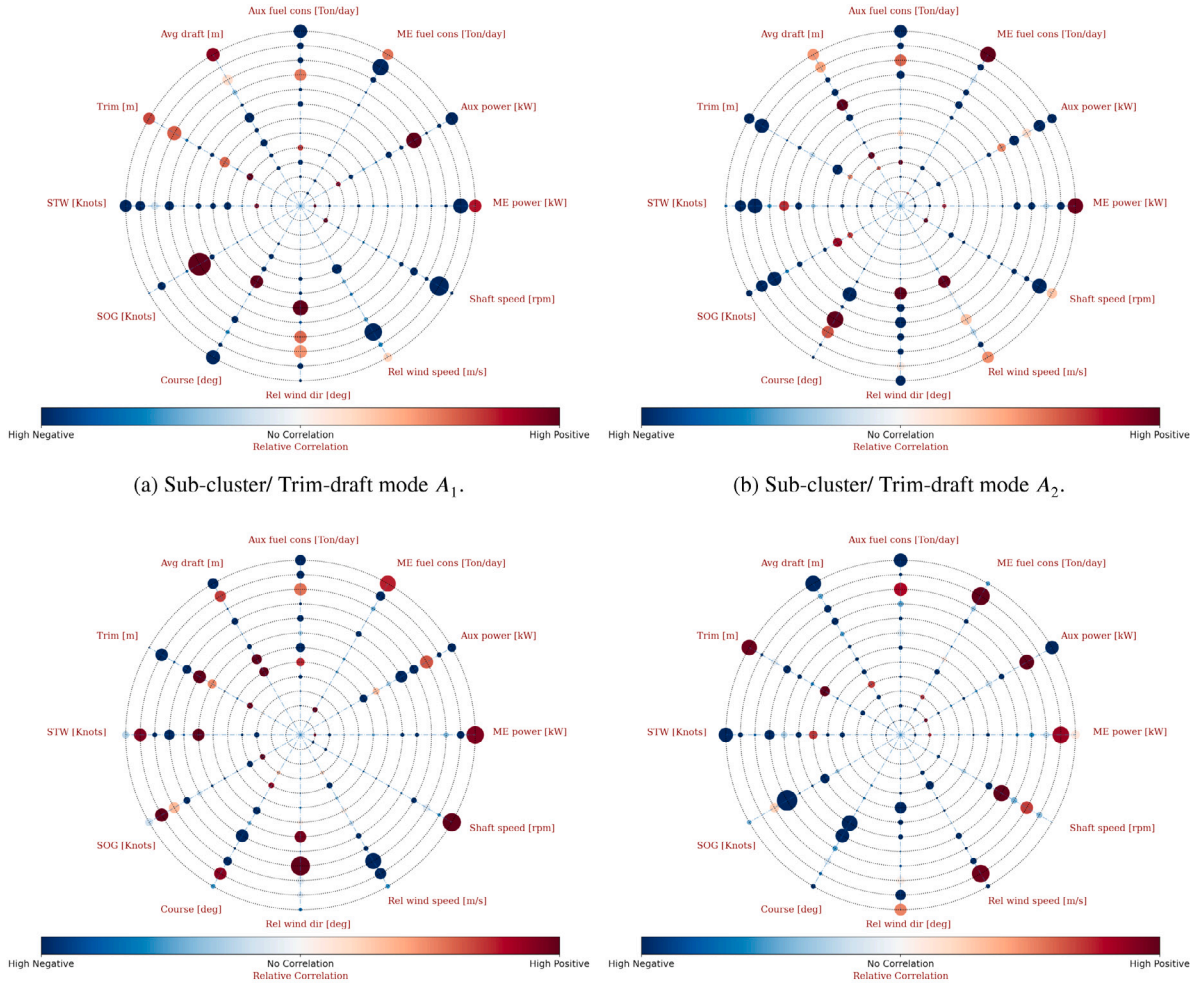

(a) Sub-cluster/ Trim-draft mode A_1.

(b) Sub-cluster/ Trim-draft mode A_2.

(c) Sub-cluster/ Trim-draft mode A_3.

(d) Sub-cluster/ Trim-draft mode A_4.

Fig. 17. Visual analytics of data cluster A under trim-draft modes.

these bottom singular vectors. The remaining results on this analytics of other sub-clusters (e.g., A_1, A_2, and A_4) can be explained in the same manners.

5.4. Prescriptive analytics

As mentioned previously, the prescriptive analytics is proposed to provide the KPI, expressed by the ship performance index SPI, in order to quantify the ship's performance under the identified localized operational modes. Table 4 compares the SPI results of trim-draft modes under the respective engine modes, as defined in Eq. (18). Considering engine mode A, trim-draft mode A_1 appears to be the best performance mode because of its lowest SPI value ($SPI = 0,0797$ [Ton/NM]). Looking at engine mode B, the SPI value of trim-draft mode B_4 ($SPI = 0,0805$ [Ton/NM]) indicates that this trim-draft mode is the best performance mode. Turning to engine mode C, based on the SPI value of trim-draft mode C_1 ($SPI = 0,0699$ [Ton/NM]), this is the best performance trim-draft mode. It is apparent from this table that, overall, trim-draft mode C_1 has the lowest SPI value among other trim-draft modes. It can thus be suggested that this is the best performance mode of the selected ship. However, with the ship performance and navigation parameters available in the data set were considered, caution should be applied. The lack of the loading conditions in the data set added the caution regarding the generalizability of these results for energy efficiency quantification. For this reason, 'ship performance quantification' was addressed rather than 'energy efficiency quantification'.

Table 4
SPI value for ship performance quantification.

Cluster (Engine Mode)	Sub-cluster (Trim-draft Mode)	SPI [Ton/NM]
A	A_1	0,0797
	A_2	0,1030
	A_3	0,1121
	A_4	0,1468
B	B_1	0,0936
	B_2	0,0992
	B_3	0,1080
	B_4	0,0805
C	C_1	0,0699
	C_2	0,0728
	C_3	0,0748
	C_4	0,0753

6. Conclusion

Prior studies have only focused on predicting ship fuel consumption or optimizing engine speed/trim as regards the improvement of operational energy efficiency. To the best of our knowledge, no other authors have studied the ship's performance in a local scale with respect to its operational conditions. The novelty of this study is to quantify the performance of a selected ship under localized operational conditions (i.e., engine and trim-draft modes) by developing an advanced data analytics framework. It was demonstrated through a data set collected

from a bulk carrier. The research findings obtained from the proposed framework have been summarized as follows.

- Descriptive analytics has proposed two data anomaly detectors that were be able to detect and isolate a number of data anomalies existing in the data set. Furthermore, it has offered a better understanding of the ship's localized operational conditions. This can be perceived by the engine and the trim-draft modes. With the help of the KDE and the GMMs, the investigation of the digital model has shown that the selected ship was operating in three engine modes, represented by clusters A, B and C. The digital model was further examined for trim-draft data with respect to these clusters. The findings of this examination have shown that several trim-draft modes were identified, represented by sub-clusters.
- Diagnostic analytics has suggested two main reasons why there are data anomalies in almost data sets collected from data acquisition systems. In this regard, sensor faults and/or abnormal events were identified as the causes strongly associated with these data anomalies.
- Visual analytics has revealed the relative relationships or correlations among the ship performance and navigation parameters in relation to the respective engine modes and trim-draft modes.
- Prescriptive analytics has provided a KPI in order to quantify the ship's performance under the respective engine modes and trim-draft modes. The KPI was expressed by the ship performance index SPI (i.e. the average ME fuel cons per nautical mile). Based on the SPI findings, it is likely that sub-cluster C_1 was the best performance trim-draft mode of the selected ship.

Taken together, the findings suggest a role for the domain knowledge in every step of the proposed framework. Moreover, the findings have the potential to serve as an operational energy efficiency measure that is of value for both ship operators (captains, chief-engineers, ship officers) and decision-makers (ship owners, fleet managers, technical divisions) for improving energy efficiency through operational practices. In this respect, the findings can be integrated into the ship performance monitoring systems. Specifically, they can be simulated and displayed on the on-board user interfaces. Therefore, ship operators are equipped with meaningful visualizations and indicators in order to evaluate their practices and raise their awareness with respect to energy efficiency. By considering the KPI proposed in this study, ship operators could know in which engine/trim-draft mode they should facilitate the eco-maneuvering, e.g. operating the engine under the load range with the lowest specific fuel oil consumption. This KPI will change depending on system's operational conditions and hull fouling conditions. Hence, ship operators can also consult with technical divisions ashore in order to trouble-shoot their operational problems via remote communication. Furthermore, such visualizations and indicators can assist ship owners/fleet managers in achieving performance improvement across their fleet.

Looking ahead towards Shipping 4.0, the ship performance monitoring systems can be transformed into digital platforms by the Digital Twin technology. The Digital Twin is a virtual representation which serves as the real-life counterpart of the ship. The digital model proposed in the study has the potential for exploiting the Digital Twin. In this way, the Digital Twin has the capabilities to become an automated, self-aware anomaly detection, self-visualization platform that enables ship operators and fleet managers to monitor the instantaneous performance of the ship in real-time.

Nonetheless, the findings in this study are subject to a limitation. The SPI findings on the account of ship performance quantification maybe somewhat limited by the absence of the loading conditions parameter in the data set. Therefore, these findings need to be interpreted with caution. This is the main reason why 'ship performance quantification' was concerned in this study, rather than 'energy efficiency quantification'. Further studies, which take the loading conditions and other factors into account for energy efficiency quantification, will need to be undertaken. Moreover, the issue of data quality is an intriguing one which could be usefully explored in the further studies.

CRediT authorship contribution statement

Khanh Q. Bui: Methodology, Software, Formal analysis, Writing - original draft, Visualization. **Lokukaluge P. Perera:** Conceptualization, Methodology, Writing - review & editing, Supervision.

Declaration of competing interest

The authors declare that they have no known competing financial interests or personal relationships that could have appeared to influence the work reported in this paper.

References

Akaike, H., 1974. A new look at the statistical model identification. IEEE Trans. Automat. Control 19 (6), 716–723. http://dx.doi.org/10.1109/TAC.1974.1100705.

Bal Beşikçi, E., Arslan, O., Turan, O., Ölçer, A.I., 2016. An artificial neural network based decision support system for energy efficient ship operations. Comput. Oper. Res. 66, 393–401. http://dx.doi.org/10.1016/j.cor.2015.04.004.

Balcombe, P., Brierley, J., Lewis, C., Skatvedt, L., Speirs, J., Hawkes, A., Staffell, I., 2019. How to decarbonise international shipping: Options for fuels, technologies and policies. Energy Convers. Manage. 182, 72–88. http://dx.doi.org/10.1016/j.enconman.2018.12.080.

Bishop, C., 2006. Pattern Recognition and Machine Learning. In: Information Science and Statistics, Springer-Verlag, New York.

Bouman, E.A., Lindstad, E., Rialland, A.I., Strømman, A.H., 2017. State-of-the-art technologies, measures, and potential for reducing GHG emissions from shipping – A review. Transp. Res. D 52, 408–421. http://dx.doi.org/10.1016/j.trd.2017.03.022.

Brandsæter, A., Vanem, E., 2018. Ship speed prediction based on full scale sensor measurements of shaft thrust and environmental conditions. Ocean Eng. 162, 316–330. http://dx.doi.org/10.1016/j.oceaneng.2018.05.029.

Brunton, S.L., Kutz, J.N., 2019. Data-Driven Science and Engineering: Machine Learning, Dynamical Systems, and Control. Cambridge University Press, Cambridge, http://dx.doi.org/10.1017/9781108380690.

Brynolf, S., Baldi, F., Johnson, H., 2016. Energy efficiency and fuel changes to reduce environmental impacts. In: Andersson, K., Brynolf, S., Lindgren, J.F., Wilewska-Bien, M. (Eds.), Shipping and the Environment : Improving Environmental Performance in Marine Transportation. Springer, Berlin, Heidelberg, pp. 295–339. http://dx.doi.org/10.1007/978-3-662-49045-7_10.

Bui, K.Q., Ölçer, A.I., Kitada, M., Ballini, F., 2020. Selecting technological alternatives for regulatory compliance towards emissions reduction from shipping: An integrated fuzzy multi-criteria decision-making approach under vague environment. Proc. Inst. Mech. Eng. M http://dx.doi.org/10.1177/1475090220917815.

Bui, K.Q., Perera, L.P., 2019. The compliance challenges in emissions control regulations to reduce air pollution from shipping. In: OCEANS 2019 - Marseille. pp. 1–8. http://dx.doi.org/10.1109/OCEANSE.2019.8867420.

Bui, K.Q., Perera, L.P., 2020. A decision support framework for cost-effective and energy-efficient shipping. In: ASME 2020 39th International Conference on Ocean, Offshore and Arctic Engineering. American Society of Mechanical Engineers Digital Collection, http://dx.doi.org/10.1115/OMAE2020-18368.

Capezza, C., Coleman, S., Lepore, A., Palumbo, B., Vitiello, L., 2019. Ship fuel consumption monitoring and fault detection via partial least squares and control charts of navigation data. Transp. Res. D 67, 375–387. http://dx.doi.org/10.1016/j.trd.2018.11.009.

Cheliotis, M., Lazakis, I., Theotokatos, G., 2020. Machine learning and data-driven fault detection for ship systems operations. Ocean Eng. 216, 107968. http://dx.doi.org/10.1016/j.oceaneng.2020.107968.

Coraddu, A., Oneto, L., Baldi, F., Anguita, D., 2017. Vessels fuel consumption forecast and trim optimisation: A data analytics perspective. Ocean Eng. 130, 351–370. http://dx.doi.org/10.1016/j.oceaneng.2016.11.058.

Dalheim, Ø.Ø., Steen, S., 2020. Preparation of in-service measurement data for ship operation and performance analysis. Ocean Eng. 212, 107730. http://dx.doi.org/10.1016/j.oceaneng.2020.107730.

Erto, P., Lepore, A., Palumbo, B., Vitiello, L., 2015. A procedure for predicting and controlling the ship fuel consumption: Its implementation and test. Qual. Reliab. Eng. Int. 31 (7), 1177–1184. http://dx.doi.org/10.1002/qre.1864.

Farag, Y.B.A., Ölçer, A.I., 2020. The development of a ship performance model in varying operating conditions based on ANN and regression techniques. Ocean Eng. 198, 106972. http://dx.doi.org/10.1016/j.oceaneng.2020.106972.

Gkerekos, C., Lazakis, I., Theotokatos, G., 2019. Machine learning models for predicting ship main engine fuel oil consumption: A comparative study. Ocean Eng. 188, 106282. http://dx.doi.org/10.1016/j.oceaneng.2019.106282.

IMO, 2014. Third IMO GHG Study 2014. International Maritime Organization (IMO), London, UK.

IMO, 2020. Fourth IMO GHG Study 2020. International Maritime Organization (IMO).

Isermann, R., 2006. Fault detection with limit checking. In: Isermann, R. (Ed.), Fault-Diagnosis Systems: an Introduction from Fault Detection to Fault Tolerance. Springer, Berlin, Heidelberg, pp. 95–110. http://dx.doi.org/10.1007/3-540-30368-5_7.

Karagiannidis, P., Themelis, N., 2021. Data-driven modelling of ship propulsion and the effect of data pre-processing on the prediction of ship fuel consumption and speed loss. Ocean Eng. 222, 108616. http://dx.doi.org/10.1016/j.oceaneng.2021.108616.

Kitada, M., Ölçer, A., 2015. Managing people and technology: The challenges in CSR and energy efficient shipping. Res. Transp. Bus. Manag. 17, 36–40. http://dx.doi.org/10.1016/j.rtbm.2015.10.002.

Lajic, Z., Blanke, M., Nielsen, U.D., 2009. Fault detection for shipboard monitoring – Volterra kernel and Hammerstein model approaches. IFAC Proc. Vol. 42 (8), 24–29. http://dx.doi.org/10.3182/20090630-4-ES-2003.00004.

Lajic, Z., Nielsen, U.D., 2010. Fault detection for shipboard monitoring and decision support systems. In: ASME 2009 28th International Conference on Ocean, Offshore and Arctic Engineering. American Society of Mechanical Engineers Digital Collection, pp. 679–686. http://dx.doi.org/10.1115/OMAE2009-79367.

Lazakis, I., Gkerekos, C., Theotokatos, G., 2019. Investigating an SVM-driven, one-class approach to estimating ship systems condition. Ships Offshore Struct. 14 (5), 432–441. http://dx.doi.org/10.1080/17445302.2018.1500189.

Lee, H., Aydin, N., Choi, Y., Lekhavat, S., Irani, Z., 2018. A decision support system for vessel speed decision in maritime logistics using weather archive big data. Comput. Oper. Res. 98, 330–342. http://dx.doi.org/10.1016/j.cor.2017.06.005.

Man, Y., Sturm, T., Lundh, M., MacKinnon, S.N., 2020. From ethnographic research to big data analytics—A case of maritime energy-efficiency optimization. Appl. Sci. 10 (6), 2134. http://dx.doi.org/10.3390/app10062134.

Nielsen, U.D., Lajic, Z., Jensen, J.J., 2012. Towards fault-tolerant decision support systems for ship operator guidance. Reliab. Eng. Syst. Saf. 104, 1–14. http://dx.doi.org/10.1016/j.ress.2012.04.009.

Ölçer, A.I., 2018. Introduction to maritime energy management. In: Ölçer, A.I., Kitada, M., Dalaklis, D., Ballini, F. (Eds.), Trends and Challenges in Maritime Energy Management. In: WMU Studies in Maritime Affairs, Springer International Publishing, pp. 1–12. http://dx.doi.org/10.1007/978-3-319-74576-3_1.

Olivier, J.G., Janssens-Maenhout, G., Muntean, M., Peters, J.A., 2016. Trends in Global CO2 Emissions: 2016 Report. Technical Report 2315, PBL Netherlands Environmental Assessment Agency, The Hague, p. 86.

Perera, L.P., 2016. Marine engine centered localized models for sensor fault detection under ship performance monitoring. IFAC-PapersOnLine 49 (28), 91–96. http://dx.doi.org/10.1016/j.ifacol.2016.11.016.

Perera, L.P., Mo, B., 2017. Machine intelligence based data handling framework for ship energy efficiency. IEEE Trans. Veh. Technol. 66 (10), 8659–8666. http://dx.doi.org/10.1109/TVT.2017.2701501.

Perera, L.P., Mo, B., 2020. Ship performance and navigation information under high-dimensional digital models. J. Mar. Sci. Technol. 25 (1), 81–92. http://dx.doi.org/10.1007/s00773-019-00632-5.

Perera, L., Ventikos, N., Rolfsen, S., Öster, A., 2021. Advanced data analytics towards energy efficient and emission reduction retrofit technology integration in shipping. In: 31st International Ocean and Polar Engineering Conference (ISOPE2021). Rhodes, Greece.

Petersen, J.P., Jacobsen, D.J., Winther, O., 2012a. Statistical modelling for ship propulsion efficiency. J. Mar. Sci. Technol. 17 (1), 30–39. http://dx.doi.org/10.1007/s00773-011-0151-0.

Petersen, J.P., Winther, O., Jacobsen, D.J., 2012b. A machine-learning approach to predict main energy consumption under realistic operational conditions. Ship Technol. Res. 59 (1), 64–72. http://dx.doi.org/10.1179/str.2012.59.1.007.

Pyle, D., 1999. Data Preparation for Data Mining, first ed. Morgan Kaufmann Publishers Inc., San Francisco, CA, USA.

Raptodimos, Y., Lazakis, I., 2018. Using artificial neural network-self-organising map for data clustering of marine engine condition monitoring applications. Ships Offshore Struct. 13 (6), 649–656. http://dx.doi.org/10.1080/17445302.2018.1443694.

Rasmussen, H.B., Lützen, M., Jensen, S., 2018. Energy efficiency at sea: Knowledge, communication, and situational awareness at offshore oil supply and wind turbine vessels. Energy Res. Soc. Sci. 44, 50–60. http://dx.doi.org/10.1016/j.erss.2018.04.039.

Rødseth, Ø.J., Perera, L.P., Mo, B., 2016. Big data in shipping - Challenges and opportunities. In: Proceedings of the 15th International Conference on Computer Applications and Information Technology in the Maritime Industries (COMPIT 2016). Lecce, Italy.

Sasa, K., Terada, D., Shiotani, S., Wakabayashi, N., Ikebuchi, T., Chen, C., Takayama, A., Uchida, M., 2015. Evaluation of ship performance in international maritime transportation using an onboard measurement system - in case of a bulk carrier in international voyages. Ocean Eng. 104, 294–309. http://dx.doi.org/10.1016/j.oceaneng.2015.05.015.

Schwarz, G., 1978. Estimating the dimension of a model. Ann. Statist. 6 (2), http://dx.doi.org/10.1214/aos/1176344136.

Soner, O., Akyuz, E., Celik, M., 2018. Use of tree based methods in ship performance monitoring under operating conditions. Ocean Eng. 166, 302–310. http://dx.doi.org/10.1016/j.oceaneng.2018.07.061.

Soner, O., Akyuz, E., Celik, M., 2019. Statistical modelling of ship operational performance monitoring problem. J. Mar. Sci. Technol. 24 (2), 543–552. http://dx.doi.org/10.1007/s00773-018-0574-y.

Sullivan, B.P., Desai, S., Sole, J., Rossi, M., Ramundo, L., Terzi, S., 2020. Maritime 4.0 – Opportunities in digitalization and advanced manufacturing for vessel development. Procedia Manuf. 42, 246–253. http://dx.doi.org/10.1016/j.promfg.2020.02.078.

Tran, T.A., 2020. Effect of ship loading on marine diesel engine fuel consumption for bulk carriers based on the fuzzy clustering method. Ocean Eng. 207, 107383. http://dx.doi.org/10.1016/j.oceaneng.2020.107383.

UNCTAD, 2019. Review of Maritime Transport 2019. UNITED NATIONS, New York, NY, USA.

Vanem, E., Brandsæter, A., 2019. Unsupervised anomaly detection based on clustering methods and sensor data on a marine diesel engine. J. Mar. Eng. Technol. 1–18. http://dx.doi.org/10.1080/20464177.2019.1633223.

Viktorelius, M., Lundh, M., 2019. Energy efficiency at sea: An activity theoretical perspective on operational energy efficiency in maritime transport. Energy Res. Soc. Sci. 52, 1–9. http://dx.doi.org/10.1016/j.erss.2019.01.021.

Wang, S., Ji, B., Zhao, J., Liu, W., Xu, T., 2018. Predicting ship fuel consumption based on LASSO regression. Transp. Res. D 65, 817–824. http://dx.doi.org/10.1016/j.trd.2017.09.014.

Wang, K., Yan, X., Yuan, Y., Jiang, X., Lodewijks, G., Negenborn, R.R., 2017. Study on route division for ship energy efficiency optimization based on big environment data. In: 2017 4th International Conference on Transportation Information and Safety (ICTIS). pp. 111–116. http://dx.doi.org/10.1109/ICTIS.2017.8047752.

Yan, R., Wang, S., Du, Y., 2020. Development of a two-stage ship fuel consumption prediction and reduction model for a dry bulk ship. Transp. Res. E 138, 101930. http://dx.doi.org/10.1016/j.tre.2020.101930.

Yan, X., Wang, K., Yuan, Y., Jiang, X., Negenborn, R.R., 2018. Energy-efficient shipping: An application of big data analysis for optimizing engine speed of inland ships considering multiple environmental factors. Ocean Eng. 169, 457–468. http://dx.doi.org/10.1016/j.oceaneng.2018.08.050.

Yuan, Y., Li, Z., Malekian, R., Yan, X., 2017. Analysis of the operational ship energy efficiency considering navigation environmental impacts. J. Mar. Eng. Technol. 16 (3), 150–159. http://dx.doi.org/10.1080/20464177.2017.1307716.

Zaman, I., Pazouki, K., Norman, R., Younessi, S., Coleman, S., 2017. Challenges and opportunities of big data analytics for upcoming regulations and future transformation of the shipping industry. Procedia Eng. 194, 537–544. http://dx.doi.org/10.1016/j.proeng.2017.08.182.

Zhang, S., Zhang, C., Yang, Q., 2003. Data preparation for data mining. Appl. Artif. Intell. 17 (5–6), 375–381. http://dx.doi.org/10.1080/713827180.

Paper III

Life-Cycle Cost Analysis on a Marine Engine Innovation for Retrofit: A Comparative Study

Khanh Quang Bui, Lokukaluge Prasad Perera, Jan Emblemsvåg and Halvor Schøyen (2022)

Published in *Proceedings of the ASME 2022 41st International Conference on Ocean, Offshore and Arctic Engineering. Volume 5A: Ocean Engineering.* Hamburg, Germany. June 5–10, 2022. V05AT06A029. ASME.

https://doi.org/10.1115/OMAE2022-79488.

Paper IV

Life cycle cost analysis of an innovative marine dual-fuel engine under uncertainties

Khanh Quang Bui, Lokukaluge Prasad Perera and Jan Emblemsvåg (2022)

Published in *Journal of Cleaner Production, 380*, 134847.

https://doi.org/10.1016/j.jclepro.2022.134847.

Journal of Cleaner Production 380 (2022) 134847

Contents lists available at ScienceDirect

Journal of Cleaner Production

journal homepage: www.elsevier.com/locate/jclepro

Life-cycle cost analysis of an innovative marine dual-fuel engine under uncertainties

Khanh Q. Bui [a,b,*], Lokukaluge P. Perera [a], Jan Emblemsvåg [c]

[a] Department of Technology and Safety, UiT The Arctic University of Norway, Tromsø, Norway
[b] Faculty of Navigation, Vietnam Maritime University, Hai Phong, Viet Nam
[c] Department of Ocean Operations and Civil Engineering, NTNU Norwegian University of Science and Technology, Norway

ARTICLE INFO

Handling Editor: Mingzhou Jin

Keywords:
Life-cycle cost analysis
Dual-fuel marine engine
Net present cost
Emissions reduction
Uncertainties
Market-based measures

ABSTRACT

As innovative technologies are being deployed to accelerate shipping decarbonization in response to air emission regulations, there is considerable concern about the cost effectiveness of such technologies from a life-cycle perspective. This study conducts a life-cycle cost analysis (LCCA) on an innovative marine dual-fuel engine under uncertainties, comparing the total life-cycle cost performance of such an engine with that of a conventional diesel engine. By proposing several economic Key Performance Indicators (KPIs) such as the Net Present Cost (NPC), the Net Saving (NS) and the Saving-to-Investment Ratio (SIR), the findings indicate that the dual-fuel engine is more cost-effective than the diesel engine under a given fuel price scenario. The uncertainties are meticulously treated by using scenario sensitivity analyses and a Monte Carlo simulation. The scenario sensitivity analyses reveal that the cost effectiveness of the dual-fuel engine is sensitive to the high gas price scenarios. It is uncovered from the Monte Carlo simulation that there is an adequate degree of confidence when opting for the dual-fuel engine. Furthermore, fuel prices are found to be the most influential cost driver. Different foreseeable carbon pricing scenarios are also simulated to show that the dual-fuel engine is still the most favorable option. Regardless of fuel prices and carbon pricing scenarios, the dual-fuel engine provides a considerable environmental benefit with a CO_2 emission reduction potential of 33%. The findings of this study are of interest within the field of shipping investment appraisals and relevant to decision-makers (i.e. ship-owners and investors).

1. Introduction

1.1. Background

International shipping has been in the limelight recently, following the daunting challenge of decarbonization. The international shipping industry carries 80% of global trade by volume (UNCTAD, 2021). During this process, ships emit approximately 1 billion metric tons of carbon dioxide (CO_2) each year, i.e. equivalent to Japan's annual CO_2 emissions (Ritchie and Roser, 2020). During the period from 2012 to 2018, the total GHG emissions from shipping rose from 977 million tonnes to 1,076 million tonnes. This is an increase by 9.6%. In the same period, there was also an increase (from 2.76% to 2.89%) in the share of shipping emissions in global anthropogenic (man-made) emissions. As trade demand grows, so too will CO_2 emissions from shipping. It is envisaged that these emissions will represent 90% to 130% of 2008 emissions by 2050 under the business-as-usual scenario (IMO, 2020).

International shipping is not directly included in the Paris Climate Change Agreement, with responsibility for emissions reductions lying on the International Maritime Organization (IMO) (Bullock et al., 2022). However, the IMO has made a commitment to the Paris Agreement by adopting an Initial Strategy with a target to halve the total annual GHG emissions from international shipping by 2050, compared with 2008 levels. It also aims at lowering the carbon intensity of international shipping by at least 40% by 2030 and pursuing efforts towards 70% by 2050, compared with 2008 levels (IMO, 2018).

The Initial Strategy comprises a variety of measures that can be listed in short-, medium- and long-term visions: (i) design measures, (ii) operational measures, (iii) market-based measures (MBMs), and (iv) the use of low or zero-carbon fuels. The Energy Efficiency Design Index (EEDI) is a design measure which is mandatory for new-built ships while the Ship Energy Efficiency Management Plan (SEEMP) is an operational measure applied to all ships. The EEDI and SEEMP have been enforced since 2011 under Annex VI Chapter 4 of the International

* Corresponding author at: Department of Technology and Safety, UiT The Arctic University of Norway, Tromsø, Norway.
E-mail address: khanh.q.bui@uit.no (K.Q. Bui).

https://doi.org/10.1016/j.jclepro.2022.134847
Received 8 June 2022; Received in revised form 21 September 2022; Accepted 20 October 2022
Available online 27 October 2022

Nomenclature

Abbreviations

APS	Announced Pledges Scenario
CBS	Cost Breakdown Structure
CERs	Cost Estimation Relationships
CII	Carbon Intensity Indicator
CO_2	Carbon Dioxide
DWT	Deadweight Ton
EBS	Engine Breakdown Structure
ECAs	Emission Control Areas
EEDI	Energy Efficiency Design Index
EEXI	Energy Efficiency Existing Ship Index
ETS	Emissions Trading System
EU	European Union
GHG	Greenhouse Gas
HFO	Heavy Fuel Oil
IMO	International Maritime Organization
ISO	International Organization for Standardization
KPIs	Key Performance Indicators
LCA	Life-cycle Assessment
LCC	Life-cycle Costing
LCCA	Life-cycle Cost Analysis
LNG	Liquefied Natural Gas
LOA	Length Overall
MARPOL	International Convention for the Prevention of Pollution from Ships
MBMs	Market-based Measures
MCR	Maximum continuous rating
MEPC	Marine Environment Protection Committee
MGO	Marine Gas Oil
NO_x	Nitrogen Oxide
NPV	Net Present Value
NZE	Net Zero Emissions by 2050 Scenario
O&MMs	Operation & Maintenance Manuals
RPM	Revolutions Per Minute
SCR	Selective Catalytic Reduction
SDS	Sustainable Development Scenario
SEEMP	Ship Energy Efficiency Management Plan
SSS	Short-sea Shipping
STEPS	Stated Policies Scenario
TCO	Total Cost of Ownership
ULSD	Ultra Low Sulphur Diesel
VLSFO	Very Low Sulphur Fuel Oil
WEO2021	Energy Outlook 2021

Variables

$\mathcal{N}$	The number of years in the study period
$\mathcal{P}$	Price of a product [€]
ΔI_t	The additional investment-related costs in year t associated with the alternative
C_F	Carbon emission conversion factor [t-CO_2/t-Fuel]
H	The annual operating hours for each engine mode [h/y]
I	Inflation rate [%]
i	The i^{th} engine mode associated with the corresponding engine load
M_{CO_2}	The annual amount of CO_2 emissions generated from fuel combustion [t-CO_2/y]
N	The total number of engine modes
P	The engine power required for each engine mode [kW]
r	Discount rate [%]
r'	Discount rate for calculating the carbon emission costs [%]
S_t	The savings in year t in operational costs associated with the alternative
t	Year of occurrence, $t = 0$ is the base year
CST	Construction cost [€]
EOL	End-of-life value [€]
FC	The annual fuel consumption [t-Fuel/y]
FGC	The annual fuel gas consumption [t-Fuel/y]
FOC	The annual fuel oil consumption [t-Fuel/y]
FV	Future value of the cost or benefit [€]
LOC	The annual lubricating oil consumption [t-Fuel/y]
MTN	Maintenance cost [€]
NPC	Net present cost [€]
NS	Net Saving [€]
OPR	Operation Cost [€]
PFC	The annual pilot fuel consumption [t-Fuel/y]
PV	Present value of the cost or benefit [€]
SFGC	The specific fuel gas consumption [g/kWh] under specific engine power output, as the function of the engine load [g/kWh]
SFOC	The specific fuel oil consumption [g/kWh] under specific engine power output, as the function of the engine load [g/kWh]
SIR	The saving-to-investment ratio of the alternative relative to the base case
SLOC	The specific lubricating oil consumption under specific engine power output [g/kWh]
SPFC	The specific pilot fuel consumption under specific engine power output [g/kWh]

Convention for the Prevention of Pollution from Ships (MARPOL) (IMO, 2011).

A new wave of mandatory measures will be enforced from 2023 with the IMO's adoption of new amendments to the MARPOL Annex VI including the Energy Efficiency Existing Ship Index (EEXI), the carbon intensity indicator (CII) and the enhanced SEEMP. Being considered the sister to the EEDI, the EEXI is a design measure, applicable to existing ships. The CII, related to an operational measure, measures the operational carbon intensity performance levels of a ship based on a rating scheme (from A to E). The EEXI and the CII are the short-term measures to lower carbon intensity while MBMs are considered the mid-term measures. Lagouvardou et al. (2022) augured that MBMs also have both short-term (logistical) and long-term (technological) consequences.

Such measures are expected to create a profound impact on the shipping industry in its transition towards decarbonization. To accelerate such transition, various available emissions reduction options, extensively reviewed by Bouman et al. (2017) together with under-development innovative options are needed. From the ship-owner perspective, it is a challenging task for them to choose the best option that

will gain traction in the industry. This is due to the fact that it is a multi-criteria decision-making process in which a broad range of criteria, including technical, environmental and economic criteria is taken into consideration (Bui et al., 2021a). In addition, investments in such options are costly with a recent study reporting at least $1 trillion needed by 2050 in order to meet the IMO's emission targets (Carlo et al., 2020). Furthermore, there are still significant uncertainties concerning the technical feasibility and economics of these options.

Since the shipping industry is a capital-intensive industry associated with long ship lifespans and a high dependence on the global fuel supply, decisions made today will have a strong effect on the future operations and economic performance of a fleet for many years to come. The total lifespan cost of any appropriate emissions reduction technology can be significant if unwise decisions are made at the early stage. For this reason, it is required a strategic long-term approach that can oversee and control the costs before they are incurred. In this regard, life-cycle cost analysis (LCCA) on such technologies is attracting considerable attention. When adopting such technologies, there is a large uncertainty over fuel prices and the future fuel and energy mix. This seems to be a reason why ship-owners are reluctant to make investments. Therefore, it is important to take these uncertainties into consideration when conducting LCCA.

1.2. Dual-fuel engine retrofit

Apart from the regulatory pressure to achieve the IMO's emission targets, shipowners are coming under commercial pressure to be more competitive in the charter market (DNV, 2021). In order to have a better performance on emissions, shipowners are in need of upgrading their existing fleet to higher operational standards. From this perspective, retrofitting, i.e., the installation of innovative technologies on-boards existing ships is attracting considerable interest. In this respect, dual-fuel engines could be potentially applied for the main propulsion system on retrofitted ships. The subject of this study is a high-efficiency modern dual-fuel engine. The dual-fuel engine provides flexibility because it can be run in either liquid-fueled diesel mode or gas mode. In the diesel mode, it functions similar to a normal diesel engine. In the gas mode, a lean burn combustion process is achieved, thus lowering nitrogen oxides (NO_x) emissions and enhancing efficiency. Furthermore, utilizing a clean and low-carbon fuel (i.e. liquefied natural gas (LNG)) leads to very low exhaust gas emissions. The gas is injected into the engine at a low pressure and it is then ignited by a small amount of pilot diesel fuel injected into the combustion chamber (Wärtsilä, 2020).

The dual-fuel engine can be potentially retrofitted or installed on ships operating in short-sea shipping (SSS). In the context of the European SSS, one should consider the expansion of the EU Emissions Trading System (ETS) to the maritime sector (European Commission (EC), 2021). This is a result of the Fit for 55 package which is a green transition plan set by the EU, aiming to reduce the EU's total GHG emissions by at least 55% by 2030. In this regard, all ships will be required to purchase allowances for each ton of CO_2 they emit. The EU ETS, based on the "polluter pays" principle, is advocated as an efficient MBM at a regional level (Cariou et al., 2021). The IMO MBMs, on the other hand, are intended to impose a tax on emitted GHG emissions at a global level.

There will be a considerable correlation between the utilization of innovative technologies (e.g. the dual-fuel engine) and the introduction of MBMs (e.g. the IMO MBMs and the EU ETS). If ship-owners decide to retrofit their existing fleet with the dual-fuel engine, the economic aspect from a life-cycle perspective will be of paramount importance. At this point, LCCA will become a useful tool to assess and predict the economic performance of this engine over its lifespan.

The remaining part of this study proceeds as follows: Section 2 reviews the life-cycle costing (LCC) studies in the maritime research domain, Section 3 discusses the details of the proposed LCC framework, Section 4 describes the application of the proposed LCC framework to a case study pertaining to the dual-fuel engine and a conventional diesel engine and finally, Section 5 highlights and discusses the findings. Suggestions for future work are also offered in this section.

2. Literature review

2.1. Review on the LCC studies

LCC is an economic method for evaluating the total cost of an asset by considering initial costs and discounted future expenditures that will incur throughout the asset's life cycle. This method was introduced by the U.S. Department of Defense in the 1960s as an attempt to improve its cost-effectiveness in granting competitive awards (Sherif and Kolarik, 1981). Since then, it has been successfully employed in the industrial and consumer sectors.

In the maritime research domain, it has received considerable scholarly attention in recent years. From the methodological perspective, it has been combined with existing approaches for evaluating different options from an economic viewpoint. By combining the LCC method with activity-based costing, Emblemsvåg (2003) proposed an effective cost management method under an uncertain environment. The proposed method was applied in the context of a platform supply vessel operating in the North Sea. With the adoption of systems engineering and sustainable principles, Utne (2009) provided a LCC framework that can be used as a tool for enhancing sustainable designs of the Norwegian fishing fleet.

Furthermore, the LCC method has been integrated with the Life-cycle Assessment (LCA) method to assess the economic and environmental impacts of alternative technologies and ship systems. Having a different view to the ISO 14000 standard, Emblemsvåg and Bras (2012) evaluated the life-cycle economic and environmental impacts of a platform supply vessel by proposing an activity-based cost and environmental management approach. Blanco-Davis and Zhou (2014) conducted a cost-benefit analysis for the retrofitting evaluation of ballast water treatment systems. However, a major drawback of this study is the omission of the maintenance phase. A framework with an integration of the LCC and LCA methods was proposed for the selection of propulsion systems (Jeong et al., 2018). The proposed framework was demonstrated in two case studies. The first one examined the advantages of battery usage in a short-route hybrid ferry. The second one found the optimal engine configuration for an offshore tug vessel.

Favi et al. (2018) developed a framework combining the LCA and LCC methods to assess the environmental and economic performance of recreation vessels (i.e. luxury yachts). From a life-cycle perspective, the environmental and commercial benefits of using solar panel applied to short route ferries were investigated (Wang et al., 2019; Zito et al., 2022). Wang et al. (2021) proposed a framework in which a life cycle emission inventory and the corresponding costs of innovative battery power plants applied on a catamaran ferry were compared to that of conventional diesel engines. In the context of SSS in Croatia, Perčić et al. (2020) proposed strategies to improve the environmental impacts and lifespan costs of passenger ferries. In this study, a combined LCA–LCC method was performed to evaluate the potential of various alternative marine fuels compared to the conventional diesel fuel. Andersson et al. (2020) conducted a comparative analysis to select the marine scrubber systems. The LCC method was applied in this study to compare the payback time of the installation costs of these systems.

Huang et al. (2021) undertook a LCCA on alternatives for the compliance of the IMO's 2020 global sulphur cap under uncertainties. In this study, three alternatives, including fuel switch from Heavy Fuel Oil (HFO) to Very Low Sulphur Fuel Oil (VLSFO) and Marine Gas Oil (MGO), the installation of scrubber and the use of LNG as fuel, were compared in two container vessels of 5000 and 10,000 TEUs.

The total cost of ownership (TCO), a synonym of LCC, of various alternative fuels and corresponding ship power systems was evaluated

Table 1
Review on the LCC studies.

Reference	Software	Target subject	ISO 14040/14044	ISO 15686-5	Uncertainty treatment[a]
Blanco-Davis and Zhou (2014)	Gabi	Ballast water treatment systems	✓		No
Emblemsvåg (2003)	Crystal Ball	A platform supply vessel	*	*	Yes
Emblemsvåg and Bras (2012)	Crystal Ball	A platform supply vessel	*	*	Yes
Utne (2009)	N/M	Norwegian fishing vessels		✓	No
Jeong et al. (2018)	Gabi	Marine propulsion systems Battery usage in a short-route hybrid ferry	✓		No
Favi et al. (2018)	Excel, Visual Basic	Complex vessels (luxury yachts)	✓	✓	No
Wang et al. (2019)	Gabi, RETScreen	Solar panel system applied to a short route ferry	✓		No
Zito et al. (2022)	Gabi, MATLAB	Solar panel system applied to a short route ferry	✓		No
Wang et al. (2021)	Gabi	Battery power plants in a high-speed ferry	✓		No
Perčić et al. (2020)	GREET	Passenger ferries	✓		No
Wang et al. (2018)	Gabi	An optimal hull maintenance strategy for a short route ferry	✓		No
Andersson et al. (2020)	Gabi	Marine scrubber systems	✓		No
Gualeni et al. (2019)	In-house software	Different propulsion layout solutions	✓		No
Huang et al. (2021)	@RISK	Alternatives for container vessels	N/M	N/M	Yes
Lagemann et al. (2022)	Gurobi, Python	Alternative fuels and ship power systems	N/M	N/M	No

N/M: Not mentioned.
*: A different approach was proposed.
[a]Uncertainty treatment by a probabilistic approach such as Monte Carlo simulation.

by using an optimization model (Lagemann et al., 2022). By applying this model to a supramax bulk carrier under a low fuel price and a carbon tax setting, bio-fuels were uncovered to be the most cost-effective and LNG powered-system is considered reliable for several GHG reduction ambitions.

Several studies were mainly oriented to LCA under the maintenance perspective. An optimal maintenance strategy was derived from a study conducted by Wang et al. (2018) after evaluating the life-cycle cost of a short route ferry considering the steel renewal and re-coating processes. Gualeni et al. (2019) proposed a life-cycle performance assessment tool to select the best propulsion layout solution with regard to cost performance.

2.2. Research gaps and contribution

It is perceived from these studies reviewed in the last section that the application of the LCC method is normally situated along with the LCA method, rather than in a stand-alone context. In this regard, from the methodological point of view, most of these studies have adopted the ISO 14040/14044 standards of environmental management. This may lead to misunderstandings or confusions when a specific LCC framework is conducted. The ISO 15686-5 standard on LCC applying to the building sector could be used as a standardized approach that offers a methodological procedure for conducting LCCA (Mondello et al., 2021). Another aspect emerged from the literature review that the uncertainty inherent to any LCC models has not been addressed thoroughly. Prior studies have dealt with the uncertainty by only using deterministic approaches (e.g. sensitivity analysis) which do not offer direct insights into the probabilities of different outcomes. As a result, decision-makers select between alternatives based on their judgements. On the other hand, probabilistic approaches provide a more detailed consideration of the uncertainty by taking into account probability. An example of the probabilistic approach is Monte Carlo simulation. However, only three out of the reviewed studies carried out the uncertainty analysis using Monte Carlo simulation, as demonstrated in Table 1. Favi et al. (2018) suggested the use of Monte Carlo simulation to consider uncertainties throughout the lifespan of studied vessels as future work. Furthermore, to the best of the authors' knowledge, there are not many studies focusing on the life-cycle cost performance of a marine dual-fuel engine in the context of retrofitting practices. In addition, there has been no detailed investigation of the main components and systems of studied subjects with an engineering approach.

The current study aims to address these gaps in the existing literature by proposing a LCC framework that integrates a standardized approach for LCCA (i.e. the ISO 15686-5) for investigating the potential economic benefits of an innovative engine technology (i.e. the dual-fuel engine), taking into account the uncertainties involved over the lifetime of the engine. The ultimate goal is to compare the life-cycle cost performance of the dual-fuel engine with that of a conventional diesel engine. The proposed framework includes the development of a cost model with an engineering build-up approach, resulting in interpretable and effective results using data from numerous sources. Specifically, different cost categories are calculated among the engines' life cycle phases, ranging from construction, operation, maintenance to end-of-life. In addition, the external costs (i.e. carbon emission costs) due to air pollution from internal combustion engines are included in the cost model. Furthermore, the uncertainties are thoroughly treated under scenario sensitivity analyses and a Monte Carlo simulation correspondingly. The former considers the effects of changing key uncertain input variables on the relative merits of the engine alternative, i.e. the dual-fuel engine. The latter is concerned with conducting a statistical technique using the Monte Carlo simulation. In this respect, by introducing uncertainty into the cost model, the probabilities of different outcomes can be calculated.

The application of the proposed framework should make the following contributions to the current literature: (i) it offers a better understanding on a methodological procedure for LCCA, (ii) it conducts a thorough examination of uncertainties by means of the scenario sensitivity analyses and the Monte Carlo simulation, (iii) it will be a useful aid for decision-makers (i.e. ship-owners, investors) as regards retrofitting decision-making and (iv) it provides the assessment of the impacts of carbon pricing on technology investments, contributing to recent discussions concerning MBMs.

3. The proposed LCC framework

As previously mentioned, a uniform LCC framework has not yet been established or some LCC studies have just followed what is needed in the ISO 14040/14044 standards. Having a more detailed perspective, this study proposes a LCC framework in which several steps are demonstrated, as shown in Fig. 1. The framework encompasses the principles taken from the ISO15686-5 standard (ISO, 2017) and processes proposed by Utne (2009), Bui et al. (2021b) and Bui et al. (2022).

3.1. Goal and scope

- Goal: The goal of this study is to evaluate the total life-cycle cost performance of the dual-fuel engine compared with that of a conventional engine. The economic benefits of utilizing the

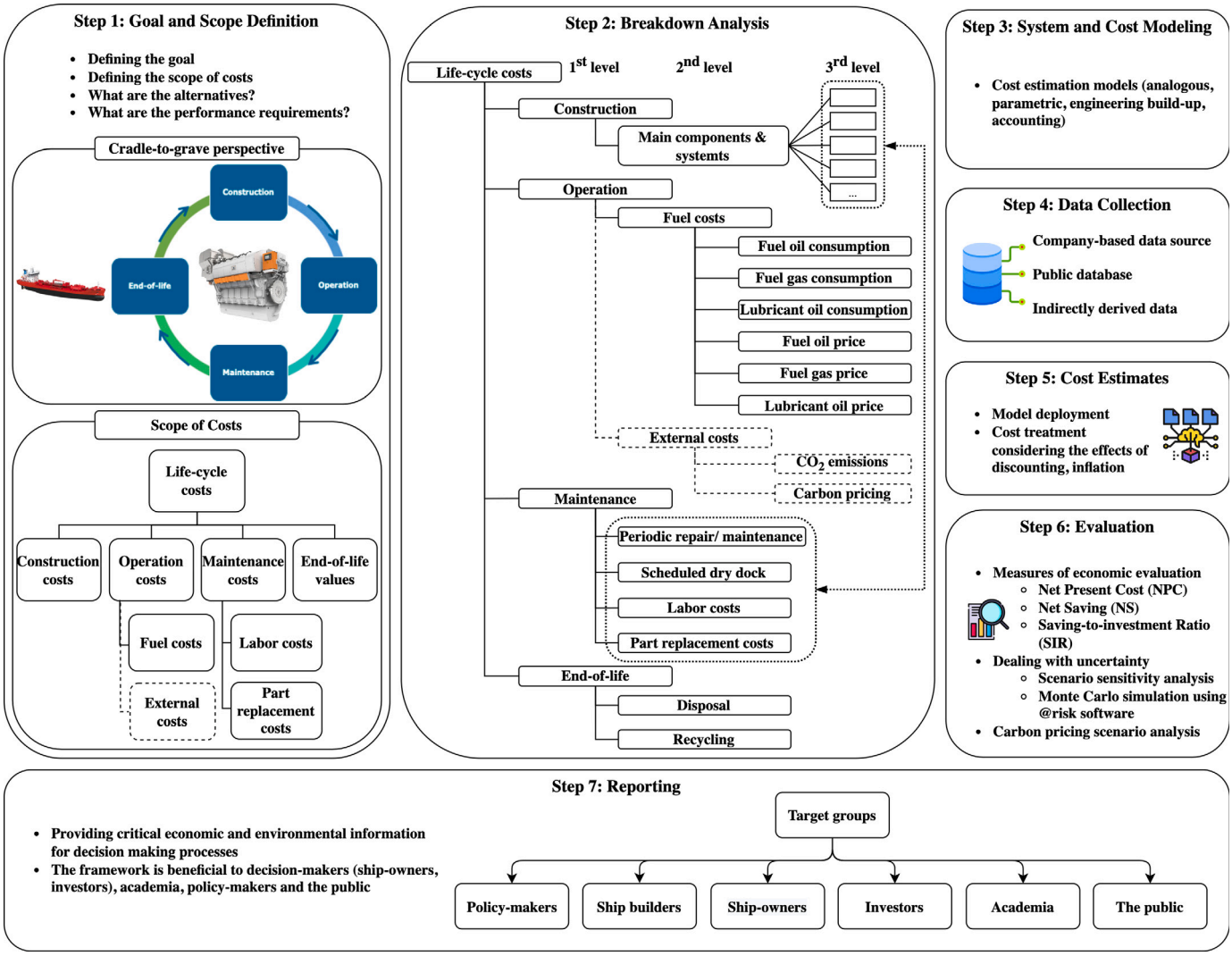

Fig. 1. The proposed LCC framework.

dual-fuel engine are demonstrated from a life-cycle perspective. Furthermore, the environmental benefits of utilizing the dual-fuel engine during its operation are also under consideration.

- Scope: The scope of this study can be revised along the analysis because of the iterative approach. The system is bounded to the use of such engines as the main propulsion systems. From a cradle-to-grave perspective, there are four cost components associated with the engines' life-cycle phases: construction costs, operation costs, maintenance costs and end-of-life values. Apart from that, the external costs (i.e. carbon emission costs) are also taken into account under the operation phase.

3.2. Breakdown analysis

To further define the scope of costs included in this study, a Cost Breakdown Structure (CBS) is devised to provide a structured basis in which cost categories are classified on different levels as shown in Step 2 of Fig. 1. The first level comprises the main cost components connected with four life-cycle phases of the engines, i.e., construction, operation, maintenance, and end-of-life. The second and third level includes local costs and factors that are intended to accommodate in the respective phases of the engines.

3.2.1. Construction costs

The construction costs include those for assembling the engines before putting them into initial service. In this regard, an Engine Breakdown Structure (EBS) of a conventional diesel engine is provided to indicate the costs of its main components and systems, as shown in Table 2. The EBS is a basis for a structural comparison between the diesel engine and the dual-fuel engine. One of the structural differences between these engines is the fuel injection system because the dual-fuel engine is equipped with a gas system. Furthermore, the installation of the Selective Catalytic Reduction (SCR) system is not applicable to the dual-fuel engine due to its low emissions when operating in the gas mode. The EBS will also play an important role in the later stage when calculating the part replacement costs of the engines' components.

3.2.2. Operation costs

The operation costs are the annual expenses incurred in the routine operations of the engines. Fuel costs are the most important cost component of the cost of running ships, accounting for two-thirds of the voyage costs (Stopford, 2009). For this reason, the operation costs used in the base case of this study refer to fuel costs. These costs can be derived from the annual fuel consumption and the annual lubricating oil consumption (LOC).

As regards the diesel engine, the total annual fuel oil consumption (FOC) and the total annual LOC can be determined by using the

Table 2
A general Engine Breakdown Structure (EBS).

2nd Level	3rd Level	Cost	
		Diesel engine	Dual-fuel engine
Main components & systems	Engine basement		
	Camshaft & Valve Mechanism		
	Fuel Injection System		
	Turbocharging & Scavenging System		
	Ancillary System		
	Automation System		
	Low-value Parts		
	Exhaust Gas Cleaning System[a]		N/A
	Total	989K	1,200K

[a]Selective Catalytic Reduction (SCR) technology for NO_x reduction. The SCR cost for the diesel engine was adopted from the International Association for Catalytic Control of Ship Emissions to Air (IACCSEA) (IACCSEA, 0000). The SCR system is not required for the dual-fuel engine. Other costs were obtained from the engine manufacturer (Wärtsilä, 2021a).
Unit K = 1000€.

following equations (Wang et al., 2019).

$$\mathrm{FOC} = \sum_{i=1}^{N} P_i \times \mathrm{SFOC}_i \times H_i \quad (1)$$

$$\mathrm{LOC} = \sum_{i=1}^{N} P_i \times \mathrm{SLOC}_i \times H_i \quad (2)$$

In the case of the dual-fuel engine, it can be run either in diesel mode or gas mode. In the diesel mode, it is a normal diesel engine, therefore the total annual FOC can also be found by adopting Eq. (1). In the gas mode, the main fuel is LNG which is injected into the engine at a low pressure. The lean air–gas mixture is ignited by injecting a small amount of pilot diesel fuel (Wärtsilä, 2020). The total annual pilot fuel consumption (PFC) can also be obtained by adopting Eq. (1). The total annual fuel gas consumption (FGC) can be determined as follows.

$$\mathrm{FGC} = \sum_{i=1}^{N} P_i \times \mathrm{SFGC}_i \times H_i \quad (3)$$

The total annual LOC of the dual-fuel engine can also be calculated by adopting Eq. (2).

Besides the internal costs borne by the engine operations during their lives, the scope of this study is also expanded by including the external costs (also termed externalities) that are expected to be internalized in the near future. They are carbon emission costs that will be included in the operation costs in the later stage where carbon pricing scenarios are taken into account. The carbon emission costs refer to the costs of emitting CO_2 equivalent emissions. These can be perceived as carbon taxes under the IMO MBMs or the carbon allowance under the EU ETS that can be received, bought, or even traded. In order to determine these costs, the environmental impacts of the engines need to be quantified based on the estimation of the annual CO_2 emissions emitted from fuel combustion, as expressed in the following equation (IMO, 2020).

$$M_{CO_2} = \mathrm{FC} \times C_F \quad (4)$$

3.2.3. Maintenance costs

The maintenance costs refer to the costs of regular maintenance tasks that should be done to avoid engine malfunction and extend its lifespan. The practices for such maintenance tasks are based on a time-based maintenance schedule, i.e. the Operation & Maintenance Manual (O&MM) given by the engine manufacturer, where the maintenance intervals for each engine's main component and system are provided. These components and systems are corresponding to the third level of the EBS as indicated previously. Table 3 briefly illustrates the maintenance tasks and the associated intervals of each part of the fuel injection system of the dual-fuel engine. The routine maintenance tasks are normally conducted by crew members from the engine department (i.e., Chief Engineers, Engine Officers, Engine Cadets) when the ship is in service. The heavy maintenance tasks (i.e. major overhauls) are generally performed by technical personnel from the engine manufacturer when the ship is out of service (i.e. on dry-docking). Occasionally, several engine parts can be sent to the engine manufacturer's workshops ashore. In this study, the maintenance costs are categorized into:

- Labor costs for doing the maintenance tasks for the engines' components.
- Part replacement costs (i.e. spare costs) of the engines' components according to the O&MMs.

3.2.4. End-of-life values

Around 96% of ships are recycled when they reach the final phase of their lives (McKenna et al., 2012). Along with hull structure and other significant parts of the ship, the main engine will also be recycled. Therefore, in this study, the values of the engines at the end of their lives are the negative costs or the benefits.

3.3. System and cost modelling

The following is a brief description of models to perform LCCA. It has been perceived in the literature that four cost estimation models exist: analogous, parametric, engineering build-up, and cost accounting. Their characteristics, advantages and disadvantages will be explained as follows.

3.3.1. Analogous model

In this method, the cost of a product can be estimated from the similarities and differences between it and known variants from past projects. It is based on an assumption that similar products have similar costs. Domain knowledge from experts is required to establish similarity functions and analogy rules. With actual historical data available, reasonable cost approximation can be made in a short span of time. This case-based method can be applicable to the cost estimation during the early design stage (Curran et al., 2004; Hueber et al., 2016).

3.3.2. Parametric model

The principle of this method is to formalize the so-called "Cost Estimation Relationship" (CER) which is derived from the mathematical relationships between the costs of a product and its parameters. Such parameters are typically referred to as "Cost Drivers" and they have great influence on the cost changes or at least they are relative to the cost changes. An example of the cost driver is the part size of the product, as the part size increases, so does the manufacturing costs. Statistical analysis can be used under one part family of the product in order to estimate the part costs with regard to the part size. Different CERs can be developed with more cost drivers (e.g., size, weight) in one parametric model. There are several drawbacks of this method:

Table 3
An extraction of the O&MM regarding the fuel injection system of the dual-fuel engine.
Source: Wärtsilä.

3rd level of the EBS	Part	Maintenance task	Interval
Fuel injection system	Fuel filters	Check the pressure drop Change the filter cartridges if a high pressure drop is indicated	50 h
	Fuel system	Check that there are no fuel leaks from the engine	24 h
	Fuel system	Check the clean leak fuel quantity	50 h
	Fuel system	Replace the valve block for Pressure Drop and Safety Valve (PDSV) and Circulation Valve (CV)	24,000 h
	Fuel system	Replace the high-pressure fuel pipes	48,000 h
	HP fuel pump(s)	Replace the HP fuel pump(s)	24,000 h
	Fuel injectors	Replace the fuel injectors	8,000 h
	Centrifugal oil filter	Clean the centrifugal filter	2,000 h
	Fuel feed pump	Overhaul the fuel feed pump	16,000 h
	Main gas admission valve	Replace the main gas admission valves	16,000 h
	Gas system	Monitor the gas leak detection system. Make sure that the gas monitoring system is functioning Check for external gas leaks on the engine by using a portable gas detector.	24 h
	Gas system	Perform a tightness test, after the overhaul, before the engine is started.	32,000 h

This table provides only parts of the fuel injection system of the dual-fuel engine for reference. Remaining parts from other main components and systems are not listed here.

it depends upon a historical database; using this model outside of the database range should be avoided; and it is incapable of demonstrating technological changes or altered system requirements (Curran et al., 2004; Hueber et al., 2016).

3.3.3. Engineering build-up model

The bottom-up or engineering build-up model identifies parts, materials, and associated tasks of a product. Their costs are then added up to produce the final cost estimate of the product. As the name suggests, this method is based on a detailed engineering analysis in which a deep understanding of the process interactions, the product design and configuration, and the product system components is required. Additionally, other accounting information regarding material, equipment, and labor is necessary. Unlike the analogous and parametric models, the engineering build-up model is not limited to the range of the underlying historical data. Furthermore, it is capable of providing the level of detail and the causation. When it comes to innovative or new technologies to the industry, it is considered the only available option for cost estimation. On the other hand, domain knowledge and a large amount of data regarding the product details need to be acquired in this method (Curran et al., 2004; Hueber et al., 2016).

3.3.4. Accounting model

Cost management and accounting considering the overhead costs are the focal points in this method. In the literature, cost accounting models and systems can be divided into three categories: volume-based costing systems, unconventional costing methods, and modern cost management systems. More information on the accounting model can be found in Emblemsvåg (2003).

With a focus on the development of the EBS, the chosen cost estimation model in the current study is the engineering build-up model. Depending on the amount of data available, the other model such as the analogous model will also be used.

3.4. Data collection

Since the engineering build-up model is a systematic approach, the amount of collected data is extensive. The collected data can best be divided into three main categories: company-based data source, public database, and indirectly derived data. The involvement of an engine manufacturer (i.e. Wärtsilä) and several ship-owners in this study was of concern. Table 4 is an illustration of these data categories and their associated sources.

3.5. Cost estimates

In the section that follows, a cost model is built and deployed while considering the effects of several important aspects of LCCA (i.e., inflation, discounting, and present value). Furthermore, several measures of economic performance that will be used in the evaluation step are discussed.

3.5.1. Inflation and discounting

Since the above-mentioned costs are accumulated over the engine's lifespan, it should be noted that the monetary flows occur at different times. For this reason, the two following aspects should be considered. The first is inflation, which reduces the purchasing power of currency over time. This can be seen by a gradual increase in the general price of goods and services because of the market dynamics. Costs in different year with different purchasing power should not be added together directly to arrive at a meaningful amount. Assuming an inflation rate I, the price $\mathcal{P}$ of a product at time t (in years) can be calculated as expressed in Eq. (5) (Rödger et al., 2018).

$$\mathcal{P}(t) = (1 + I)^t \times \mathcal{P}(0) \tag{5}$$

The second aspect is discounting, which is related to the varying time value of money. The value of money today is not equal to the one projected to be spent in the future. As a result, present and future costs that occur at different points in the life of an engine cannot be compared directly. By using a discount rate chosen to represent the time value of money, all future costs are discounted back to present value costs through the following equation (Rödger et al., 2018; Welch, 2017).

$$\mathrm{PV} = \mathrm{FV}\frac{1}{(1+r)^t} \tag{6}$$

3.5.2. Net present cost (NPC)

Once all the costs associated with each phase of the engine's life cycle are estimated and computed, the net present cost (NPC), i.e. the total present value of all costs, can be calculated as the summation of the following costs in present value terms (Kneifel and Webb, 2022).

$$\mathrm{NPC} = \mathrm{PV(CST)} + \mathrm{PV(OPR)} + \mathrm{PV(MTN)} - \mathrm{PV(EOL)} \tag{7}$$

3.5.3. Net saving (NS)

Net saving (NS) is a useful measure of economic performance for an alternative investment that reduces the operational costs. NS, expressed in present value terms, can be determined by subtracting the NPC of the alternative (i.e. the dual-fuel engine) from the NPC of the base case (i.e. the diesel engine), as follows (Kneifel and Webb, 2022).

$$\mathrm{NS} = \mathrm{NPC}_{BaseCase} - \mathrm{NPC}_{Alternative} \tag{8}$$

Table 4
Data categories and sources.

Category	Source
Company-based data source	
Construction costs	Wärtsilä (2021a)
Operational profile	Wärtsilä
Engine technical data	Wärtsilä (0000)
Maintenance schedule (O&MMs)	Wärtsilä
Engine materials	Wärtsilä
Engine weights	Engine product guide Wärtsilä (2020, 2021b)
Public database	
Material recycling rates	Greengate Metals (0000)
Marine fuel (gas, oil) prices	Ship & Bunker (2021), Global Maritime Hub (2021)
Wages	Eurostat (2022)
Currency exchange rates	xe.com/currencyconverter
Discount rate	Hunkeler et al. (2008), Rödger et al. (2018)
Indirectly derived data	
Maintenance hour consumption	Questionnaires & Interviews with Chief-Engineers, Engine Officers
Part replacement costs	Interviews with a Technical Manager, Chief-Engineers

O&MMs: Operation & Maintenance Manuals.

3.5.4. Saving-to-investment ratio (SIR)

Saving-to-investment Ratio (SIR), another measure of economic performance of an alternative investment, is a ratio between its saving and its increased investment cost (in present value terms). The formula for the SIR is shown in Eq. (9) (Kneifel and Webb, 2022).

$$\mathrm{SIR} = \sum_{t=0}^{\mathrm{N}} \frac{S_t}{(1+r)^t} \Bigg/ \sum_{t=0}^{\mathrm{N}} \frac{\Delta I_t}{(1+r)^t} \tag{9}$$

3.6. Evaluation

3.6.1. Measures of economic performance

The essence of this evaluation is to use the above-mentioned measures as critical economic KPIs (i.e. key performance indicators) for the overall decision-making process. To be more specific, these measures will be used to compare the life-cycle cost performance of the dual-fuel engine with that of the diesel engine. The alternative engine is considered economically justified relative to the base engine if its NPC is lower than the NPC of the base engine. This is equivalent to having the NS greater than zero. In addition, the engine alternative is cost-effective relative to the base engine if its SIR is greater than 1.0.

3.6.2. Dealing with uncertainty

LCCA requires assumptions about future behaviors with regard to cost projection, making "best-guess" estimates as if they were certain. However, investments in such an innovative engine are long-lived and necessarily involve some uncertainties regarding fuel prices, the engine's annual operating hours, etc. If there is a substantial uncertainty regarding cost and time information, LCCA may have little value for the final decision-making process. Therefore, it is necessary to assess the degree of uncertainty associated with the results and consider it as additional information when making final decisions. Although it might be uncertain about some input variables occurring in the future, it is worth including them in the economic evaluation instead of relying solely on the first costs.

There are two main approaches to dealing with uncertainty in terms of investment decisions (Kneifel and Webb, 2022). One is the deterministic approach, which measures the impact of investment outcomes by changing one uncertain key input variable or a combination of variables at a time. The result reflects upon how the changes in the input variable change the outcome while all other things remain constant. In contrast, the probabilistic approach assumes that no single input variable can sufficiently express the full range of possible outcomes of a risky investment. Instead, many alternative outcomes must be taken into consideration, and each outcome must be associated with a probability. If the outcome is represented by a probability distribution, statistical analysis can be carried out to measure the degree of risk. With regard to the deterministic approach, the degree of risk is obtained on a subjective basis.

Scenario sensitivity analysis, which falls under the deterministic approach, will be used in this study. In this technique, for input variables with varying degrees of uncertainty, a set of more pessimistic or optimistic variables than the expected ones can be simultaneously tested in various scenarios. In this respect, the NPC is recalculated for testing its sensitivity with regard to the changes in input variables. Regarding the probabilistic approach, a Monte Carlo simulation will be performed in this study. In this regard, a range of values called a probability distribution is assigned for any input variable that has inherent uncertainty. By using something called "random sampling", the simulation is run repeatedly, generating random values from the variable probability distributions. As a result, a cost range of possible NPC outcomes can be achieved, expressed by a probability distribution. The advantage of performing the Monte Carlo simulation is that the entire cost range of the NPC can be sampled accurately and the effects of simultaneous changes in uncertain variables can be assessed (Emblemsvåg, 2022).

3.7. Reporting

The LCCA conducted in this study is from the ship-owner perspective who is striving to comply with emission control regulations by considering retrofitting investment decisions on the dual-fuel engine. At the same time, they are also aware of the life cycle cost performance of such an engine. Therefore, ship-owners are the main target group. Apart from ship-owners, the findings reported in this study can be used as a reference for investors with regard to investment appraisal of the dual-fuel engine. In addition, the findings gained from this study would be beneficial to other target groups such as policy-makers, ship builders, academia and the public.

4. Case study

This section presents a case study of utilizing the proposed framework to compare the total life cycle cost performance of the dual-fuel engine against that of a conventional diesel engine. The selected case ship is a bulk carrier with the deadweight of 7600 [t], and the Length-Over-All (LOA) of 112 [m]. The specifications of these engines are demonstrated in Table 5.

Based on the domain knowledge from experts and the availability of data, the following assumptions have been made in this study without having significant effects on the final results.

- The common lifespan of ships and their associated systems is 20+. However, the period of analysis chosen in this study is 20 years, which matches those observed in previous studies (Wang et al., 2019).

Table 5
Specifications of two engines.

Specification	Diesel engine	Dual-fuel engine
Cylinder configuration	8L32	8V31DF
No of cylinder	8	8
Cylinder bore [mm]	320	310
Power per cylinder [kW]	580	600
Power [kW]	4640	4800
RPM	750	750
Fuel type	MGO	ULSD (in diesel mode) LNG (in gas mode)

MGO: Marine Gas Oil; ULSD: Ultra Low Sulphur Diesel.

- For being consistent throughout this study, the currency used is Euro (€) with the exchange rate as follows. 1 US dollar (USD) equals to €1.132.
- In the construction phase, the costs of engine delivery are omitted. This is due to the fact that these costs can be the same for these engines. In addition, the installation costs of the MGO tank system for the diesel engine and the LNG tank system for the dual-fuel engine are not considered.
- In the maintenance phase, the costs of handling LNG storage facilities are not included.
- The external costs from the construction phase are omitted. This may be explained as follows. One of the main sources of CO_2 emissions from this phase is the iron and steel-making processes. However, the CO_2 emissions from such processes are significantly less, compared to the CO2 emissions from the operation phase.
- The external costs due to air pollution from disposal or recycling process at the end of lives of the engines are not included.

This section is organized in the following way: the first part presents a base case where the carbon emission costs do not come under the umbrella of the operation costs, the second part deals with the presence of the carbon emission costs when taking into account several carbon pricing scenarios.

4.1. The base case

4.1.1. Construction costs

The construction costs for the diesel engine and the dual-fuel engine were determined after a discussion with the engine manufacturer, as given in Table 2.

4.1.2. Operation costs

Table 6 presents an operational profile of the case ship operating the diesel engine. The engine load, as a percentage of the maximum continuous rating (MCR) of the engine, varies under different engine modes. The SFOC is expressed as a function of the engine load. For these reasons, the SFOC needs to be adjusted in connection with the changes of the engine load. The SFOC adjustment of the engine was determined by interpolation/extrapolation with reference to the values given in Table 7 (Wärtsilä, 0000). Fig. 2 indicates graphically the relation curve between the engine load and the relative SFOC. For a diesel medium-sized four-stroke engine, it is desirable to maintain the engine load at around 80% for optimal fuel consumption and engine performance (Jalkanen et al., 2012). The total annual FOC and LOC of the diesel engine can be obtained with the help of Eqs. (1) and (2) respectively, as shown in Table 6.

In terms of the case ship operating the dual-fuel engine, the same operational profile was used with the following assumptions:

- The dual-fuel engine is running on Ultra Low Sulphur Diesel (ULSD) in the diesel mode, i.e. in "Manoeuvring".
- The dual-fuel engine is running on LNG in the gas mode, i.e., in "Engine Mode 1" and "Engine Mode 2".

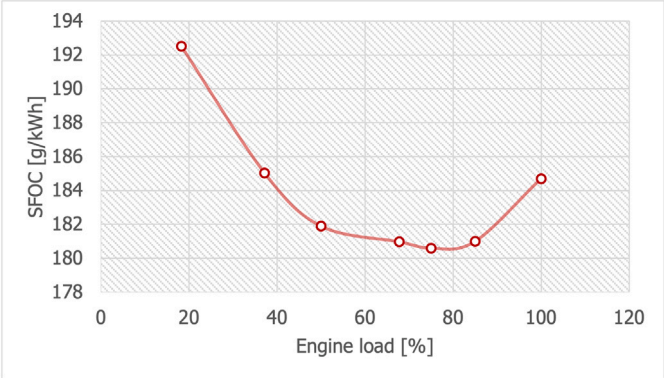

Fig. 2. SFOC-engine load relation curve of the diesel engine.

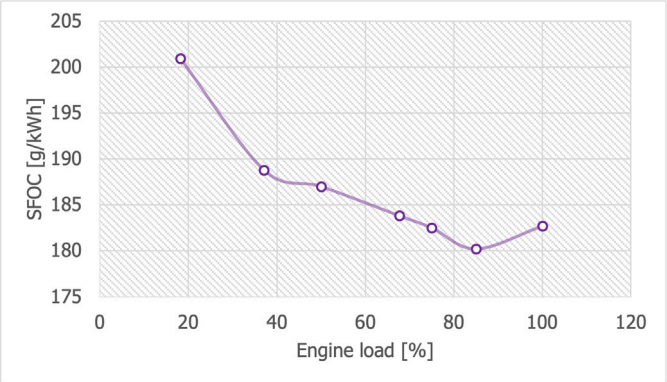

Fig. 3. SFOC-engine load relation curve of the dual-fuel engine in the diesel mode.

As mentioned before, in the diesel mode, the dual-fuel engine operates as a normal diesel engine. Therefore, the total annual FOC and LOC can be achieved in a similar way to what has been done for the diesel engine. Fig. 3 depicts the relation curve between the engine load and the relative SFOC in the diesel mode. The interpretation of this figure is similar to Fig. 2. The engine load should be with the lowest SFOC in order to reduce fuel consumption and enhance engine performance.

In the gas mode, it is essential to find the total annual PFC and the total annual FGC. The PFC can be calculated by adopting Eq. (1). The FGC can be calculated with the help of Eq. (3). Table 9 provides the reference values for the SFOC, SLOC, the specific pilot fuel consumption (SPFC) and the specific fuel gas consumption (SFGC) (Wärtsilä, 0000). Fig. 4 displays the relation curves between the engine load and the relative SFGC, SPFC in the gas mode. The differences between the SFGC in different engine loads are marginal. Taken together, Table 8 demonstrates the operational profile and the total annual FOC, LOC, FGC, and PFC of the dual-fuel engine.

There is a rather significant outcome when comparing the annual fuel consumption (by mass) of these two engines. Due to having a higher low heating value (i.e. net calorific value), the dual-fuel engine uses less amount of gas than the amount of diesel the diesel engine uses (1767.3 [t] versus 2447.8 [t]). In order to calculate the operation costs of these engines, fuel prices were derived from real public data sources in the Rotterdam region as presented in Table 10.

4.1.3. Maintenance costs

As previously stated, there are two cost categories of the maintenance costs, which are further explained as follows.

Table 6
The case ship's operational profile operating the diesel engine.

Operation mode	Annual hours [h/y]	Speed [Knot]	Percentage [%]	Power [kW]	Engine load [%]	SFOC [g/kWh]	Annual FOC [t/y]	SLOC [g/kWh]	Annual LOC [t/y]
Port	1200	0	14%	0	0	0	0	0	0
Manoeuvring	100	0	1%	846.7	18.2%	192.5	16.3	0.06	0.01
Engine Mode 1	300	18.1	3%	3139.6	67.7%	181.0	170.5	0.24	0.22
Engine Mode 2	7100	15.3	82%	1720.9	37.1%	185.0	2261.1	0.13	1.59
Total	8700						2447.8		1.81

Table 7
Reference values for the SFOC & SLOC of the diesel engine.

Engine load [%]	SFOC [g/kWh]	SLOC [g/kWh]
100	184.7	0.35
85	181	
75	180.6	
50	181.9	

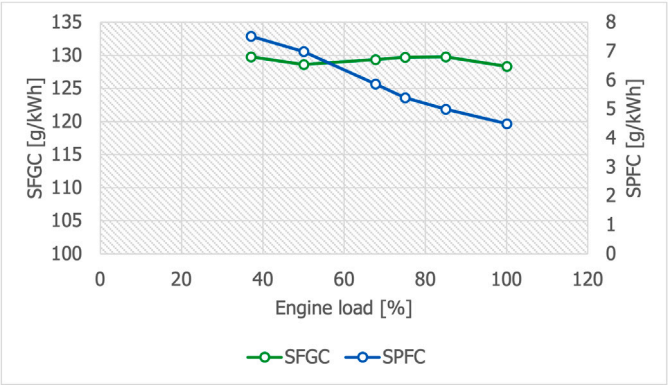

Fig. 4. SFGC/SPFC-engine load relation curves of the dual-fuel engine in the gas mode.

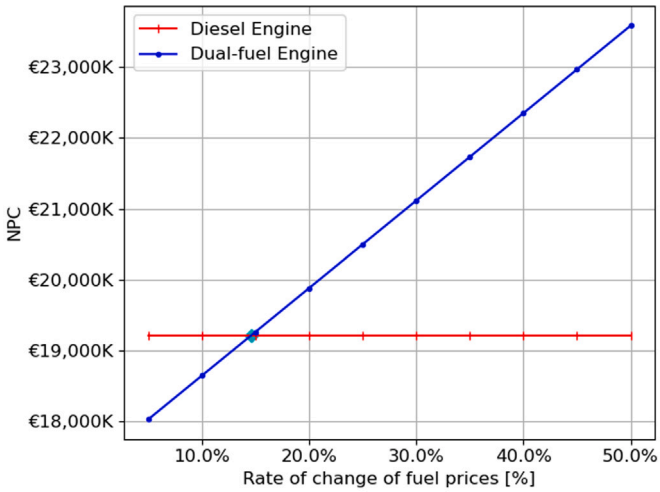

Fig. 5. Rising LNG price and steady MGO price scenarios.

- The labor costs for doing the maintenance tasks for the engines' components. These costs are driven by the engines' annual operating hours, the period of analysis, the recommended maintenance intervals, the number of components, the hourly wages, and the maintenance hour consumption. It should be borne in mind that the actual operation conditions, the quality of the fuel used, the fuel type, and the annual operating hours have a significant impact on the recommended maintenance intervals. The hourly wages selected in this case study are 30 [€/h] (Eurostat, 2022). Domain knowledge is required to obtain the maintenance hour consumption. In this regard, in-depth interviews were carried out with crew members from various shipping companies. They are Chief Engineers and Engine Officers who have at least 5 years of seafaring experience. They were asked to provide information about the amount of time they spent doing the maintenance tasks for every engine component.
- The part replacement costs (i.e. spare costs) of the engines' components according to the O&MMs. These costs were obtained by using an analogous model and conducting thorough interviews with a Technical Manager and Chief Engineers from several shipping companies. Based on their domain knowledge and available historical data of similar engines, the part replacement costs were estimated in a satisfactory way.

4.1.4. End-of-life values

The engines reach the recycling yard for demolition at the end of their lives. Therefore, the materials of the engines and their associated components will be recycled. Table 11 lists the most important structural materials of the engines. The benefits of recycling such materials are presented in the same table. The weights of the engines are provided in Table 12. Such information is contributing to the calculation of the end-of-life values of the engines.

4.1.5. LCC appraisal

Table 13 provides an overview of the cash flow for the LCC appraisal, consisting of the above-mentioned costs accumulated over the period of 20 years. It needs to be said that the maintenance costs, including the labor costs and the part replacement costs are inflated values where they are exposed to the effects of the inflation rate of 3.1%. Furthermore, all future costs are discounted back to their present values by using a nominated discounted rate. The selection of an appropriate discounted rate is dependent on the type of cost. For internal costs, it is associated with the cost of borrowing. In the private sector, a discount rate might fall into the range of 5%–15%, depending on the required return on investment (Hunkeler et al., 2008). A lower discount rate can be chosen following the financial crisis in 2008 (Rödger et al., 2018). For the public sector, the discount rate is generally specified between 3% and 5% for the economic analysis of publicly funded projects (Langdon, 2007). Under the scope of the private sector, the chosen nominated discounted rate in this study is 5%.

It is apparent from the Table 13 that the operation costs have the biggest impact on the life-cycle cost performances of these engines. Albeit having higher construction costs and maintenance costs, the dual-fuel engine has a better performance with regard to the operation costs. The life-cycle cost performances of these engines can be compared by evaluating the measures of economic performance (i.e. economic KPIs), as shown in Table 14. These measures reveal that the dual-fuel engine is clearly cost-effective with the lowest NPC and the NS greater than 0. Furthermore, the SIR of 4.95 means that the dual-fuel engine will generate an average return of €4.95 for every €1 invested.

Table 8
The case ship's operational profile operating the dual-fuel engine.

Operation mode	Annual hours [h/y]	Speed [Knot]	Percentage [%]	Power [kW]	Engine load [%]	SFOC [g/kWh]	Annual FOC [t/y]	SLOC [g/kWh]	Annual LOC [t/y]	SFGC [g/kWh]	Annual FGC [t/y]	SPFC [g/kWh]	Annual PFC [t/y]
Port	1200	0	14%	0	0	0	0	0	0	0	0	0	0
Manoeuvring	100	0	1%	873.6	18.2%	200.9	17.6	0.08	0.01	131.1	N/A	N/A	N/A
Engine Mode 1	300	18.8	3%	3249.6	67.7%	183.8	N/A	0.30	0.30	129.4	126.2	5.9	5.7
Engine Mode 2	7100	15.9	82%	1780.8	37.1%	188.8	N/A	0.17	2.11	129.8	1641.1	7.5	95.1
Total	8700						17.6		2.42		1767.3		100.9

Table 9
Reference values for the SFOC, SLOC, SPFC & SFGC of the dual-fuel engine.

Engine load [%]	SFOC [g/kWh]	SLOC [g/kWh]	SPFC [g/kWh]	Heat rate [kJ/kWh]	SFGC [g/kWh]
100	182.7	0.45	4.5	7058	128.3
85	180.2		5.0	7138	129.8
75	182.5		5.4	7134	129.7
50	187.0		7.0	7076	128.7

The calorific value for LNG: 55000 [kJ/kg] is used to convert the heat rate into the SFGC.

Table 10
Fuel information.

Type of fuel	Price [€/t]	CF [t-CO2/t-Fuel]	Calorific value [kJ/kg]
MGO	508.1[a]	3.20600[c]	–
ULSD	576.8[b]	3.15104[c]	–
LNG	561.1[a]	2.75000[c]	55,000
Lubricating oil	2300[b]	–	–

[a]Source: Global Maritime Hub (2021).
[b]Source: Ship & Bunker (2021).
[c]Source: IMO (2020).

Table 11
Metal material content of engines.
Source: Wärtsilä, Greengate Metals (0000).

Material	Weight ratio [%]	Benefits of recycling [€/kg]
Steel	16	0.25
Cast iron	80	0.25
Aluminum	2	0.7
Cooper	2	6.35

Table 12
Engine weights.
Source: Wärtsilä (2020, 2021b).

Criteria	Diesel engine	Dual-fuel engine
Weight [t]	43.6	58.9

4.1.6. Scenario sensitivity analysis

In the section that follows, an investigation on the sensitivity of the NPCs of these engines with regard to the changes of uncertain variables is demonstrated. The uncertain variables considered are fuel prices and discount rate.

(a) Scenario sensitivity analysis on fuel prices: In order to investigate at which fuel price will the decision favor one engine over another, various price scenarios with respect to MGO and LNG were simulated. These price scenarios were treated under two aspects: the LNG price increases while the MGO price remains stable; the LNG price is kept steady while the MGO price decreases.

(i) Scenarios under the rise of LNG price: Fig. 5 depicts several scenarios where the LNG price increases while the MGO price remains constant. As marked in this figure, the break-even point, i.e. the intersection of the NPC lines, can be identified at the point when the LNG price increases by 14.6%, precisely. This is the point where the corresponding price for LNG is 643 [€/t], which is equal to 1.3 the MGO price. Therefore, when the LNG price is comparatively higher, the economic viability of the dual-fuel engine can be downgraded.

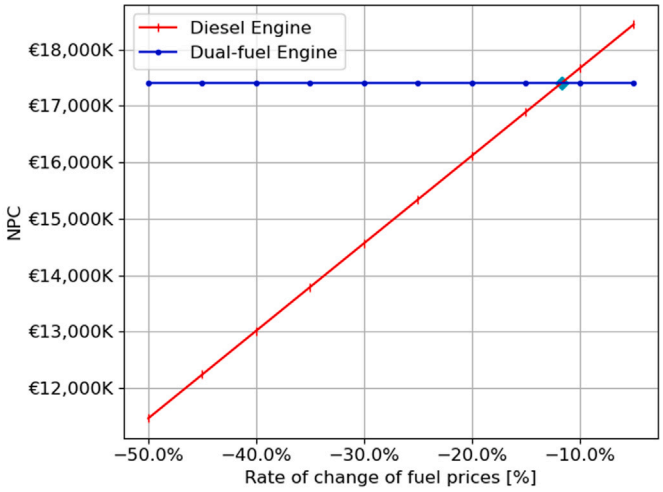

Fig. 6. Steady LNG price and decreasing MGO price scenarios.

(ii) Scenarios under the slump of MGO price: Scenarios where the MGO price decreases while the LNG price is constant were also tested. As marked in Fig. 6, the break-even point is the point when the MGO price decreases by 11.6%, precisely. This is corresponding to the price of MGO of 449 [€/t], which is equal to 0.8 the LNG price. In this respect, the dual-fuel engine becomes the cost-effective option compared to the diesel engine.

Table 13
Summary of the LCC appraisal in the base case.

Cost category	20 year cash flow: Diesel engine		20 year cash flow: Dual-fuel engine	
	Non-discounted costs	Discounted costs	Non-discounted costs	Discounted costs
Construction costs	989K	989K	1,200K	1,200K
Operation costs	24,960K	15,553K	21,308K	13,277K
Maintenance costs	4,614K[a]	2,678K	5,050K[a]	2,940K
Labor costs	697K[a]	411K	720K[a]	425K
Part replacement costs	3,917K[a]	2,267K	4,330K[a]	2,515K
End-of-life value	17K	6K	22K	8K

[a]Inflated values with the inflation rate of 3.1%.
Unit K = 1000€, Discount rate $r = 5\%$.

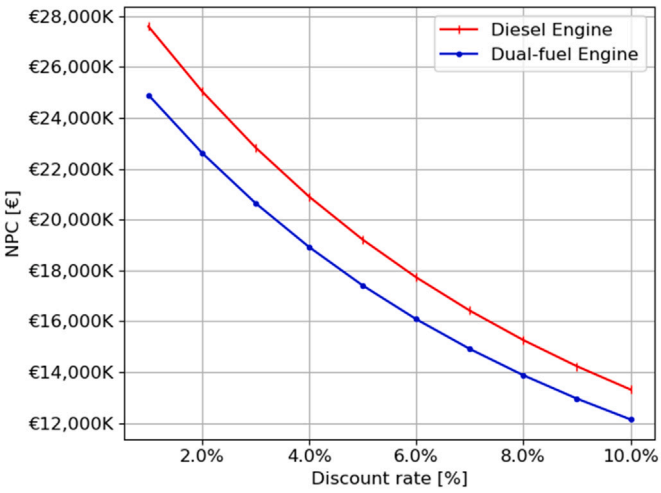

Fig. 7. Scenarios of discount rate fluctuations.

Table 14
Measures of economic performance in the base case.

Measure of economic performance	20 year economic calculations (discounted costs)	
	Diesel engine	Dual-fuel engine
Net Present Cost (NPC)	19,213K	17,409K
Net Saving (NS)	–	1,804K
Saving-to-ratio (SIR)	–	4.95

Unit K = 1000€.
Discount rate $r = 5\%$.

Table 15
Triangular distributions of variables.

Variable	(Min, Most Likely, Max)
MGO price [€/t]	(383.2, 469.4, 541.9)
LNG price [€/t]	(360.2, 482.2, 687.8)
Discount rate [%]	(1, 5, 10)
Inflation rate [%]	(1, 3.1, 5)
Annual operating hours [h/y]	(5500, 7500, 8760)
Hourly wages [€/h]	(20, 30, 46.9)

(b) Scenario sensitivity analysis on the discount rate: This was performed by varying the discount rate from 1 to 10%, as shown in Fig. 7. This figure is quite revealing in several ways. First, when the discount rate increases, there is a clear trend of decreasing the NPCs as well as the cost gap between the dual-fuel engine and the diesel engine. Second, it is more advantageous to opt for the dual-fuel engine regardless of the changes in the discount rate.

(c) Scenario sensitivity analysis on fuel prices and the discount rate: Fig. 8 provides an overall interconnected sensitivity of fuel prices and the discount rate on the NPCs of these engines. This underlines the effects of fuel prices and the discount rate on the NPCs of these engines.

4.1.7. Uncertainty analysis

What follows is an account of uncertainty analysis running the Monte Carlo simulation in which the uncertainty is introduced in the model. In this regard, it is important to model the uncertainty (i.e. variables such as fuel prices, the discount rate) as either uncertainty distributions or fuzzy numbers and intervals (Emblemsvåg, 2003). Apart from fuel prices and the discount rates, the inflation rate, the annual operating hours, and the hourly wages were identified as uncertain variables. To model these variables, triangular distributions were chosen for several reasons. First, these variables are believed to be normally distributed but the uncertainty is quite large. When the uncertainty is quite large, a normal distribution appears to express too little on the ends of the distribution, and this is undesirable. Second, triangular distributions deal with asymmetry better than the normal ones. The triangular distributions of these variables are shown in Table 15. It needs to be mentioned that the min, most likely and max values of the variable distributions with regard to fuel prices were derived from a real public data source (Ship & Bunker, 2021).

The Monte Carlo simulation was run using the @RISK software. The number of iterations was set at 10,000. Fig. 9 depicts the results of the Monte Carlo simulation, demonstrating a distribution overlay of the NPCs of the respective engines. Given 10,000 iterations that were randomly generated, the NPC range of the diesel engine can be found from €26.7 million to €29.8 million with the probability of 62%. The probability of the NPC of the dual-fuel engine falling under this range is 68.6%. Therefore, it can be concluded that the dual-fuel engine is adequately superior to the diesel engine.

Apart from handling the uncertainty in the model, the @RISK software is capable of tracing the critical cost drivers. It can be seen from Fig. 10 that fuel prices are the dominant cost driver, influencing the NPC results the most.

4.2. The case of carbon pricing

Although MBMs (e.g., the IMO MBMs and EU ETS) have not yet been enforced, their relevance for the shipping industry is envisaged to grow in the near future. For this reason, carbon pricing will have an impact on the investment appraisal of emissions reduction technologies (Metzger, 2022). Therefore, it is worth considering them as external costs in the LCCA conducted in this study. Trivyza et al. (2019) and Perčić et al. (2020) examined the impacts of carbon pricing/carbon allowance on the life-cycle costs of the studied subjects in several scenarios based on the data obtained from World Energy Outlook 2019 and 2020 respectively. Recent years have witnessed an increasing trend in carbon prices. In this study, several carbon pricing scenarios corresponding to the latest data obtained from World Energy Outlook 2021 (WEO2021) were considered. It is noted that carbon prices in the WEO2021 were applied to other non-CO_2 emissions, such

NPC of the Diesel Engine [€]		Discount rate [%]									
		1%	2%	3%	4%	5%	6%	7%	8%	9%	10%
MGO price [€/t]	-50.0%	16,378K	14,883K	13,584K	12,453K	11,463K	10,595K	9,829K	9,153K	8,553K	8,020K
	-45.0%	17,501K	15,900K	14,509K	13,298K	12,238K	11,308K	10,488K	9,764K	9,121K	8,549K
	-40.0%	18,623K	16,917K	15,435K	14,143K	13,013K	12,021K	11,147K	10,374K	9,689K	9,079K
	-35.0%	19,745K	17,933K	16,360K	14,988K	13,788K	12,734K	11,806K	10,985K	10,257K	9,608K
	-30.0%	20,868K	18,950K	17,285K	15,833K	14,563K	13,448K	12,465K	11,596K	10,824K	10,138K
	-25.0%	21,990K	19,967K	18,210K	16,679K	15,338K	14,161K	13,124K	12,206K	11,392K	10,667K
	-20.0%	23,112K	20,984K	19,136K	17,524K	16,113K	14,874K	13,783K	12,817K	11,960K	11,197K
	-15.0%	24,234K	22,001K	20,061K	18,369K	16,888K	15,588K	14,441K	13,427K	12,527K	11,726K
	-10.0%	25,357K	23,018K	20,986K	19,214K	17,663K	16,301K	15,100K	14,038K	13,095K	12,255K
	-5.0%	26,479K	24,035K	21,911K	20,059K	18,438K	17,014K	15,759K	14,649K	13,663K	12,785K
	508.1	27,601K	25,052K	22,837K	20,905K	19,213K	17,728K	16,418K	15,259K	14,231K	13,314K
	5.0%	28,723K	26,069K	23,762K	21,750K	19,988K	18,441K	17,077K	15,870K	14,798K	13,844K
	10.0%	29,846K	27,086K	24,687K	22,595K	20,763K	19,154K	17,736K	16,480K	15,366K	14,373K
	15.0%	30,968K	28,103K	25,612K	23,440K	21,538K	19,868K	18,394K	17,091K	15,934K	14,903K
	20.0%	32,090K	29,119K	26,538K	24,285K	22,314K	20,581K	19,053K	17,702K	16,501K	15,432K
	25.0%	33,212K	30,136K	27,463K	25,131K	23,089K	21,294K	19,712K	18,312K	17,069K	15,962K
	30.0%	34,335K	31,153K	28,388K	25,976K	23,864K	22,008K	20,371K	18,923K	17,637K	16,491K
	35.0%	35,457K	32,170K	29,313K	26,821K	24,639K	22,721K	21,030K	19,533K	18,204K	17,021K
	40.0%	36,579K	33,187K	30,238K	27,666K	25,414K	23,434K	21,689K	20,144K	18,772K	17,550K
	45.0%	37,701K	34,204K	31,164K	28,511K	26,189K	24,148K	22,348K	20,755K	19,340K	18,080K
	50.0%	38,824K	35,221K	32,089K	29,356K	26,964K	24,861K	23,006K	21,365K	19,908K	18,609K

NPC of the Dual-fuel Engine [€]		Discount rate [%]									
		1%	2%	3%	4%	5%	6%	7%	8%	9%	10%
LNG price [€/t]	-50.00%	15,958K	14,520K	13,271K	12,183K	11,231K	10,395K	9,659K	9,008K	8,431K	7,917K
	-45.00%	16,853K	15,331K	14,009K	12,857K	11,849K	10,964K	10,184K	9,495K	8,884K	8,339K
	-40.00%	17,748K	16,141K	14,746K	13,530K	12,466K	11,532K	10,709K	9,982K	9,336K	8,762K
	-35.00%	18,642K	16,952K	15,484K	14,204K	13,084K	12,101K	11,235K	10,468K	9,789K	9,184K
	-30.00%	19,537K	17,763K	16,222K	14,878K	13,702K	12,670K	11,760K	10,955K	10,241K	9,606K
	-25.00%	20,432K	18,573K	16,959K	15,552K	14,320K	13,238K	12,285K	11,442K	10,694K	10,028K
	-20.00%	21,326K	19,384K	17,697K	16,225K	14,938K	13,807K	12,810K	11,929K	11,146K	10,450K
	-15.00%	22,221K	20,195K	18,434K	16,899K	15,556K	14,376K	13,335K	12,415K	11,599K	10,872K
	-10.00%	23,115K	21,005K	19,172K	17,573K	16,174K	14,944K	13,861K	12,902K	12,052K	11,294K
	-5.00%	24,010K	21,816K	19,910K	18,247K	16,791K	15,513K	14,386K	13,389K	12,504K	11,716K
	561.1	24,905K	22,627K	20,647K	18,921K	17,409K	16,082K	14,911K	13,876K	12,957K	12,138K
	5.00%	25,799K	23,437K	21,385K	19,594K	18,027K	16,650K	15,436K	14,362K	13,409K	12,560K
	10.00%	26,694K	24,248K	22,122K	20,268K	18,645K	17,219K	15,962K	14,849K	13,862K	12,982K
	15.00%	27,589K	25,059K	22,860K	20,942K	19,263K	17,788K	16,487K	15,336K	14,314K	13,404K
	20.00%	28,483K	25,869K	23,597K	21,616K	19,881K	18,356K	17,012K	15,823K	14,767K	13,826K
	25.00%	29,378K	26,680K	24,335K	22,289K	20,498K	18,925K	17,537K	16,310K	15,220K	14,249K
	30.00%	30,273K	27,491K	25,073K	22,963K	21,116K	19,493K	18,062K	16,796K	15,672K	14,671K
	35.00%	31,167K	28,301K	25,810K	23,637K	21,734K	20,062K	18,588K	17,283K	16,125K	15,093K
	40.00%	32,062K	29,112K	26,548K	24,311K	22,352K	20,631K	19,113K	17,770K	16,577K	15,515K
	45.00%	32,957K	29,923K	27,285K	24,985K	22,970K	21,199K	19,638K	18,257K	17,030K	15,937K
	50.00%	33,851K	30,733K	28,023K	25,658K	23,588K	21,768K	20,163K	18,743K	17,482K	16,359K

Fig. 8. Fuel prices and the discount rate sensitivity.

Table 16
CO_2 price scenarios.
Source: OECD (2021).

Scenario	Price (€/t-CO_2)		
	2030	2040	2050
Stated Policies Scenario (STEPS)	57.46	66.3	79.56
Sustainable Development Scenario (SDS)	106.08	150.28	176.8
Net Zero Emissions by 2050 (NZE)	114.92	181.22	221

as methane (OECD, 2021). Table 16 provides information regarding the carbon pricing forecast for these scenarios in the EU region in 2030, 2040 and 2050 respectively. These values were used as reference values for interpolation of the annual carbon prices. Assuming 2022 is the base date for this study, the carbon price for 2022 is zero since neither MBMs (e.g., the IMO MBMs and EU ETS) is implemented in the shipping industry. Fig. 11 displays the results of the annual carbon prices. The considered carbon pricing scenarios are summarized as follows.

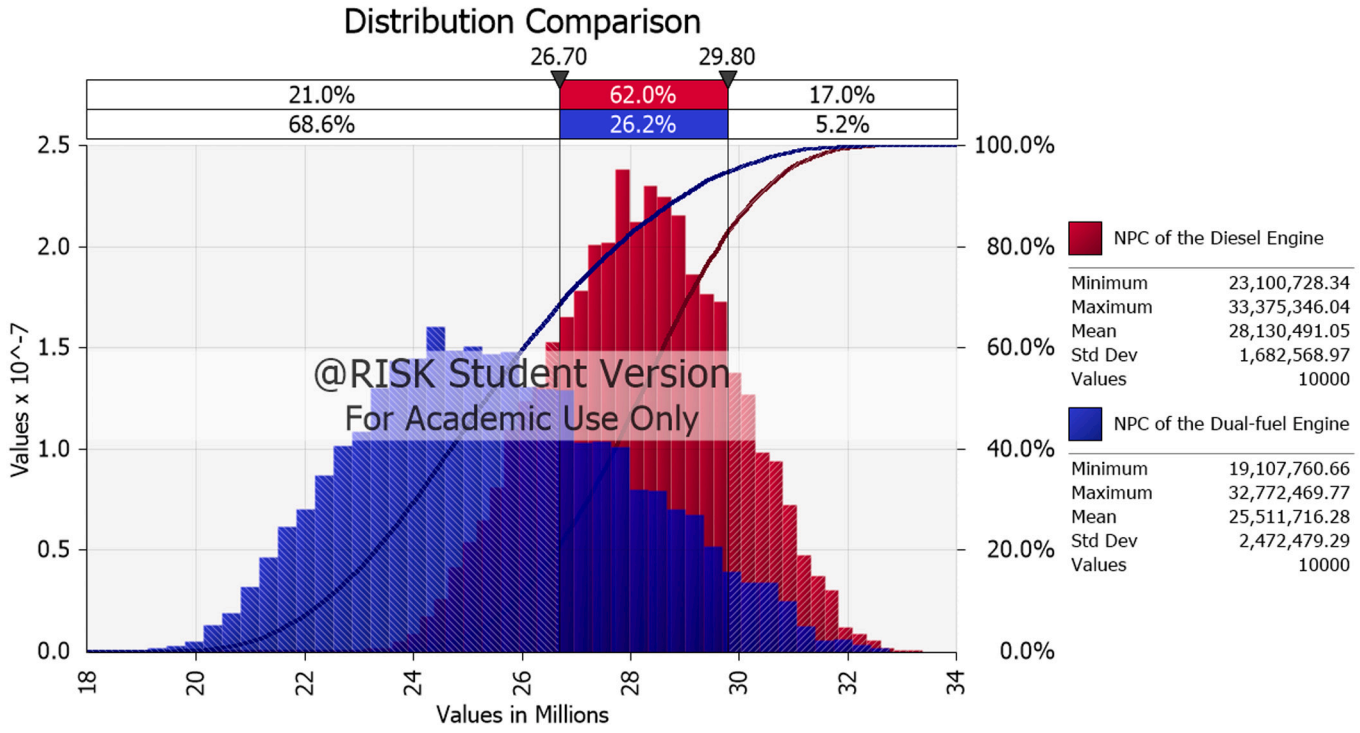

Fig. 9. Overlay graph of the NPC of the diesel engine and the NPC of the dual-fuel engine.

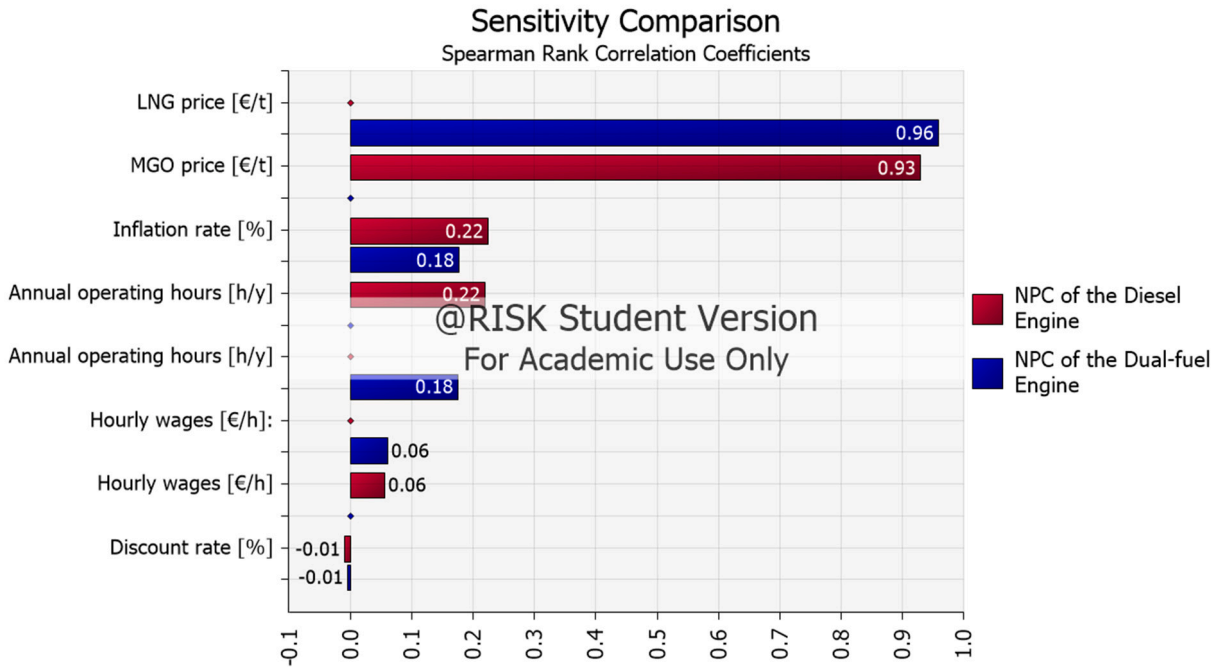

Fig. 10. Sensitivity chart.

(i) Stated Policies Scenario (STEPS) includes not just existing policies and measures but also those that are under development. An example of a measure that is under development is the EU's Fit for 55 package.

(ii) Sustainable Development Scenario (SDS) is the so-called "well below 2°" pathway to meet the Paris Agreement targets. It is noted here that the WEO21 also included the Announced Pledges Scenario (APS) which entails all of the climate commitments made by governments all over the world. However, the carbon prices for the SDS and the APS in the EU region were set the same. For this reason, only the SDS was considered in this study.

(iii) Net Zero Emissions by 2050 Scenario (NZE) is a narrow but achievable pathway for the global energy sector to reach net

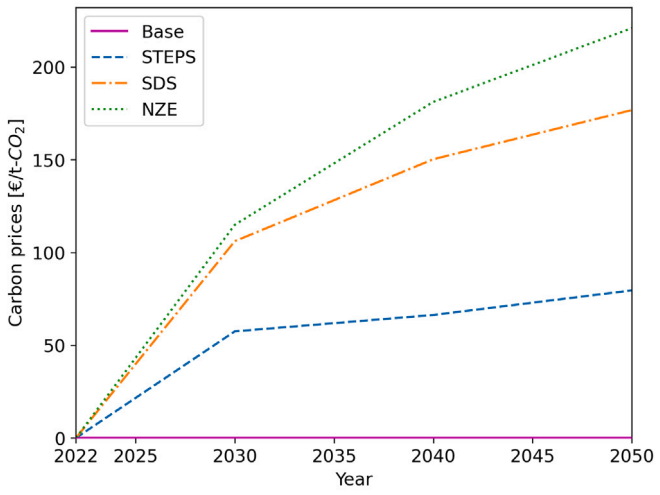

Fig. 11. Carbon pricing scenarios.

zero CO_2 emissions by 2050. Advanced economies are expected to achieve this target ahead of others.

Table 17 compares the NPC and NS results derived from the carbon pricing scenario analysis of the diesel engine and the dual-fuel engine. Fig. 12 depicts the cost category results (i.e. 20 year discounted costs). As stated earlier, the operation costs in the base case only consider the fuel costs while the operation costs in the three carbon pricing scenarios take into account the carbon emission costs. These costs were derived from the annual CO_2 emissions (Eq. (4)) and the annual carbon prices (Table 16). Since emitting CO_2 to the atmosphere has a detrimental effect on society, a lower discount rate should be chosen for long time periods. For this reason, calculations for the carbon emission costs were done by accounting for the discount rate of 3.5% (Smith, 2021). The effects of carbon pricing on the cost performances of these engines in the respective scenarios can be seen in Fig. 12. If either the IMO MBMs or EU ETS is implemented, it would lead to substantially higher carbon emission costs, thereby increasing the NPCs of these engines considerably in the higher carbon price scenarios (i.e., SDS and NZE). However, the dual-fuel engine is more cost-effective than the diesel engine because it yields lower NPCs in all carbon pricing scenarios. The carbon prices above 100 [€/t-CO_2] in the SD and NZE scenarios lends support to previous findings in the literature where Metzger (2022) argued that carbon prices of 100 [USD/t-CO_2] might increase substantially the Net Present Value (NPV) of a technology investment. The impacts driven by the carbon prices might be even higher as mentioned by ben Brahim et al. (2019). The proposal of the carbon levy of 100 [USD/t-CO_2] (i.e equivalent emissions) was submitted by the Marshall Islands and the Solomon Islands in the IMO's Marine Environment Protection Committee (MEPC76) meeting (Lagouvardou et al., 2022). The results are suggestive of a correlation between the cost effectiveness of emissions reduction technologies (e.g. the dual-fuel engine) and the potential introduction of MBMs. This indicates that MBMs are required to promote the adoption of future energy technologies.

It is also worth noting that the dual-fuel engine can offer an environmental benefit irrespective of fuel prices or carbon pricing scenarios. The environmental benefit of switching over to the dual-fuel engine can be quantified by using Eqn. (4) and the carbon emission conversion factor C_F given in Table 10. Given 20 years of operation, Table 18 details a considerable reduction in CO_2 emissions when opting for the dual-fuel engine. To be specific, a reduction in CO_2 emissions of 33% can be achieved, or 52,291 [t] of CO_2 would be eliminated.

Table 17
Measures of economic performance in carbon pricing scenarios.

Scenario	NPC		NS
	Diesel engine	Dual-fuel engine	
STEPS	30,487K	24,927K	5,560K
SDS	42,585K	32,994K	9,591K
NZE	46,261K	35,446K	10,815K

Unit K = 1000€.
Discount rate $r = 5\%$, inflation rate $I = 5\%$.
Discount rate for calculating the carbon emission costs $r' = 3.5\%$.

Table 18
20-year CO_2 emissions in operation.

Criteria	Diesel engine	Dual-fuel engine
Total CO_2 emissions [t]	156,954	104,663
Amount saving [t]		52,291
Percentage reduction [%]		33%

5. Conclusion

This study has proposed a LCC framework for evaluating the life-cycle cost performance of an innovative marine dual-fuel engine considering uncertainties involved over its lifetime. There are several important areas where this study makes noteworthy contributions to the current literature. First, it proposes a methodological framework for LCCA integrating the ISO 15686-5 standard and a detailed engineering build-up approach. Second, the uncertainties are extensively treated by the scenario sensitivity analyses and the Monte Carlo Simulation, filling the gap in the existing literature. Third, the insights gained from this study may be of assistance to decision makers (i.e., ship-owners and investors) as regards retrofitting decision-making. Fourth, it has an important policy implication for developing MBMs to promote the adoption of future emissions reduction technologies.

The proposed framework includes the development of a life-cycle cost model for the engine's life phases (i.e., construction, operation, maintenance and end-of-life) taking into account cases with and without carbon pricing (i.e. the base case). Furthermore, the KPIs pertinent to the measures of economic performance (i.e. the NPC, NS and SIR) have been offered to compare the potential benefits of adopting the dual-fuel engine against a conventional diesel engine. The main findings of this study are summarized as follows:

- The most dominant phase in the life cycles of the studied engines is the operation phase (i.e. the one with the highest cost).
- In the base case, the dual-fuel engine appears to be more cost-effective than the diesel engine since it has lower NPC (€17,409K versus €19,213K), the NS (€1,804K) greater than zero and the SIR (4.95) greater than 1.0.
- The uncertainty analysis using scenario sensitivity analyses uncovers that fuel prices are highly influential in affecting changes in the NPCs of these engines. Specifically, the cost effectiveness of the dual-fuel engine is sensitive to the high gas scenarios.
- The uncertainty analysis using the Monte Carlo simulation provides an adequate degree of confidence when opting for the dual-fuel engine. Furthermore, fuel prices are found to be the dominant cost driver.
- In the case of carbon pricing, the carbon prices result in significantly higher NPCs of these engines in the high carbon price scenarios. Nevertheless, the dual-fuel engine is still more cost-attractive than the diesel engine.
- Regardless of fuel prices and carbon pricing scenarios, a 33% reduction in CO_2 emissions can be achieved by opting for the dual-fuel engine.

It is critical to note that the fuel prices considered in this paper were derived from the current high price situation in the market in

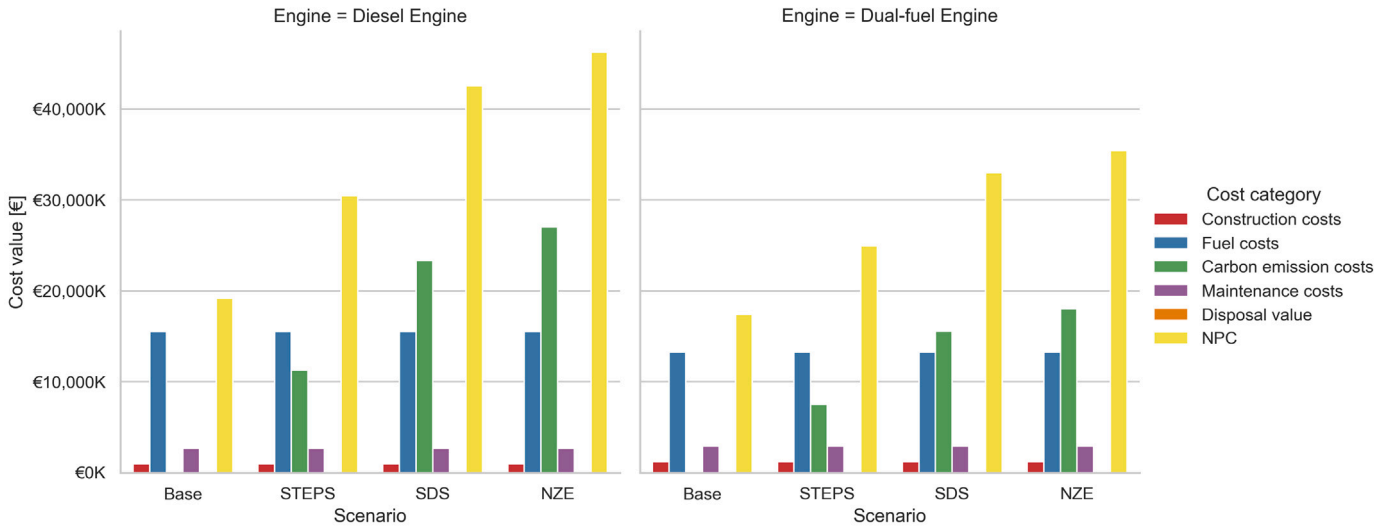

Fig. 12. Results of 20 year discounted costs under carbon pricing scenarios.

which the LNG price is higher than the MGO price. Looking into the past, this is unusual and regarded as temporary since the LNG price is expected to decrease in the near future (Ship & Bunker, 2021; The Loadstar, 2021). If the high LNG price persists, the dual-fuel engine is still a promising option since it brings flexibility for ship operators to switch to ULSD or VLSO in the diesel mode. The switch between fuels can be done seamlessly without loss of power or speed. Such fuel flexibility ensures regulatory compliance in Emission Control Areas (ECAs), while providing ship operators with the option of choosing the fuel according to cost and availability. It should also bear in mind that LNG has been well-established around the world with available bunkering infrastructure. Earlier studies have also demonstrated that LNG has been considered reliable today and for near future regulatory compliance (Trivyza et al., 2019; DNV, 2021).

However, the findings in this study are subject to a limitation in terms of lacking the costs of handling LNG tanks in the maintenance phase and the external costs incurred by air pollution from the construction and end-of-life phases. The monetization of the external costs from these phases would provide a complete socio-economic assessment. Additionally, this study is limited by the fact that the installation costs of the fuel tank systems, i.e., MGO for the diesel engine and LNG for the dual-fuel engine were not included. The possibility of having a higher installation cost for the LNG tank system cannot be ruled out. These limitations highlight the difficulty of collecting data on the respective phases. Considerably more work will need to be done when more data and information on these costs are available. LCCA is an intriguing area that could be usefully explored in further research on techno-economic assessment of future energy technologies.

CRediT authorship contribution statement

Khanh Q. Bui: Methodology, Software, Formal analysis, Investigation, Writing – original draft, Visualization. **Lokukaluge P. Perera:** Conceptualization, Writing – review & editing, Supervision. **Jan Emblemsvåg:** Writing – review & editing, Supervision.

Declaration of competing interest

The authors declare that they have no known competing financial interests or personal relationships that could have appeared to influence the work reported in this paper.

Data availability

The authors do not have permission to share data.

Acknowledgements

The project has received funding from the European Union's Horizon 2020 research and innovation program under the grant agreement No 857840. The opinions expressed in this document reflect only the author's view and in no way reflect the European Commission's opinions. The European Commission is not responsible for any use that may be made of the information it contains.

References

Andersson, K., Jeong, B., Jang, H., 2020. Life cycle and cost assessment of a marine scrubber installation. J. Int. Marit. Saf. Environ. Aff. Shipp. 4 (4), 162–176. http://dx.doi.org/10.1080/25725084.2020.1861823.

ben Brahim, T., Wiese, F., Münster, M., 2019. Pathways to climate-neutral shipping: A Danish case study. Energy 188, 116009. http://dx.doi.org/10.1016/j.energy.2019.116009.

Blanco-Davis, E., Zhou, P., 2014. LCA as a tool to aid in the selection of retrofitting alternatives. Ocean Eng. 77, 33–41. http://dx.doi.org/10.1016/j.oceaneng.2013.12.010.

Bouman, E.A., Lindstad, E., Rialland, A.I., Strømman, A.H., 2017. State-of-the-art technologies, measures, and potential for reducing GHG emissions from shipping – A review. Transp. Res. D 52, 408–421. http://dx.doi.org/10.1016/j.trd.2017.03.022.

Bui, K.Q., Ölçer, A.I., Kitada, M., Ballini, F., 2021a. Selecting technological alternatives for regulatory compliance towards emissions reduction from shipping: An integrated fuzzy multi-criteria decision-making approach under vague environment. Proc. Inst. Mech. Eng. M 235 (1), 272–287. http://dx.doi.org/10.1177/1475090220917815.

Bui, K.Q., Perera, L.P., Emblemsvåg, J., 2021b. Development of a life-cycle cost framework for retrofitting marine engines towards emission reduction in shipping. In: 13th IFAC Conference on Control Applications in Marine Systems, Robotics, and Vehicles CAMS 2021, vol. 54. Oldenburg, Germany, pp. 181–187. http://dx.doi.org/10.1016/j.ifacol.2021.10.091.

Bui, K.Q., Perera, L.P., Emblemsvåg, J., Schøyen, H., 2022. Life-cycle cost analysis on a marine engine innovation for retrofit: A comparative study. In: ASME 2022 41st International Conference on Ocean, Offshore and Arctic Engineering. American Society of Mechanical Engineers Digital Collection, Hamburg, Germany.

Bullock, S., Mason, J., Larkin, A., 2022. The urgent case for stronger climate targets for international shipping. Clim. Policy 22 (3), 301–309. http://dx.doi.org/10.1080/14693062.2021.1991876.

Cariou, P., Lindstad, E., Jia, H., 2021. The impact of an EU maritime emissions trading system on oil trades. Transp. Res. D 99, 102992. http://dx.doi.org/10.1016/j.trd.2021.102992.

Carlo, R., Marc, B.J., Fuente, S., Smith, T., Søgaard, K., 2020. Aggregate investment for the decarbonisation of the shipping industry.

Curran, R., Raghunathan, S., Price, M., 2004. Review of aerospace engineering cost modelling: The genetic causal approach. Prog. Aerosp. Sci. 40 (8), 487–534. http://dx.doi.org/10.1016/j.paerosci.2004.10.001.

DNV, 2021. Maritime Forecast to 2050. Technical Report, DNV.

Emblemsvåg, J., 2003. Life-Cycle Costing: Using Activity-Based Costing and Monte Carlo Methods to Manage Future Costs and Risks. Wiley, Hoboken, N.J.

Emblemsvåg, J., 2022. Wind energy is not sustainable when balanced by fossil energy. Applied Energy 305, 117748. http://dx.doi.org/10.1016/j.apenergy.2021.117748.
Emblemsvåg, J., Bras, B., 2012. Activity-Based Cost and Environmental Management: A Different Approach to ISO 14000 Compliance, Softcover reprint of the original first ed. 2001 ed. Springer, Boston, MA.
European Commission (EC), 2021. Proposal for a directive of the European parliament and of the council amending directive 2003/87/EC establishing a system for greenhouse gas emission allowance trading within the union, decision (EU) 2015/1814 concerning the establishment and operation of a market stability reserve for the union greenhouse gas emission trading scheme and regulation (EU) 2015/757.
Eurostat, 2022. Hourly labour costs. https://ec.europa.eu/eurostat/statistics-explained/index.php?title=Hourly_labour_costs.
Favi, C., Campi, F., Germani, M., Manieri, S., 2018. Using design information to create a data framework and tool for life cycle analysis of complex maritime vessels. J. Clean. Prod. 192, 887–905. http://dx.doi.org/10.1016/j.jclepro.2018.04.263.
Global Maritime Hub, 2021. Bunker prices weekly outlook – Week 24. https://globalmaritimehub.com/bunker-prices-weekly-outlook-week-24.html.
Greengate Metals, UK scrap metal prices 2021, Manchester - Greengate metals scrap yard, https://www.greengatemetals.co.uk/scrapmetal/prices.
Gualeni, P., Flore, G., Maggioncalda, M., Marsano, G., 2019. Life cycle performance assessment tool development and application with a focus on maintenance aspects. J. Mar. Sci. Eng. 7 (8), 280. http://dx.doi.org/10.3390/jmse7080280.
Huang, D., Hua, Y., Loughney, S., Blanco-Davis, E., Wang, J., 2021. Lifespan cost analysis of alternatives to global sulphur emission limit with uncertainties. Proc. Inst. Mech. Eng. M 235 (4), 921–930. http://dx.doi.org/10.1177/1475090220983140.
Hueber, C., Horejsi, K., Schledjewski, R., 2016. Review of cost estimation: Methods and models for aerospace composite manufacturing. Adv. Manuf. Polym. Compos. Sci. 2 (1), 1–13. http://dx.doi.org/10.1080/20550340.2016.1154642.
Hunkeler, D., Lichtenvort, K., Rebitzer, G., Ciroth, A., SETAC-Europe (Eds.), 2008. Environmental Life Cycle Costing. SETAC ; CRC Press, Pensacola, Fla.: Boca Raton.
IACCSEA, Marine SCR - A proven and viable technology, https://www.iaccsea.com/faq/marine-scr/.
IMO, 2011. Inclusion of Regulations on Energy Efficiency for Ships in MARPOL Annex VI. Technical Report, International Maritime Organization (IMO), London, UK.
IMO, 2018. Initial IMO Strategy on Reduction of GHG Emissions from Ships. IMO Resolution MEPC.304(72). Technical Report, International Maritime Organization (IMO), London, UK.
IMO, 2020. Fourth IMO GHG Study 2020. Technical Report, International Maritime Organization (IMO), London, UK.
ISO, 2017. ISO 15686-5:2017 Buildings and constructed assets — Service life planning — Part 5: Life-cycle costing.
Jalkanen, J.-P., Johansson, L., Kukkonen, J., Brink, A., Kalli, J., Stipa, T., 2012. Extension of an assessment model of ship traffic exhaust emissions for particulate matter and carbon monoxide. Atmospheric Chemistry and Physics 12 (5), 2641–2659. http://dx.doi.org/10.5194/acp-12-2641-2012.
Jeong, B., Wang, H., Oguz, E., Zhou, P., 2018. An effective framework for life cycle and cost assessment for marine vessels aiming to select optimal propulsion systems. J. Clean. Prod. 187, 111–130. http://dx.doi.org/10.1016/j.jclepro.2018.03.184.
Kneifel, J., Webb, D., 2022. NIST Handbook 135 Life-Cycle Costing Manual for the Federal Energy Management Program.
Lagemann, B., Lindstad, E., Fagerholt, K., Rialland, A., Ove Erikstad, S., 2022. Optimal ship lifetime fuel and power system selection. Transp. Res. D 102, 103145. http://dx.doi.org/10.1016/j.trd.2021.103145.
Lagouvardou, S., Psaraftis, H.N., Zis, T., 2022. Impacts of a bunker levy on decarbonizing shipping: A tanker case study. Transp. Res. D 106, 103257. http://dx.doi.org/10.1016/j.trd.2022.103257.
Langdon, D., 2007. Life Cycle Costing (LCC) as a Contribution to Sustainable Construction: A Common Methodology. Final Report, European Commission, Brussels.
McKenna, S.A., Kurt, R.E., Turan, O., 2012. A methodology for a 'design for ship recycling': International conference on the environmentally friendly ship. In: The Environmentally Friendly Ship. Royal Institution of Naval Architects, London, pp. 37–44.
Metzger, D., 2022. Market-based measures and their impact on green shipping technologies. WMU J. Marit. Aff. 21 (1), 3–23. http://dx.doi.org/10.1007/s13437-021-00258-8.
Mondello, G., Salomone, R., Saija, G., Lanuzza, F., Gulotta, T.M., 2021. Life cycle assessment and life cycle costing for assessing maritime transport: A comprehensive literature review. Marit. Policy Manag. 1–21. http://dx.doi.org/10.1080/03088839.2021.1972486.
OECD, 2021. World Energy Outlook 2021. Organisation for Economic Co-operation and Development (OECD), Paris.
Perčić, M., Vladimir, N., Fan, A., 2020. Life-cycle cost assessment of alternative marine fuels to reduce the carbon footprint in short-sea shipping: A case study of Croatia. Appl. Energy 279, 115848. http://dx.doi.org/10.1016/j.apenergy.2020.115848.
Ritchie, H., Roser, M., 2020. CO_2 and Greenhouse Gas Emissions. https://ourworldindata.org/co2/country/japan.
Rödger, J.-M., Kjær, L.L., Pagoropoulos, A., 2018. Life cycle costing: An introduction. In: Hauschild, M.Z., Rosenbaum, R.K., Olsen, S.I. (Eds.), Life Cycle Assessment: Theory and Practice. Springer International Publishing, Cham, pp. 373–399. http://dx.doi.org/10.1007/978-3-319-56475-3_15.
Sherif, Y.S., Kolarik, W.J., 1981. Life cycle costing: Concept and practice. Omega 9 (3), 287–296. http://dx.doi.org/10.1016/0305-0483(81)90035-9.
Ship & Bunker, 2021. World Bunker Prices. https://shipandbunker.com/prices.
Smith, C., 2021. Government Investment Programmes: The 'Green Book'. In: Government Investment Programmes. https://lordslibrary.parliament.uk/government-investment-programmes-the-green-book/.
Stopford, M., 2009. Maritime Economics, third ed. Routledge, London ; New York.
The Loadstar, 2021. Carriers watch as price of LNG 'transition fuel' sails past the cost of diesel. https://theloadstar.com/carriers-watch-as-price-of-lng-transition-fuel-sails-past-the-cost-of-diesel/.
Trivyza, N.L., Rentizelas, A., Theotokatos, G., 2019. Impact of carbon pricing on the cruise ship energy systems optimal configuration. Energy 175, 952–966. http://dx.doi.org/10.1016/j.energy.2019.03.139.
UNCTAD, 2021. Review of Maritime Transport 2021. Technical Report.
Utne, I.B., 2009. Life cycle cost (LCC) as a tool for improving sustainability in the Norwegian fishing fleet. J. Clean. Prod. 17 (3), 335–344. http://dx.doi.org/10.1016/j.jclepro.2008.08.009.
Wang, H., Boulougouris, E., Theotokatos, G., Zhou, P., Priftis, A., Shi, G., 2021. Life cycle analysis and cost assessment of a battery powered ferry. Ocean Eng. 241, 110029. http://dx.doi.org/10.1016/j.oceaneng.2021.110029.
Wang, H., Oguz, E., Jeong, B., Zhou, P., 2018. Life cycle cost and environmental impact analysis of ship hull maintenance strategies for a short route hybrid ferry. Ocean Eng. 161, 20–28. http://dx.doi.org/10.1016/j.oceaneng.2018.04.084.
Wang, H., Oguz, E., Jeong, B., Zhou, P., 2019. Life cycle and economic assessment of a solar panel array applied to a short route ferry. J. Clean. Prod. 219, 471–484. http://dx.doi.org/10.1016/j.jclepro.2019.02.124.
Wärtsilä, Engine online configurator | Wärtsilä, https://www.wartsila.com/marine/engine-configurator.
Wärtsilä, 2020. Wärtsilä 31DF product guide.
Wärtsilä, 2021a. A discussion with the Project Manager on the construction costs of the engines studied.
Wärtsilä, 2021b. Wärtsilä 32 Product Guide.
Welch, I., 2017. Corporate Finance, fourth ed. Ivo Welch, Los Angeles.
Zito, T., Park, C., Jeong, B., 2022. Life cycle assessment and economic benefits of a solar assisted short route ferry operating in the Strait of Messina. J. Int. Marit. Saf. Environ. Aff. Shipp. 6 (1), 24–38. http://dx.doi.org/10.1080/25725084.2021.1968664.